

THE PETROCHEMISTRY OF THE BULL ARM FORMATION
NEAR RANTEM STATION, SOUTHEAST NEWFOUNDLAND

CENTRE FOR NEWFOUNDLAND STUDIES

**TOTAL OF 10 PAGES ONLY
MAY BE XEROXED**

(Without Author's Permission)

JOHN G. MALPAS

312129



THE PETROCHEMISTRY OF THE BULL ARM FORMATION
NEAR RANTEM STATION, SOUTHEAST NEWFOUNDLAND

by



John G. Malpas, B.A.

A Thesis
Submitted in Partial Fulfilment of the Requirements
for the degree of
MASTER OF SCIENCE

Memorial University of Newfoundland

December, 1971



FRONTISPIECE: View looking SW to
Placentia Bay from the Doe Hills.

TABLE OF CONTENTS

	<u>Page</u>
Abstract:	(vi)

CHAPTER I: INTRODUCTION

(A) Location and Access	1
(B) Physiography and Climate	1
(C) Previous Geological Work	2
(D) Present Study	3
(E) Acknowledgements	3

CHAPTER II: GEOLOGICAL SETTING

(A) General Geology of the Avalon Peninsula	4
(B) Precambrian Stratigraphy	4
Eastern Avalon: (i) Harbour Main Group	4
(ii) Conception Group	8
(iii) Holyrood Granite Series	9
(iv) Cabot and Hodgewater Groups	9
Western Avalon: (i) Connecting Point Group	11
(ii) Musgravetown Group	11
(iii) The Random Formation	12
(C) Palaeozoic Stratigraphy	13
(D) Structural History	13
(E) Interpretation of Stratigraphy and Structure	15

CHAPTER III: THE BULL ARM FORMATION

(A) General Lithology	18
(B) Structure and Metamorphism	19
(C) Geology of the Map Area	19
Rock Types: (i) Rhyolite Flows and Ignimbrites	21
(ii) Basalt Flows	24
(iii) Tuffs	24
(iv) Volcanogenic Deposits	26

CHAPTER IV: MINERALOGY AND PETROLOGY

(A) Rhyolites	28
(i) Rhyolites from Serrated Hill	28
(ii) Rhyolites from Doe Hills	30
(B) Rhyodacites	32
(C) Ignimbrites	33
(D) Basalts	34
(E) Tuffs	35

CHAPTER V: PETROCHEMISTRY

Introduction	37
Group I Rhyolites and Ignimbrites	37
Group II Rhyolites	54
Rhyodacites	60
Basalts	60
Tuffs	65
Sediments	66

CHAPTER VI: SIGNIFICANCE OF PETROCHEMISTRY AND MINERALOGY

(1) Origin of the Albite	67
Previous Work	67
Present Work	69
(2) Metasomatism	70
Geological Significance	74
(3) Original Composition of Rocks and Volcanic Affinities. . .	77
Appendix I: ANALYTICAL METHODS	84
Bibliography	87

TABLES:

Table II-A: Avalon stratigraphic succession	5
Table IV-A: Average modes of rhyolites	28
Table IV-B: Average modes of rhyodacites	32
Table IV-C: Average modes of ignimbrites.	34
Table IV-D: Average modes of tuffs.	36
Table V-A: Analyses, C.I.P.W. Norms: Rhyolites Group I . .	38
Table V-B: Analyses, C.I.P.W. Norms: Rhyolites Group II. .	39-40
Table V-C: Analyses, C.I.P.W. Norms: Rhyodacites	41
Table V-D: Analyses, C.I.P.W. Norms: Basalts	42
Table V-E: Analyses: Tuffs.	43
Table V-F: Analyses: Sediments	44
Table V-G: Average Hawaiites and Mugearites	64

	<u>Page</u>
Table VI-A: Major Element and weighted averages for rhyolites and tuffs	76
Table A-I: Accuracies and Precisions of Analytical Methods	85-86

FIGURES:

Figure I-1: Geology of the Bull Arm near Rantem Station .	(Pocket)
Figure II-1: General Geology of the Avalon Peninsula . . .	6
Figure II-2: General Geology of the Western Avalon	(Pocket)
Figure II-3: Fault systems in the Isthmus of Avalon . . .	14
Figure II-4: Facies types of the Avalon	16
Figure II-5: Facies distribution	F.p. 17
Figure V-1: Sample locations	45
Figure V-2: Frequency distribution of analysed specimens.	46
Figure V-3: Major elements vs. SiO_2	48
Figure V-4: Major elements vs. SiO_2	49
Figure V-5: Trace elements vs. SiO_2	50
Figure V-6: Alkalinity Index vs. SiO_2	51
Figure V-7: Normative Qtz. Ab. Or. diagrams	52
Figure V-8: Trace elements vs. Differentiation Index. . .	53
Figure V-9: Correlation between K and Rb and K and Ba for Group I rhyolites	55
Figure V-10: Correlation between Ca and Sr for Group I rhyolites	56
Figure V-11: Plot of Na_2O vs K_2O for Group II rhyolites. .	58
Figure V-12: Correlation between K and Rb and K and Ba for Group II rhyolites.	59
Figure V-13: Normative An. Ab. Or. in basalts and Alks. vs. SiO_2 for basalts.	62
Figure V-14: Alkalies vs. Alumina for Basalts	63
Figure VI-1: Variation of Zr. with Differentiation Index - Alkaline suites	79
Figure VI-2: Variation of Zr with Differentiation Index - Calc-alkaline suites.	80

PLATES:

Facing Page

Frontispiece.	View looking SW to Placentia Bay from the Doe Hills.	
Plate III-1:	Flow banding in rhyolites	22
Plate III-2:	Autobrecciated rhyolite flows	23
Plate III-3:	Ignimbrite from Serrated Hill showing eutaxitic texture X 25. Plane light . .	24
Plate III-4:	Intrusive basalt breccia.	24
Plate III-5:	Conglomerate.	26
Plate III-6:	Siltstones showing sedimentary features .	27
Plate IV-1:	Chequer-board albite showing glomero- porphyritic growth. X25 X-nicols. . . .	29
Plate IV-2:	Chequer-board twinning in albite X35. X-nicols.	29
Plate IV-3:	'Fresh' albite phenocryst X 25. X-nicols.	30
Plate IV-5:	Flow-banding in rhyolite X 25. Plane light.	30
Plate IV-4:	Development of spherulites in rhyolite matrices. A: X 40; B: X 22. X-nicols.	31
Plate IV-6:	Spherulites in rhyolite in hand specimen.	31
Plate IV-7: IV-8: IV-9:	Replacement of albite by orthoclase in Doe Hills rhyolites. IV-7: X 35; IV-8: X 37; IV-9: X 27. X-nicols.	32
Plate IV-10:	Welded glass shards in ignimbrite X 37. Plane light.	33
Plate IV-11:	Welded glass shards in ignimbrite X 40. Plane light.	33
Plate IV-12.	Welded shards around basic fragment in ignimbrite X 20. X-nicols	34
Plate IV-13:	Microclites of plagioclase in basalt X 60. X-nicols.	34

Plate IV-14:	Lithic Tuffs.	A: X 30, X-nicols.	
		B: X 20, Plane light. .	35
Plate IV-15:	Crystal Tuffs.	A: X 15, X-nicols.	
		B: X 15, Plane light. .	36
Plate IV-16:	Epidote development in lithic tuff		
	X 35. X-nicols		37
Plate VI-1:	Development of Barite in veins and on		
	joint surfaces in Doe Hills Area.		84

Abstract

The Bull Arm Formation of late Precambrian volcanic rocks crops out on the Avalon Peninsula and on the Isthmus of Avalon, S.E. Newfoundland. An area of approximately nine square miles on the Isthmus was mapped and sampled in the summer of 1970. The area was chosen because it showed a complete cross section of rock types exposed in fresh roadside cuttings and therefore easily accessible.

The rock types are mainly rhyolitic flows, ignimbrites and tuffs, minor late basaltic flows and scoria, and associated volcanogenic sediments. A relative lack of intermediate derivatives makes the distribution essentially bimodal.

Features such as well preserved igneous flow structures, and the presence of ignimbrites and red sediments, suggest a subaerial environment of deposition for the volcanics, with local reworking of deposits in superficial ponds and lakes to give graded and cross-bedded sediments.

The rocks have undergone mild deformation into open folds with associated axial planar cleavage visible in some tuffaceous and sedimentary deposits. This deformation appears to be Acadian in age and was accompanied by metamorphism to low greenschist grade. In the tuffs and some flows there is a noticeable development of epidote and zoisite as matrix alteration products.

Metasomatic effects mask the original identity of the rocks and both chemically and mineralogically they may now be ascribed to a spilite/

keratophyre suite. The development of secondary albite 'phenocrysts' visibly accompanies epidotisation in thin section. These are thought to be a product of metasomatism. In one area, this metasomatism is overprinted by a (contemporaneous?) potassium enrichment which appears to be structurally controlled. Here, rhyolites with increased potassium contents have low sodium and show a progressive development of orthoclase at the expense of albite, in the phenocrysts. The metasomatism explains the anomalously young age date of 467 ± 30 m.y. and the high Rb/Sr ratios obtained for the Bull Arm Formation by previous workers. It may also account for a local barite/galena mineralisation.

Two lines of evidence, Zr values and bulk analyses, suggest an original calc-alkaline affinity for the rocks, but the bimodal distribution of rock types remains difficult to interpret.

CHAPTER I

INTRODUCTION

(A) LOCATION AND ACCESS:

The Bull Arm Formation crops out in the western part of the Avalon Peninsula, southeast Newfoundland, and in the narrow isthmus joining this peninsula to the main part of the island. The map area is located in this Isthmus and comprises approximately nine square miles between $47^{\circ}37'$ and $47^{\circ}41'$ north latitudes and $53^{\circ}52'$ west longitudes (Figure I-1). The Trans-Canada Highway approximately bisects the area and runs 74 miles eastwards to St. John's, the Provincial capital. An older gravel road, Route 1A, also serves the area and settlements on the north shore of Trinity Bay. The main Canadian National Railways line passes through the district with a short side branch to Rantem Station in the North. A number of small fishing settlements are found in the vicinity of the map area, the largest of these being Chance Cove and Bellevue. Bellevue Provincial Park, in which a base camp was established for the present work, is situated between the two on Route 1A.

(B) PHYSIOGRAPHY AND CLIMATE:

Exposure in the map area is good and has recently been increased by the road cuttings of the new Trans-Canada Highway. Bedrock geology controls topography. Volcanic rocks usually produce hills and knobs and give rise to irregular features when interbedded with sediments. The highest points in the map area are the Doe Hills and Serrated Hill. Glacial features were described by Henderson (1960) and Jenness (1960) and raised marine features by McCartney (1967). Soil is lacking in the

map area and where not outcropping, bedrock is overlain by locally derived till and waterlogged peat deposits.

Mist and fog may hamper field work on the Isthmus of Avalon even during the summer months. Temperatures rarely exceed 70°F and rainfall averages 4-5 inches per month during the summer.

(C) PREVIOUS GEOLOGICAL WORK:

J. B. Jukes (1843) divided the rocks of the Avalon Peninsula into two formations corresponding to the Precambrian and Palaeozoic with subdivisions within each formation. A geological map of the Avalon Peninsula published by A. Murray and J. P. Howley in 1881 delineates areas of extrusive and intrusive igneous rocks and subdivides the Precambrian into units corresponding to the Conception Group and the formations of the Hodgewater Group that are now recognized. A. F. Buddington studied the petrology and relationships of the Precambrian volcanic and plutonic rocks of the central Avalon (1916, 1919), in the region of Holyrood. Hayes and Rose (1948) described the geology of the Western Avalon, showing stratigraphical correlations with units to the east.

Until 1952, however, work on the Avalon was either of this broad reconnaissance nature or extremely detailed. Since then, the Geological Survey of Canada has published several memoirs on the regional geology of Avalon by E. R. Rose (1952), R. D. Hutchinson (1953), S. E. Jenness (1963), and W. D. McCartney (1967). ⁽¹⁹⁴⁸⁾ Hayes and Rose (1948) and McCartney (1967) remain the only definitive references to the Isthmus of Avalon area.

Recent work has been carried out on the Avalon Peninsula by M.U.N.

faculty members and graduate students, notably by V.S. Papezik (1969, 1970), C.J. Hughes (1970, 1971), W.D. Brückner (1969), W.D. Brückner & M.M. Anderson (1971), M.M. Anderson and S.B. Misra (1968), H. Keats (1970), and J. Maher (1971), and by several undergraduate students.

(D) PRESENT STUDY:

Field work was carried out in the summer of 1970 in order to produce a map of an area of Bull Arm volcanic rocks. Analyses were made to ascertain the composition of the volcanics and possible metasomatism. It was hoped that such a study might clarify questionable age relationships, processes of mineralisation, and the petrogenesis of the rock suites in the area.

(E) ACKNOWLEDGEMENTS:

My thanks are due to Dr. C.J. Hughes who first suggested the problem and who has guided the investigation from the outset. Many useful discussions have also been held with Professor W.D. Brückner, Dr. D.F. Strong, and other members of the Department of Geology, M.U.N. I should also like to thank Mrs. G. Andrews for instruction in Atomic Absorption techniques, and A. Harris and C. Hutchings for help in the laboratory and the field. My thanks also are due to Mr. and Mrs. S. Rowe of Chance Cove, Trinity Bay, for their hospitality.

CHAPTER II

GEOLOGICAL SETTING

(A) GENERAL GEOLOGY OF THE AVALON PENINSULA:

The Avalon Peninsula is underlain by a late Precambrian series of volcanic rocks and their sedimentary derivatives, reflecting a complex history of volcanism and sedimentation (McCartney, 1967, 1969; Poole, 1967; Brückner, 1969). Lower Palaeozoic rocks locally overlie these in central-west Avalon and in Conception Bay. The succession described by earlier workers in the area is reproduced in Table II-A, and the distribution of groups in Figure II-1.

(B) PRECAMBRIAN STRATIGRAPHY:

Precambrian sequences are described below as groups or formations named on the basis of lithology and area of outcrop. Although they thus have various names, these sequences are considered to be broadly time-equivalent.

(1) EASTERN AVALON

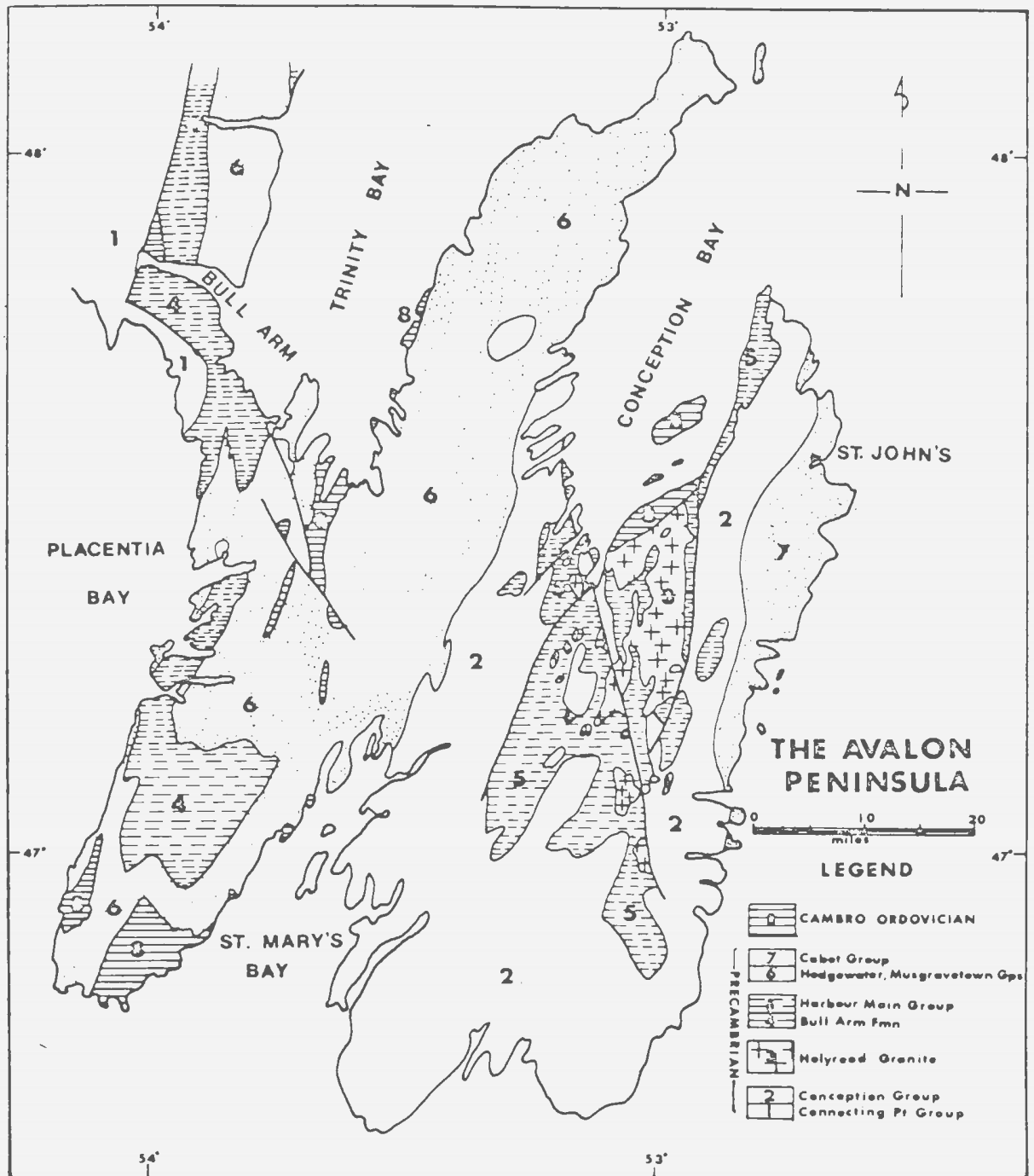
(i) Harbour Main Group:

The oldest rocks in the area, occurring in the Eastern Avalon, are a series of volcanics referred to as 'groups a and b' by Murray (1881); 'the Avondale volcanics' by Buddington (1916) and the 'Harbour Main volcanics' by Howell (1925). They are currently known as the Harbour Main Group (Rose, 1952) and have most recently been described by McCartney (1967) and Papezik (1970). The Harbour Main Group consists of a series of volcanic flows, breccias and tuffs, and volcanogenic sedimentary rocks. The base of the group is not seen but McCartney estimated their thickness

TABLE II-A:

Hayes (1948) Western Avalon		McCartney 1967 Western Avalon Eastern Avalon	
ORDOVICIAN	CLARENVILLE FORMN.		WABANA GROUP
			BELL ISLAND GROUP
			CLARENVILLE FORMN.
CAMBRIAN	ELLIOT COVE FORMN.	MANUELS R. FORMN. CHAMBERLAINS BROOK BRIGUS FORMN. SMITH POINT FORMN. BONAVISTA FORMN.	ELLIOT COVE FORMN.
	BRIGUS FORMATION (van Ingen) inc. SMITH PT. mem.		MANUELS R. FORMN.
			FORMATION
			BRIGUS FORMN.
			SMITH POINT FORMN.
			BONAVISTA FORMN.
			PRECAMBRIAN
RANDOM FORMN.	RANDOM FORMN.	RANDOM FORMN.	
disconformity	disconformity	ang. unconformity	
MUSGRAVETOWN GP. including BULL ARM FELSITE member	MUSGRAVETOWN GP. including	HODGEWATER GROUP including CARBONEAR FORMN.	
ang. unconformity	BULL ARM FORMATION		
CONNECTING POINT GROUP	CONNECTING POINT GROUP	CONCEPTION GROUP unconformity HOLYROOD GRANITE HARBOUR MAIN GP.	

FIGURE II-1: General Geology of the Avalon Peninsula.



at more than 6,000 feet. However, repetition by folding and faulting which gives rise to structures that are difficult to interpret often leads to sections with apparently greater thicknesses.

Most of the Harbour Main Group crops out to the southwest of Conception Bay, with earlier rhyolite flows and ignimbrite units overlain by basaltic and andesitic flows.

Andesitic flows, breccias and tuffs, and basalts constitute approximately two-thirds of the total volcanic rocks of the series. Andesite porphyries have been interpreted by McCartney (1967) as small necks intrusive into surrounding volcanic rocks. Rhyolite breccias are widely distributed but not abundant.

A well-preserved series of ignimbrites are of special interest (McCartney, 1967; Papezik, 1969). Analyses of some volcanic rocks from the Harbour Main Group had been given by Buddington (1916) but Papezik (1970) presented the first comprehensive series of analyses of Harbour Main rocks, indicating that they possibly comprised an alkaline sodic suite.

A range of sedimentary rock types including siliceous slates, red-beds and conglomerates have been mapped by McCartney (1967). He attributes them to possible deposition by rivers and streams and in small lakes or marine embayments within the volcanic terrane. This explanation would account for the apparent lateral discontinuities of the beds. Intercalated in the succession are sediments which were probably of proximal origin since they contain angular detrital fragments of wholly volcanic composition.

(ii) Conception Group:

A thick sequence of volcanogenic sediments and tuffs known as the Conception Group overlies the Harbour Main Group in the Eastern Avalon with apparent unconformity. Its relations with the Harbour Main are still controversial, however, with some authors regarding it as succeeding the Harbour Main Group (McCartney, 1967, 1969) and others believing the two groups to be partly contemporaneous and interfingering (Rose, 1952; Brückner, 1969; Hughes and Brückner, 1971; Maher, 1971).

At Duffs, on the east coast of Conception Bay, a basal conglomerate contains angular to subrounded boulders of quartz-monzonite derived from the nearby Holyrood Granite. Basal conglomerates pass up through a series of subgreywackes into siltstones, indicating a possible transition from shallow to deep water environments. The siltstones are generally green-grey or black in colour and are commonly laminated or show graded bedding. Remnant shards have been noted in some indicating their volcanic origin probably as waterlain tuffs. A basaltic pillow-lava, 60 feet thick is exposed within the Conception Group on the west side of Holyrood Bay, and similar pillow-lavas are known from Cape St. Francis (Maher, pers. comm.).

Abundant fossils at Cape Race (Anderson and Misra, 1968) comprise soft-bodied Metazoan forms of several types preserved below bands of waterlain tuff in Conception beds. Tillites, interbedded with Conception strata, with common striated pebbles and boulders, have been described by McCartney (1967), Brückner (1969), and Brückner and Anderson (1971).

(iii) Holyrood Granite Series:

The Holyrood Granite series, intrusive into Harbour Main rocks, crops out over an area 8 miles wide by 33 miles long extending southwards from the southern shores of Conception Bay. The predominant rock type is an equigranular quartz-monzonite but marginal granodiorite, quartz-hornblende gabbro and pegmatitic granophyre have been recognized (McCartney, 1967).

McCartney et al. (1966) have obtained an Rb/Sr isochron age of 574 ± 11 m.y. for the Holyrood Granite. McCartney (1969) considers this to represent one period of emplacement before deposition of the Conception Group. Papezik has confirmed this view for the west-central Avalon (Papezik, pers. comm.). Rose (1952) favours protracted intrusion of the granite into the lower Conception Group as well as into the Harbour Main volcanics. In either case the upper part of the Conception Group would have been laid down, assuming the isochron age to be correct, less than 574 ± 11 m.y. ago, since it contains fragments and pebbles of similar granitic rocks.

Block faulting that post-dated the granite intrusion produced a series of approximately N/S trending horst and graben structures. The resulting high relief gave rise to erosion of the Holyrood Granite, Harbour Main and Conception Group rocks on a large scale, and deposition of molasse type sediment in the grabens.

(iv) Cabot and Hodgewater Groups:

Thick clastic sequences overlies Conception Group type rocks in eastern and central Avalon. In central Avalon these grade upwards into

Cambrian sediments, but in eastern Avalon they are not seen in contact with Palaeozoic rocks. The sequences are considered equivalent in age on the basis of stratigraphical position, i.e. post-Conception and pre-Cambrian, and lithological similarity.

Brückner (1969) has divided eastern Avalon into fault-bound blocks. These blocks formed a series of horst and graben structures which were actively eroded giving different successions in each. For example, east of the Holyrood Horst lies a belt of more than 14,000 feet of sediment, collectively forming the Cabot Group. Recently Hsu (pers. comm.) has recognised tuffaceous beds within basal members of the Group representing the last stages of volcanism in the area. The lowest unit of the Group, the St. John's Formation, is composed of dark grey and red tuffaceous siltstones and there is a conformable transition from the underlying grey-green Conception slate. Overlying the St. John's Formation are thick arkoses and conglomerates, which were in part derived by erosion of Holyrood type granitic rocks. Available current directions in the Baccalieu area suggest that their derivation was from further to the N.N.E. (A.F. King, pers. comm.)

A similar sedimentary sequence occurs in the central Avalon where it is known as the Hodgewater Group. The basal unit is here known as the Carbonear Formation. It would appear to be the lateral equivalent of the St. John's Formation, as it too conformably overlies the Conception Group. Overlying this formation are a series of arkoses and red sandstones which pass with apparent conformity into the Cambrian.

(2) WESTERN AVALON

The general geology of the Western Avalon is shown in Figure II-2 (Pocket).

(i) Connecting Point Group:

Rocks with a similar lithology to the Conception Group which crop out in the western part of the Avalon Peninsula were formerly called the 'Conception Slates' (Buddington, 1919). Similarities in thickness and lithology between this group and the Conception Group were confirmed by Hayes (1948) who, however, proposed the name Connecting Point Group for them. The Connecting Point Group is in faulted contact with the Love Cove Schists further west which are presumably older since reworked schist fragments are found in sedimentary members of the Connecting Point Group. The Connecting Point Group is overlain unconformably by marine sediments, tuffs and volcanics of the Musgravetown Group.

The correlation of the Conception Group with the Connecting Point suggested by Hayes (1948) has been mentioned above. McCartney (1967) traced the Whiteways Formation, a fine-grained thin redbed unit in the middle of the Hodgewater Group, further west into red sandstones and conglomerates of the Maturin Pond Formation in the middle of the Musgravetown Group. Thus, it is probable that the Cabot, Hodgewater, and Musgravetown Group rocks are, at least in part, contemporaneous.

(ii) Musgravetown Group:

The Musgravetown Group is exposed west and northwest of the Hodgewater Group in the western Avalon and in the Isthmus of Avalon. It overlies Connecting Point Group rocks and consists of volcanic and clastic sedimentary rocks with an aggregate thickness of up to 13,000 feet. Unlike the Cabot and Hodgewater Groups, the basal beds of the Musgravetown Group are generally conglomeratic and are intercalated with volcanic rocks

known as the Bull Arm Formation. These volcanics have no counterparts in the Hodgewater or Cabot Groups.

McCartney (1956) has mapped the lowermost Bull Arm rocks as conformable with the Connecting Point Group. Much of the contact is, however, obscured by faulting. Jenness (1963) has recognised an angular unconformity between Musgravetown and Connecting Point Group rocks further north in the Bonavista area.

The Bull Arm Formation in the western Avalon and the Isthmus of Avalon is conformably overlain by a thick sequence of clastic beds. The uppermost Musgravetown Group rocks form a wedge of conglomerates which lie along the eastern edge of an apparent horst in the Isthmus area (Isthmus horst of McCartney, 1969).

(iii) The Random Formation:

The Random Formation, comprising one to four distinctive white quartzite units, is found within the upper part of the Hodgewater and Musgravetown Groups in western and central areas. These quartzites underlie Lower Cambrian fossiliferous shales and minor limestones with local discordance. McCartney (1969) interprets a shallow angular unconformity at the base of the Random in southeast Trinity Bay as a result of local structural movement. The Random Formation is absent in the Conception Bay area and Lower Cambrian beds lie with marked unconformity on Conception rocks and nonconformably on the Holyrood Granite.

The Random Formation may be interpreted by analogy with many pure quartzites of similar nature as a time-transgressive shoreline deposit.

(C) PALAEOZOIC STRATIGRAPHY:

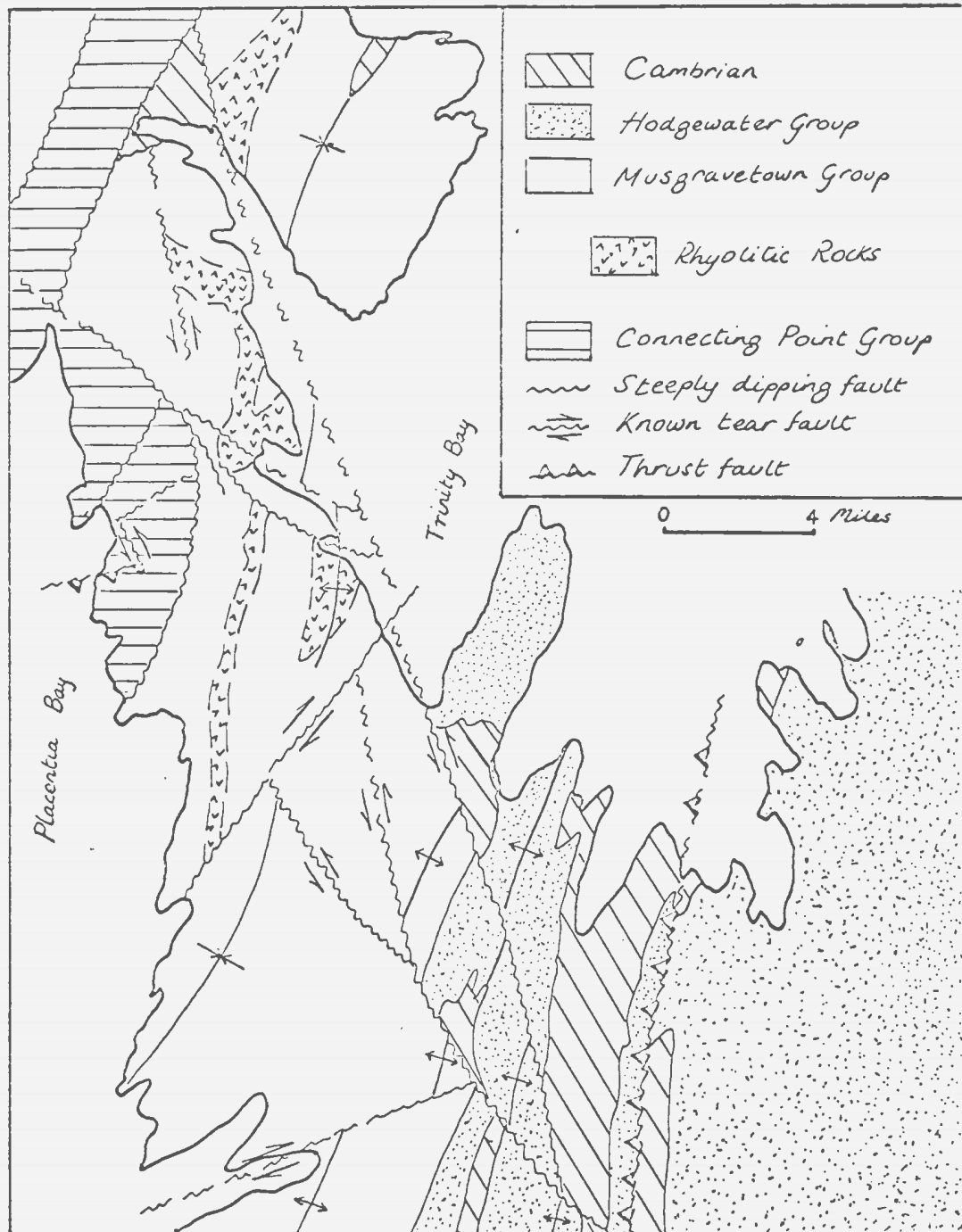
Lower, Middle and Upper Cambrian beds form a sequence of shale and limestone of approximately 1500 feet thickness and occur in the western and central Avalon Peninsula. Cambrian faunas characteristic of the Atlantic faunal realm have been noted by Hutchinson (1962). Dale (1915) and McCartney (1967) have described a marker horizon in the form of a manganese bed at the base of the Middle Cambrian in Conception and Trinity Bays. The relatively unfossiliferous Upper Cambrian is overlain by Lower Ordovician shale and sandstone beds more than 8,000 feet thick in Southern Conception Bay. These rocks are well-exposed on Bell Island and Kelly's Island and were worked on the former for sedimentary iron-ore in the Wabana Formation.

(D) STRUCTURAL HISTORY:

A period of Precambrian deformation is shown by a number of high angle faults with vertical displacements often up to several thousand feet. McCartney (1969) interprets these faults as forming a number of northerly trending horst and graben structures which dominated the sedimentary pattern during latest Precambrian time. This period of deformation has been referred to as the Avalonian orogeny by McCartney (1967), Poole (1967), and Rodgers (1967).

Post-Cambrian deformation is represented by open folds (gently plunging NNE or SSW) with moderately dipping limbs. These folds affect both Precambrian and Palaeozoic rocks, and in the less competent beds, e.g. the Cambrian shales, the dips are locally steep and an axial planar cleavage is common. The regional trend suggests that the folding was

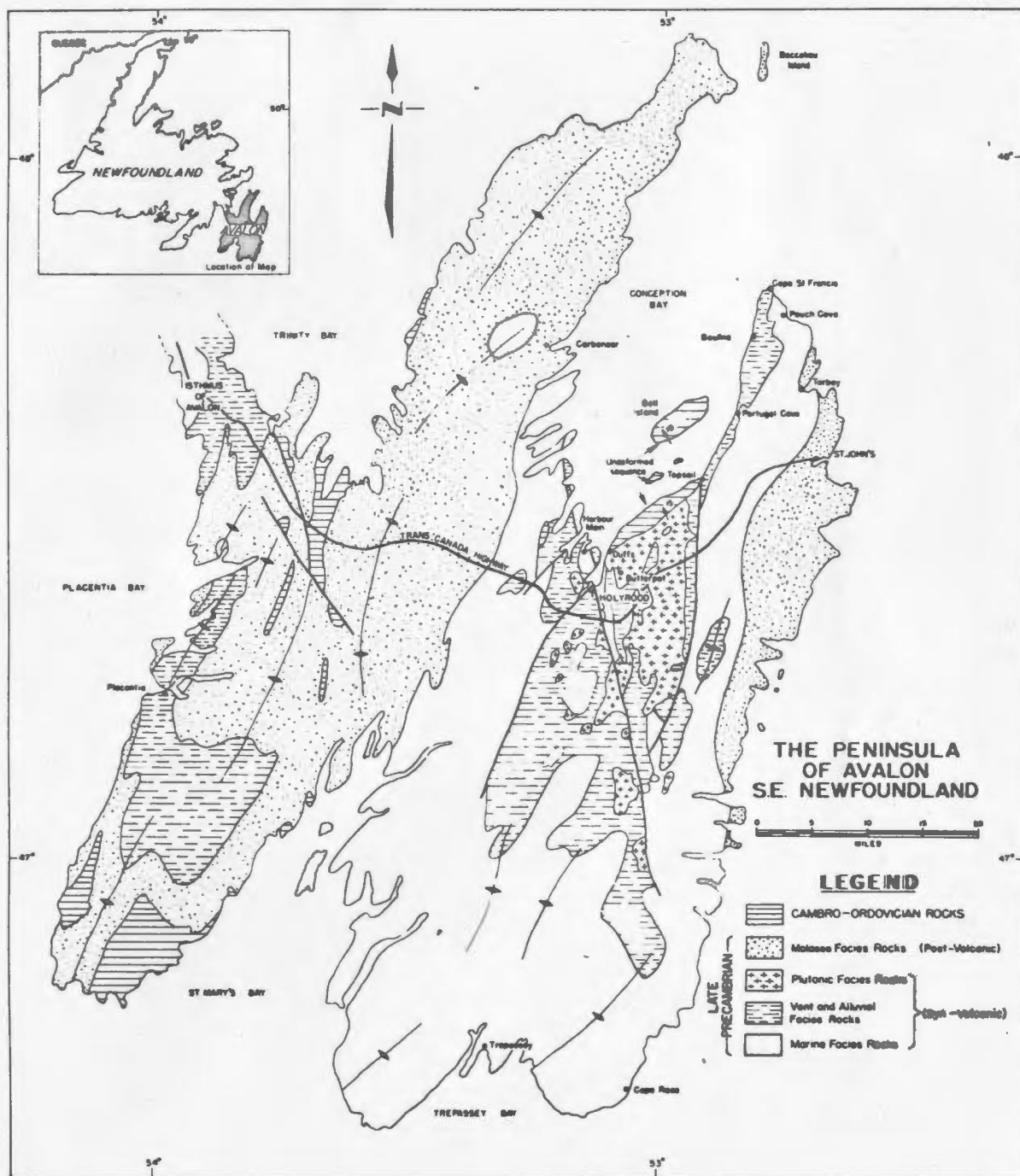
Figure II-3: Fault systems on the Isthmus of Avalon
(after McCartney '69).



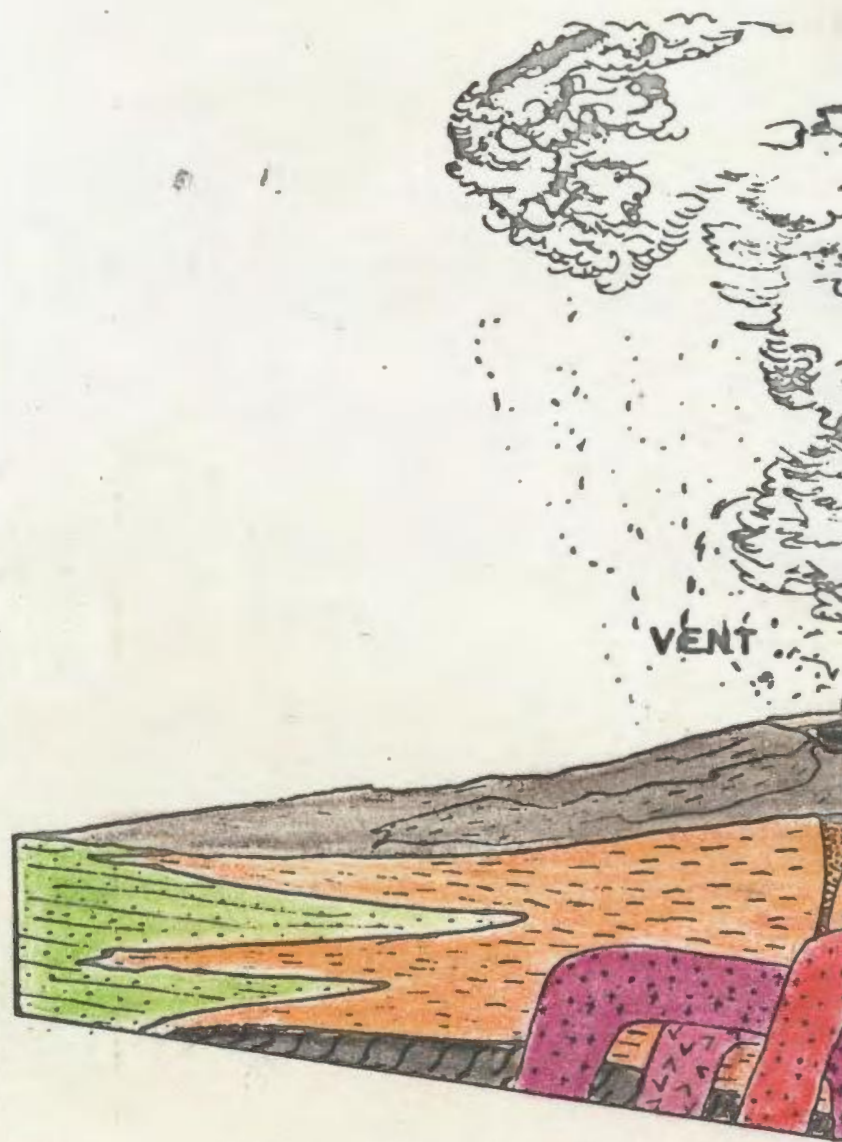
probably Acadian in age. Other post-Cambrian deformation is represented by thrust faults and tear faults. The thrust faults trend north-south and dip shallowly to either east or west. They are possibly of the same age as the folding and represent movements between units of different competence. The tear faults caused offset of fold axes in Cambrian and older strata and are well developed in the north-west Avalon (Figure II-3). Remobilisation of the older Precambrian faults is associated with this latter stage of faulting.

(E) INTERPRETATION OF THE STRATIGRAPHY AND STRUCTURE:

Several workers (Williams, 1964, 1967; Poole, 1967) have discussed the major orogenic phases that affected the Avalon Platform in Precambrian and Devonian times. The significance of the Avalonian orogeny has been further discussed by Hughes (1970) and Hughes and Brückner (1971), who conclude that the Avalon represents the remnants of an island-arc type environment that existed in late Precambrian and early Cambrian times. In this model, the older Precambrian Groups have been reinterpreted as penecontemporaneous facies. That is, the Holyrood Granite is interpreted as a plutonic facies intrusive into a syn-volcanic vent and alluvial facies rocks, the Harbour Main Group, and marine facies rocks, the Conception Group (N.B. the adjective 'marine' is here used to indicate subaqueous deposition of wide extent, not necessarily in saline waters). The Cabot, Hodgewater and Musgravetown Groups have been interpreted as essentially post-volcanic molasse facies rocks although some signs of eruptive activity is witnessed by tuff bands (Figures II-4, II-5). This type of environment would account for a calc-alkaline igneous activity suggested by Hughes (1970). The great accumulations of the molasse facies would necessarily

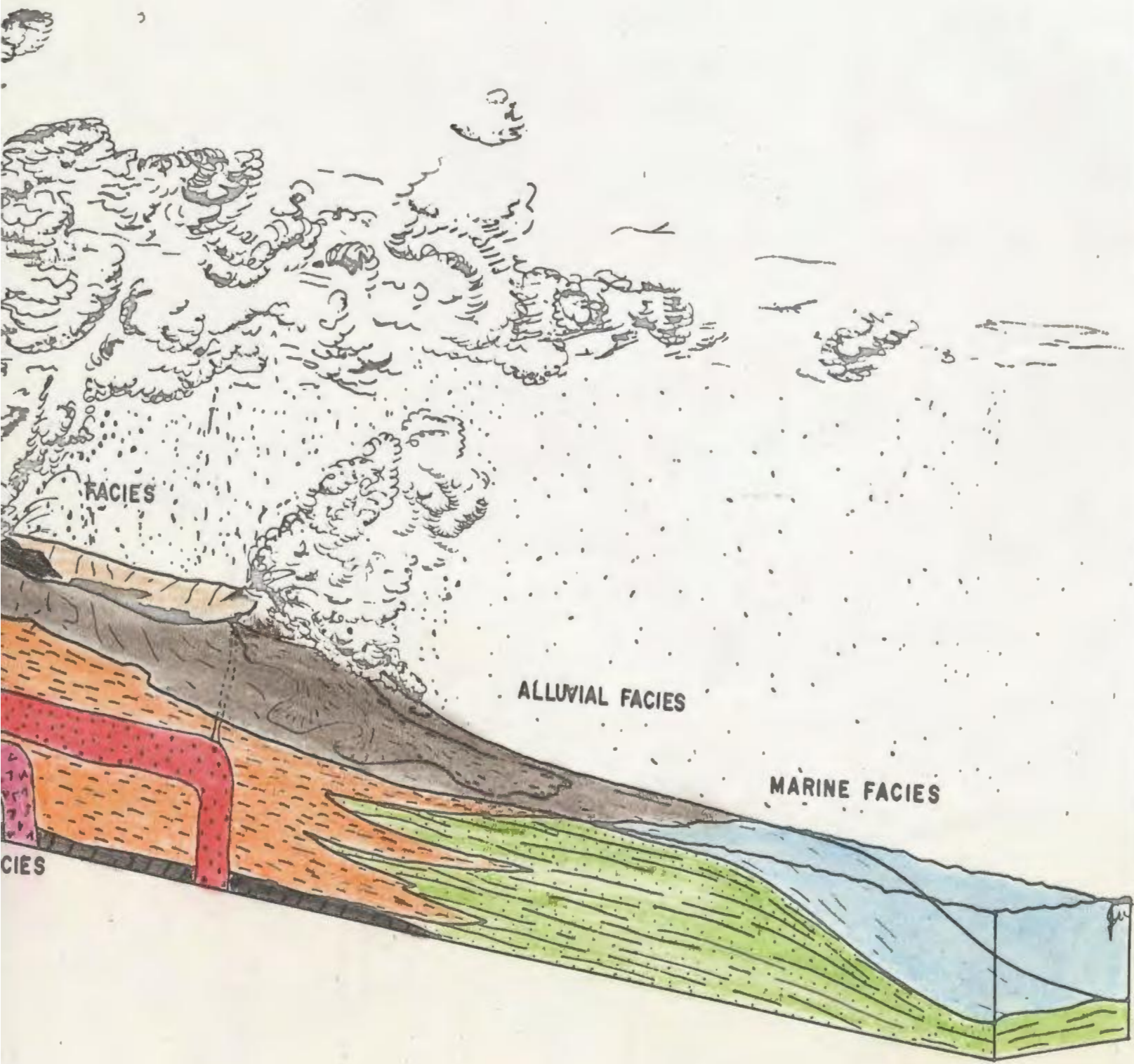


FIGU



PLUTONIC

II-5: Block diagram showing origin of facies types on the Avalon Peninsula.



involve uplift of the source area, possibly along a series of block faults, previously described. The location of the faults suggest adjustments between the rising and eroding volcanic island belt and the subsiding sedimentary basin on its flanks (Hughes, 1970, p. 188), accompanying its erosion to sea level. An island arc type of environment for the Conception and Harbour Main Groups has also been suggested by previous workers (Kay, 1953; Williams, 1964; Rodgers, 1968). Papezik (1970), on the other hand, has shown the Harbour Main to be alkaline and interprets the volcanism and block faulting as indication of Basin and Range type tectonics. These ideas are discussed in Chapter VI.

Insofar as the Cambrian appears in general to possess the same deformation as the underlying rocks, this deformation is post-Cambrian, probably Acadian, in age. The occurrence of undeformed Cambrian beds is attributed to protection by underlying batholithic rocks (Neale et al. 1961). There is no evidence of pre-Acadian compressive structures, reflecting only simple vertical movements during the 'Avalonian orogeny'.

CHAPTER III

THE BULL ARM FORMATION

Hayes (1948) had included the 'Bull Arm Felsite Member' within his definition of the Musgravetown Group and described it as composed of pyroclastics and felsitic lava flows. The same rocks were tentatively mapped further south by McCartney (1956) as the Bull Arm Group but later reduced to formation status. The term 'Bull Arm Formation' (McCartney, 1967) is thus used to designate the dominantly volcanic assemblage of rocks in the lower part of the Musgravetown Group.

(A) GENERAL LITHOLOGY:

The formation includes mafic and felsic flows, pyroclastics and breccias, and volcanogenic conglomerates, tuffaceous arkoses and siltstones. McCartney (1956) divided the Bull Arm rocks into two lithological units. One unit consists of andesitic and basaltic flows, breccias and tuffs, with associated minor intrusives, and a few rhyolite flows and tuffs and green siltstones resembling Connecting Point sediments at the base. The other unit consists solely of rhyolitic flows and tuffs which become more prominent towards the top. This strict division does not, however, seem justified in the light of the present writer's mapping, since rhyolitic flows, ignimbrites and tuffs, and small basaltic intrusive breccias recur throughout the sequence in the Isthmus area.

Although in western Avalon in general mafic rocks form approximately one-half of the total formation, acidic rocks about one quarter and tuffs and volcanogenic sediments about one quarter, on the Isthmus of Avalon and in southern Trinity Bay rhyolitic rocks are more abundant and account for some 60% of the Formation.

(B) STRUCTURE AND METAMORPHISM:

The Bull Arm Formation is deformed into open folds along NNE-SSW trending axes with moderately dipping limbs. Tuffs and fine-grained sediments often develop a marked cleavage, axial planar to the folding, and may show pronounced flattening features. Zones of more extensive flattening appear to alternate with zones showing less deformation. In general, folding becomes more intense to the northwest. On the basis of regional trend and deformational style, and the fact that Cambrian beds are affected to the same extent, this period of folding appears to be Acadian in age.

A number of tear faults affecting the Bull Arm rocks have been mapped by McCartney (1969) on the Isthmus of Avalon (Figure II-3). In an apparently complementary fault system the tear faults striking NNW are sinistral and those striking NE are dextral. This faulting offsets the fold-axes but is possibly related to the same deformation that produced the folds since principal stress orientations appear similar.

Epidote, chlorite and sericite are developed in the highly cleaved rocks. These minerals appear to have grown parallel to the cleavage and augen fragments in the tuffs. The Acadian deformation therefore seems to have been associated with a regional metamorphism to lowest greenschist facies.

(C) GEOLOGY OF THE MAP AREA:

The area mapped for this study lies within the Dildo Map Sheet (McCartney, 1956). The stratigraphic succession recognised in the map area by the present writer is as follows:

Some interfingering of rock types occurs and these are more conveniently described petrographically rather than in stratigraphic sequence.

Rock Types:

(i) Rhyolite Flows and Ignimbrites:

Rhyolitic flows and ignimbrites outcrop in the northwest-central part of the area on the west limb of a syncline (Serrated Hill area) and in the southeast-central part of the area in an anticlinal crest (Doe Hills area). They have been mapped by McCartney (1956) as a distinct member of the Bull Arm Formation (Unit 3, Dildo Map Sheet, G.S.C. 1956) since they generally appear to be contained within the central portion of the local succession. Some acidic flows and ignimbrite units occur higher in the sequence, however, and therefore this division is not a strict one.

Flows have been recognised in the field by two main criteria, flow banding and autobrecciation (Plates III-1 and III-2). Rhyolitic units are recognised which do not have flow structures but these have been traced into areas where the above criteria are seen.

Flow banding occurs generally on approximately a millimetre scale as alternating white and red bands. Coarser bands up to 1 or 2 cm thick also occur. By analogy with recent flows the banding is no doubt indicative of laminar flow in a viscous lava reflected by differential crystallisation and devitrification during cooling. It can sometimes be traced over a distance of several metres but more often becomes distorted and 'turbulent' over a short distance. This breakdown is the first sign of autobrecciation.



A



B

PLATE III-1: Flow banding in Rhyolites, Doe Hills Area. Note beginning of autobrecciation in A.

The products of autobrecciation indicate that it is a process that occurred throughout the mass of the flow more or less simultaneously and that it is not restricted to the surficial parts of the flow as in the production of aa lava. Angular rhyolite blocks are caught up in a matrix of the same composition. Often the fragments are of slightly different colour and texture to the matrix and this gives a fragmental appearance to the rock. Curtis (1954) has described a mechanism for autobrecciation which depends on the escape of small amounts of included gases. A viscous magma, almost at the surface, may have a confining pressure great enough to keep the gases in solution. On extrusion this gas is released and vesiculation takes place. Equilibrium within this lava may be such that vesiculation increases the viscosity so much that the lava cannot adjust internally purely by flow to keep pace with the moving mass behind. Joints and fractures develop within the still plastic lava along which dilation may take place. For a short time this dilation reduces the confining pressures in the area of the cracks and joints and the lava expands rapidly in these directions. This may cause spalling of the lava. Slight movement will give rise to continued spalling so that the mass may become brecciated to a considerable degree. Following autobrecciation, further movement of the mass results in additional pulverisation by attrition whereas the larger blocks become somewhat rounded.

Rhyolite flows occurring in the northwestern half of the map area contain feldspar phenocrysts but no quartz phenocrysts. Those in the major anticlinal crest of the Doe Hills area further east contain quartz and feldspar phenocrysts. However, both of these areas of rhyolitic flows



A



B

PLATE III-2: Autobrecciated Rhyolite Flows.
Doe Hills Area. Flow banded
fragment visible in B.

appear to be at a comparable stratigraphic level. Rhyodacite flows have been noted in the centre of the map area, occurring stratigraphically higher in the succession than the rhyolitic flows. These flows are not easily differentiated from other rhyolites in the field but are considered separately on the basis of chemistry and mineralogy.

'Welded tuffs' have been recognised in the map area and are of particular interest in that they have rarely been described from the Precambrian (Plate III-3). References have been made by Hjelmquist (1955) to Precambrian welded porphyritic tuffs in Dalarna, central Sweden; by McCartney (1967) and Papezik (1969) to welded tuff occurrences in the Harbour Main volcanics, Avalon; and by Thieme (1970) to ignimbrite occurrences in the Luapula Group, Zambia. Since the first descriptions of ignimbrite sequences by Marshall (1935), considerable reinterpretation of widespread dacite and rhyolite sheets has been made. Hjelmquist (1955) has summarised the following diagnostic features of ignimbrites:

- 1) The deposits have a disposition that in ordinary instances is approximately horizontal.
- 2) There is an absence of glassy selvages.
- 3) A scoriaceous surface is lacking.
- 4) The Specific Gravity is lower than flows of similar composition.
- 5) There is an increase in Specific Gravity from the top to the bottom of each formation.
- 6) There is no indication of mass flowage.
- 7) Phenocrysts, often present, are broken and fragmented rather than embayed.

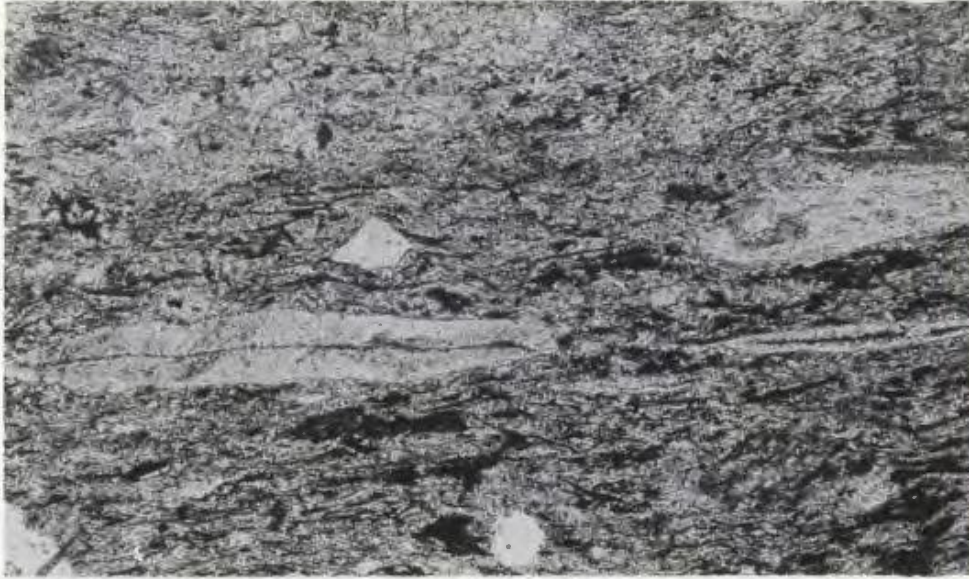


PLATE III-3: Photomicrograph of ignimbrite from Serrated Hill. Note flattened pumice fragments and well developed eutaxitic texture. Plane light x 25.

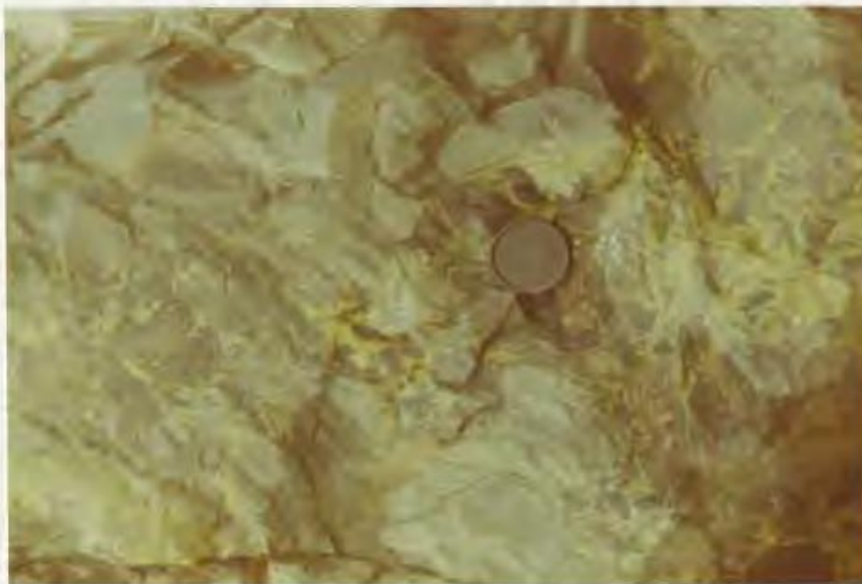


PLATE III-4: Intrusive basalt breccia with epidotised matrix. Some vesicular fragments are visible.

8) Pumice fragments and included rock fragments are often flattened and aligned to give a pronounced eutaxitic texture.

Several of these criteria are difficult to apply to lithified and devitrified welded tuffs as old as the Precambrian. This is primarily due to effects of devitrification and erosion of tops. The most conclusive criteria to use in the field are the presence of broken phenocrysts, collapsed pumice fragments, and numerous angular rock fragments which are heterolithic in character and thus distinct from fragments of flow-breccias.

(ii) Basalt Flows:

A thin series of basalt flows was mapped in the southeast corner of the area. Four flows have been recognised on the basis of interbedded scoriaceous deposits which are, in general, highly vesicular and rich in epidote. The flows are about 10 metres thick and are massive and non-vesicular.

Andesitic and dacitic rocks have not been recognised in the area, although McCartney (1967) has recorded these elsewhere in the Bull Arm Formation.

(iii) Tuffs:

Tuffaceous deposits make up approximately two-thirds of the rock types in the area. They vary from acidic lithic tuffs and crystal tuffs, which are dominant in the lower part of the succession, to more basic types, which, although present lower down, are more abundant towards the top. Tuffs are recognised in the field by the presence of a crude

stratification. They have generally been reworked by water and often show cross-bedding as well as some grain-size sorting. It is generally the latter property which serves to distinguish them from ash flow tuffs since they are highly indurated.

The acid tuffs are generally pale green or dark red in colour and vary in grain size from fine-grained, sometimes porcellanous ashes, to coarse lapilli tuffs with rock fragments up to 5-6 cm in diameter. Volcanic blocks up to 1 metre in diameter may rarely be seen in the tuffaceous matrix. The most common member of this rock suite is a pale green crystal tuff with abundant feldspar crystals and, to a lesser extent, subangular rhyolitic rock fragments. In one variety a dull arkosic matrix contains more rounded but less abundant rock fragments. Although many tuffs contain some mafic rock fragments, wholly mafic tuffs are the least common of the volcanic rocks. The most common type is a fine-grained breccia that is distinctive in its mottled purple and green colouration. Here the matrix material, commonly a mafic crystal tuff, is altered from a dull green to a purple-red colour.

Scoriaceous deposits and intrusive breccias also occur (Plate III-4). Vesicular scoria deposits are seen to overlies many of the basalt flows in the southeastern part of the area. These beds of scoria are generally between 1/2 and 1 1/2 metres thick and are also characterised by a high degree of epidotisation, especially between the fragments. Fragments of vesicular basalt, the vesicles filled with quartz, chlorite and rare feldspar, occur within a fine-grained, green epidote matrix. Blocks of more acid material have also been recorded in such deposits. These appear



PLATE III-5: Conglomerate. Reworked top of rhyolite flow gives rise to a predominance of red rhyolitic fragments.

to be 'accidental inclusions' of acidic material from lower in the succession. Some intrusive basalt breccias appear in dike-like form in the area. The matrix is generally highly epidotised and surrounds angular fragments of vesicular and non-vesicular basalt up to 2-3 cm in diameter. The intrusive origin of some basaltic breccias is difficult to establish although in certain outcrops the bedding in the surrounding tuffaceous sediments is quite clearly truncated.

(iv) Volcanogenic Sediments:

The sedimentary rock types in the area are conglomerates, tuffaceous arkoses, green-grey laminated argillites and siltstones, and red siltstones, composed entirely of volcanic rock fragments, ash and broken crystals.

Since many of the tuffaceous deposits have been waterlain or reworked by water, the distinction between tuffs and volcanogenic sediments, of the arkosic type especially, is extremely difficult. Tuffs and sediments are invariably interbedded and the most obvious differences are the degree of mixing from different sources, grain-size distribution including degrees of sorting and grain-shape, and secondary diagenetic changes.

Conglomerates: (Plate III-5). Reworking of the tops of rhyolitic flows gives rise to local conglomeratic deposits with markedly monolithic rhyolitic rock fragments. The fragments are generally enclosed within a finer-grained arkosic matrix which contains broken, semi-rounded pink feldspar phenocrysts. The fragments range in size from pebble size to boulder size and are generally poorly sorted. However, an overall fining-upwards sequence may be seen where reworked lapilli tuff and crystal tuff



A



B

PLATE III-6: A: Tuffaceous siltstone showing X-bedding.
B: Convoluted lamination in red-green siltstone.

deposits become more common and large rock fragments less so further from the flow which is supplying the clastic debris.

Arkoses: The arkoses have a poor degree of sorting and are composed of angular to subrounded and rare well-rounded fragments. These features together with a low degree of mixing indicates the proximal origin of these sediments. In the southeastern outcrops, which represent sediments higher in the succession, basic fragments are more common and are derived from the closely underlying basaltic volcanics. Elsewhere rhyolitic fragments are predominant.

Argillites and siltstones: (Plate III-6). These are generally laminated and frequently show slump structures. The laminae, if not too distorted by the slumping, can be traced for distances up to 10 metres. The banding is on a 1-5 mm scale and alternates from red-purple to green-grey in colour, presumably as a result of the oxidation state of the included iron. These laminated sediments appear to be concentrated in the higher part of the local succession, above the acidic volcanics but below the more basic types.

Lahars: Probable volcanic mudflow deposits have been mapped in two places and appear to be lenticular and not very widespread. These are recognised by a lack of bedding, an assortment of fragments both angular, subrounded and rounded, of sediments, rhyolitic and basaltic volcanics and tuffs, included in a fine-grained silty matrix. Fractures in these poorly sorted fragments are often filled by matrix material.



PLATE IV-1: Chequer-board albite crystals exhibiting
glomeroporphyritic growth. MB69. X-nicols.
X25.

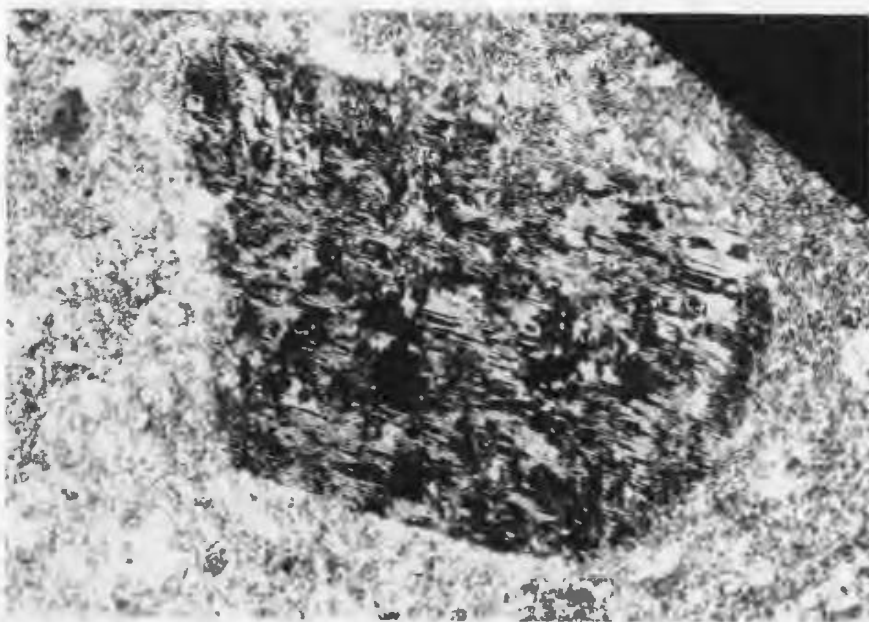


PLATE IV-2: Albite phenocryst showing development of
'chequer-board' twinning. MB56. X-nicols.
X35.

CHAPTER IV
MINERALOGY AND PETROLOGY

(A) RHYOLITES:

Rhyolite flows occur in the Serrated Hill and Doe Hills areas. No quartz phenocrysts have been recorded in rhyolites from Serrated Hill, but it is quite possible that both groups of rhyolites represent a single horizon made up of a number of overlapping flows.

TABLE IV-A: Average Modes for Rhyolites.

<u>Group I - Serrated Hill</u>		<u>Average of 8 Measurements</u>		
Matrix		Albite Phenocrysts		Opakes
86%		11%		3%
<u>Group II - Doe Hills</u>		<u>Average of 8 Measurements</u>		
Matrix	Qtz. Pheno.	Albite Pheno.	Kfd.(turbid)	Opakes
85%	6%	5%	3%	1%

(i) Rhyolites from Serrated Hill Area:

Phenocrysts:

Plagioclase forms the only phenocrysts in these flows. Staining with sodium cobaltinitrite indicates no potassium feldspar phenocrysts. Plagioclase occurs in euhedral to subhedral crystals as large as 1.5 mm which are often embayed. In some rhyolites showing good flow structures

a flow orientation of the phenocrysts has been seen. The crystals are twinned and sometimes appear to have grown in clusters (glomeroporphyritic texture), Plate IV-1. Twinning is often bent but probably as a result of later tectonic deformation rather than flow in a viscous magma (cf. Donnelly, 1963). The crystals are all of albite composition (An_{3-5}) recognised by high $2V_z$ (average on 12 measured crystals is 86° , maximum 91°) and low refractive index. Chequer-board structure has also been recognised (Plate IV-2). The chequer-albite is twinned on the albite-law, but with short lamellae which, after continuing for a length generally a little greater than their width, are abruptly truncated by a plane parallel to (001). These short lamellae are offset from one another, and in sections normal to (010) produce a chequered pattern. The crystals are tabular parallel to (001) often showing simple Manebach twinning. Battey (1955) has suggested a 'porphyroblastic' growth and inclusion of groundmass for the origin of some chequer-albites, but no evidence leading to such a conclusion has been noted in the specimens under discussion here.

Many of the albite phenocrysts appear fresh and unaltered but they are thought to reflect a sodium metasomatism as discussed in Chapter VI (Plate IV-3). Although no significant zoning has been observed, remnants of more calcic plagioclase may be represented by epidote inclusions in some crystals.

Groundmass:

The groundmass of the rhyolites is predominantly a devitrified glass as indicated by spherulites and perlitic cracks (see Plate IV-4). Textures are variable and to a large extent reflect

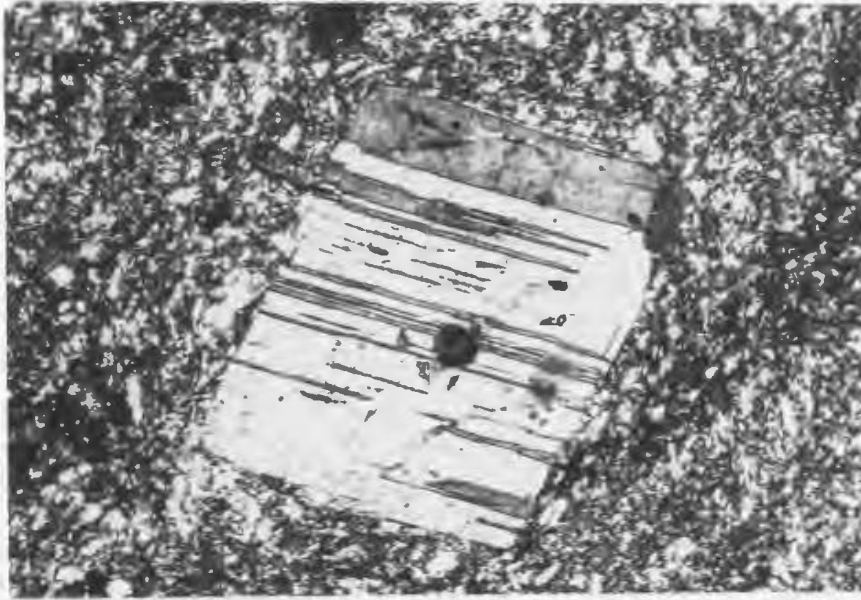


PLATE IV-3: Relatively fresh looking albite 'phenocryst'.
MB56. X-nicols, X35.

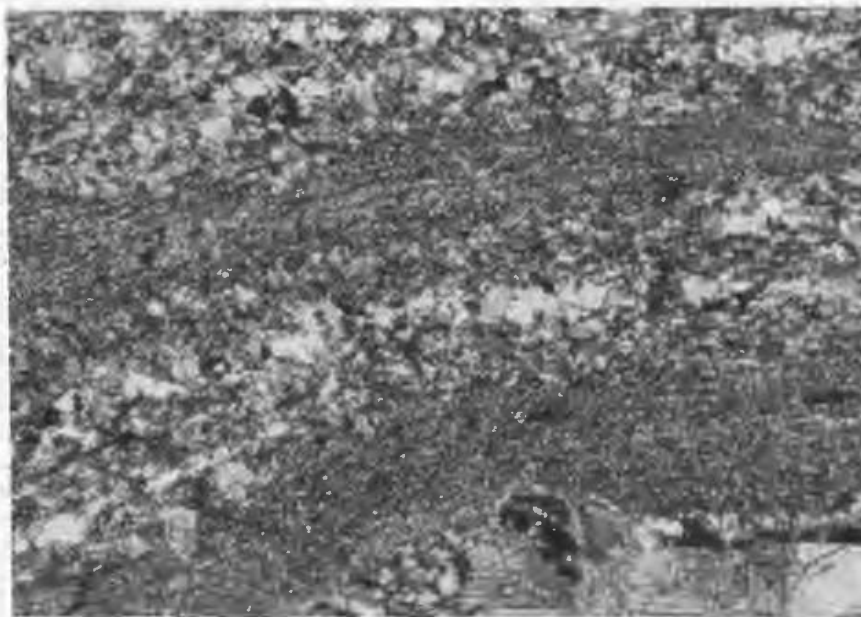


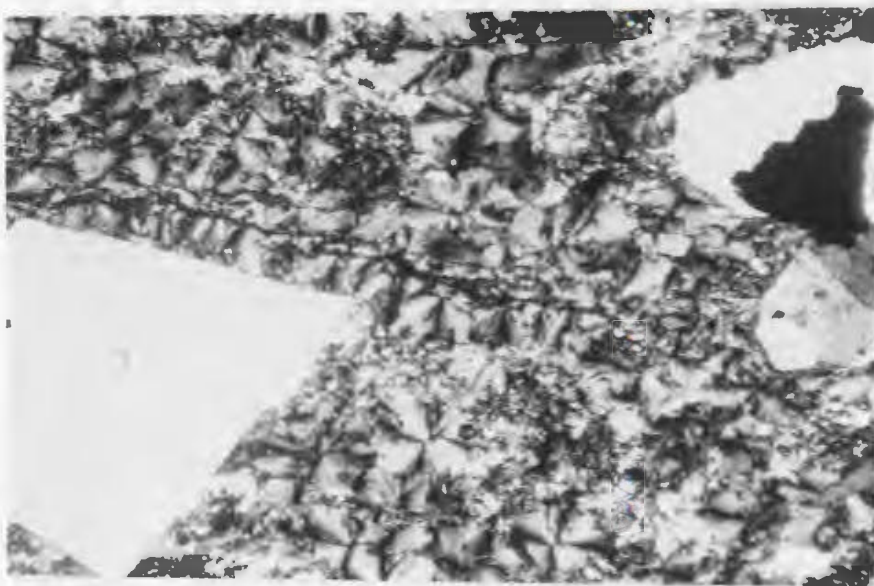
PLATE IV-5: Flow-banding in rhyolite. Plane polarised
light. X25.

devitrification rather than being of primary nature. Considerable recrystallisation of quartz has taken place in small vugs, with crystals up to 0.25 mm, considerably larger than the average in the matrix. Quartz sometimes appears to replace plagioclase and is also seen in fine-grained intergrowths with optically non-determinable feldspars. Haematite, magnetite and manganese oxide occur. Apatite, zircon and sphene have been seen. In many cases there has been a development of zoisite and sericite in the matrix, accentuating devitrification structures such as perlitic cracks. In rhyolites which are noticeably flow-banded, the lighter bands are seen to be made up of quartz alone, whilst the darker bands are formed by an intergrowth of quartz and feldspar (Plate IV-5). The quartz in the lighter bands is generally acicular with the long axis of the crystals perpendicular to the banding. Quartz and feldspar in radial growths form spherulites which occasionally reach considerable sizes (1-2 cm) and are easily recognisable in hand specimen (Plate IV-6).

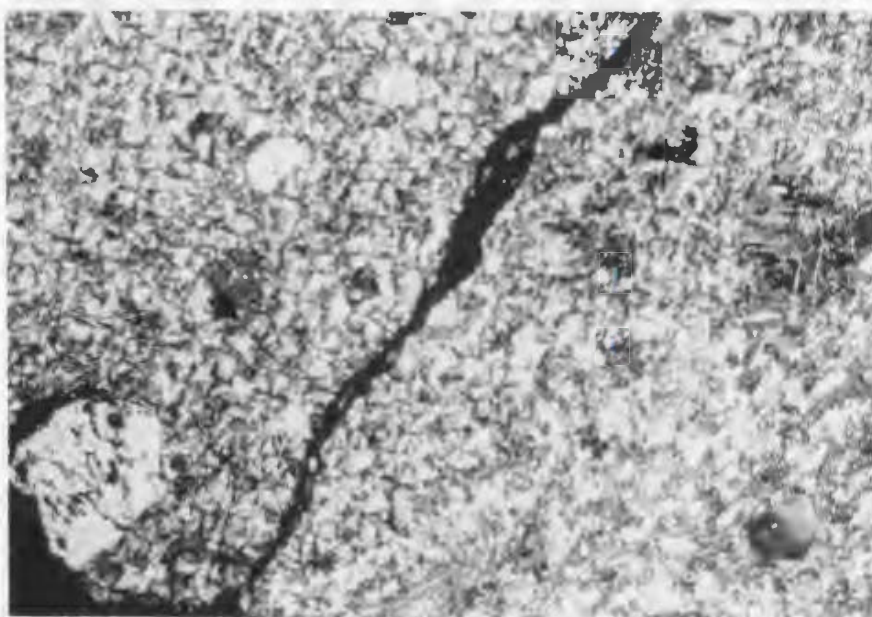
(ii) Rhyolites from the Doe Hills Area:

Phenocrysts:

Quartz phenocrysts occur as bipyramidal α - quartz paramorphs after β - quartz, showing rounding and embayment. Possible secondary growth has also been noted and the outer rims of some phenocrysts are often rich in inclusions, probably of glass. Broken and fractured phenocrysts are the result of structural deformation after consolidation of the lava. Associated with this deformation is the development of visible glide lamellae, a result of shearing within the crystal and



A



B

PLATE IV-4: Development of spherulites in Rhyolite Matrices.
 A: MB 117 x 40; B: MB 56 x 22.
 Both X-nicols.

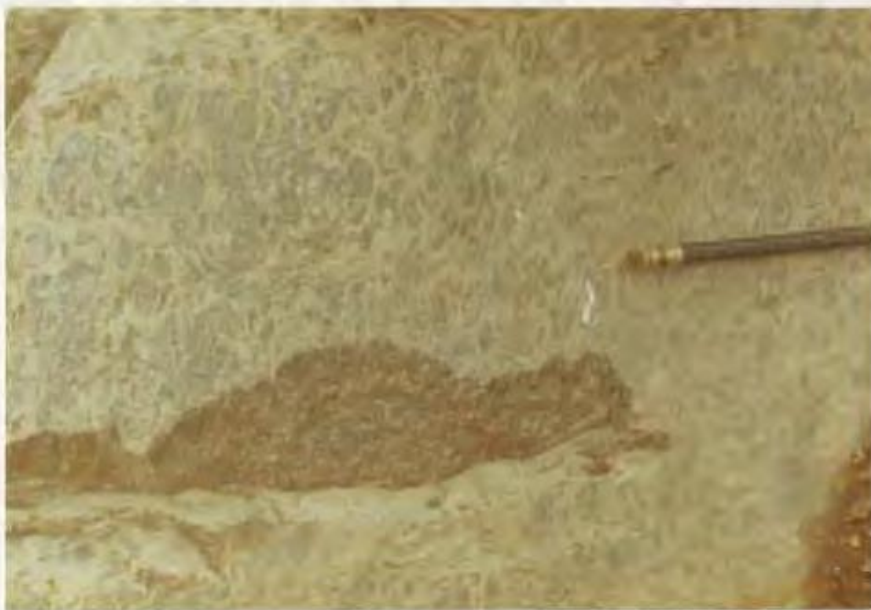


PLATE IV-6: Spherulites in rhyolite clearly visible in hand specimen (Serrated Hill region).



Glide lamellae developed in deformed quartz crystal. MJBb. X-nicols, X65.

correlatable with undulatory extinction patterns.

Plagioclase occurs in euhedral to subhedral crystals up to 1.5 mm, and where determinable by R. I. measurements has proved to be albite of composition averaging An_3 . These albite 'phenocrysts' are thus comparable with those observed in the Serrated Hill rhyolites but differ in that they show replacement by orthoclase-cryptoperthite (Tuttle, 1952). A complete series can be seen from the beginnings of potash-feldspar development in the albite, and replacement around margins and in cracks, until there results phenocrysts of turbid orthoclase (Plates IV-7, IV-8, IV-9). Staining with cobaltinitrite has confirmed that considerable amounts of plagioclase have been replaced by orthoclase and also a matrix rich in orthoclase. Some grains of orthoclase preserve the plagioclase multiple twinning, but generally the only sign of pre-existing plagioclase are small remnants of albite surrounded by potash-feldspar.

Groundmass:

Groundmass quartz and feldspar is microcrystalline and optically indeterminable. Groundmass alteration which varies widely in detail results in increased orthoclase and clinozoisite and sericite replacement. In originally glassy rocks, epidote development may accentuate perlitic cracks and flow banding. In many rocks, however, the distribution of the epidote does not appear to be controlled by any textural features apart from local concentration in or around pseudomorphed plagioclase phenocrysts. In advanced alteration the matrix may be composed entirely of quartz, epidote and sericite. Rarely piemontite is seen associated with opaque minerals.



PLATE IV-7: MBa. X-nicols X 35.



Replacement of
albite by
orthoclase,
rhyolites of Doe
Hills Area.

PLATE IV-8: MBJc. X-nicols X 37.



PLATE IV-9: MBJb. X-nicols X 27.

(B) RHYODACITES:

Light coloured, porphyritic rocks of quartz-latitude (rhyodacite) affinity are represented by specimens MB38, MB691, MB734, and MB608. These rocks generally contain microlites of plagioclase. MB38 and MB691 are both markedly flow-banded, and lines of spherulites of micrographic quartz and feldspar have been noted in thin sections. Average modes are presented in Table IV-B.

TABLE IV-B: Average modes of Rhyodacites.

<u>Average of 4 Measurements</u>			
Matrix	Albite Phenocrysts	Chlorite pseudomorphs after mafic phenoc.	Opagues
86%	9%	2%	3%

Phenocrysts:

High-quartz, albitised plagioclase and pseudomorphs after amphibole or clinopyroxene represent the phenocryst content of these rocks. Chlorite pseudomorphs after indeterminate pyroxene or amphibole are found in these rocks only, and form approximately twenty percent of the total phenocryst content. These pseudomorphs are often surrounded by concentrations of magnetite.

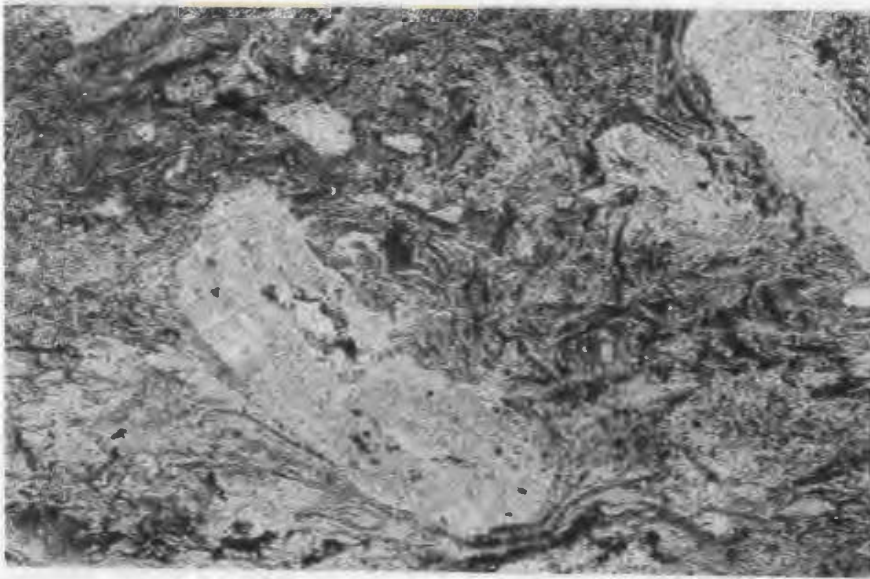


PLATE IV-10: Glass shards welded and bent around feldspar crystal in ignimbrite MB11. Plane polarised light X 37.

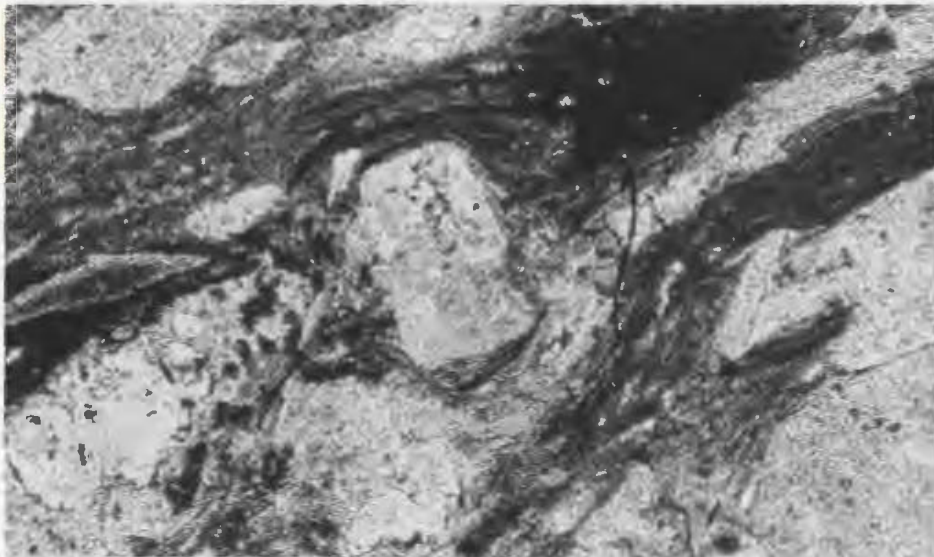


PLATE IV-11: Welded glass shards in ignimbrite MB910. Plane polarised light X 40.

Groundmass:

Microclites (albite where determinable) are common in the groundmass. The development of spherulites of micrographic quartz and feldspar represent stages in the devitrification of a glassy matrix. Perlitic cracks, accentuated by the development of epidote and chlorite, are recognisable. Common accessory minerals are magnetite, haematite, zircon, and sphene.

(C) IGNIMBRITES:

Although the ignimbrites in the Bull Arm Formation do not show the large variations in degree of welding and related textures described by Papezik (1969), Anderson (1970) and Green (1970), flattened and elongated pumice fragments are common as are lithic fragments and fiamme. A well-developed eutaxitic texture is generally preserved (Plates IV-10, IV-11).

Rock fragments range in size from 0.5 mm to several centimetres. They are mostly of acid volcanics but a few basic fragments have been observed (Plate IV-12). Some fragments, consisting of small tabular albite crystals randomly distributed in an opaque matrix, are not correlatable with any rock type seen in the area. The rock fragments form approximately 36% of the ignimbrites on average. This figure is high and may reflect the inclusion of air fall tuffs, partially welded by pneumatolysis, as ignimbrites.

The phenocrysts have the same general composition as those in the flows, i.e. albite and quartz, but are generally resorbed and shattered and account for about 20-25% of the rock. They range in size from 0.25 mm to 1.5 mm across. No potash feldspar phenocrysts have been recognised.

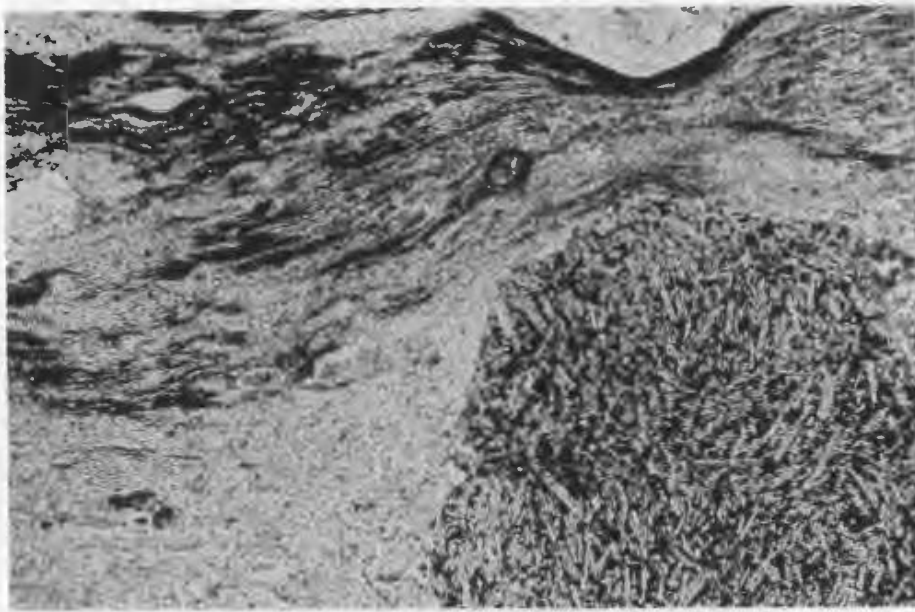


PLATE IV-12: Welded shards bent around basic fragment
in MB 910. X-nicols X 20.

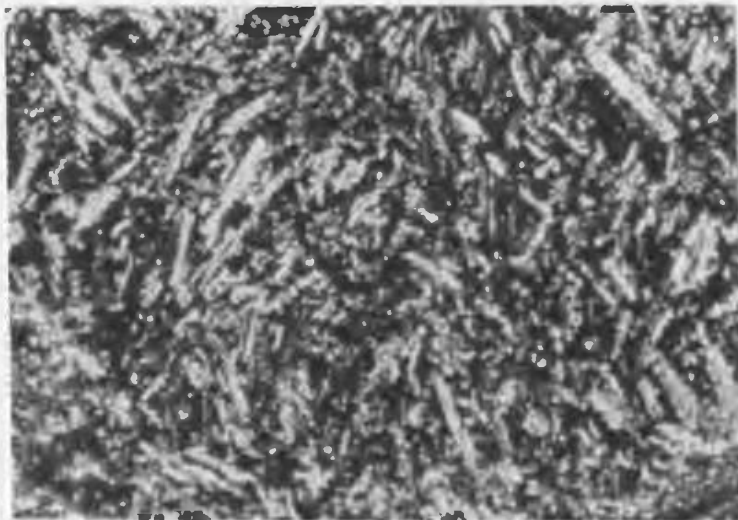


PLATE IV-13: Microlites of Plagioclase, probably albite
in basalt MB 676a. X-nicols X 60.

Rare ferromagnesian minerals, probably originally clinopyroxene, are pseudomorphosed by chlorite. Shards outlined by dusty haematite and leucoxene are recognisable, and are flattened around rock fragments and broken phenocrysts.

The matrix is conspicuously stained red by dusty haematite. Leucoxene, epidote, chlorite and sericite are also present. The groundmass feldspar and quartz are not determinable by optical methods.

TABLE IV-C: Average Modes of Ignimbrites.

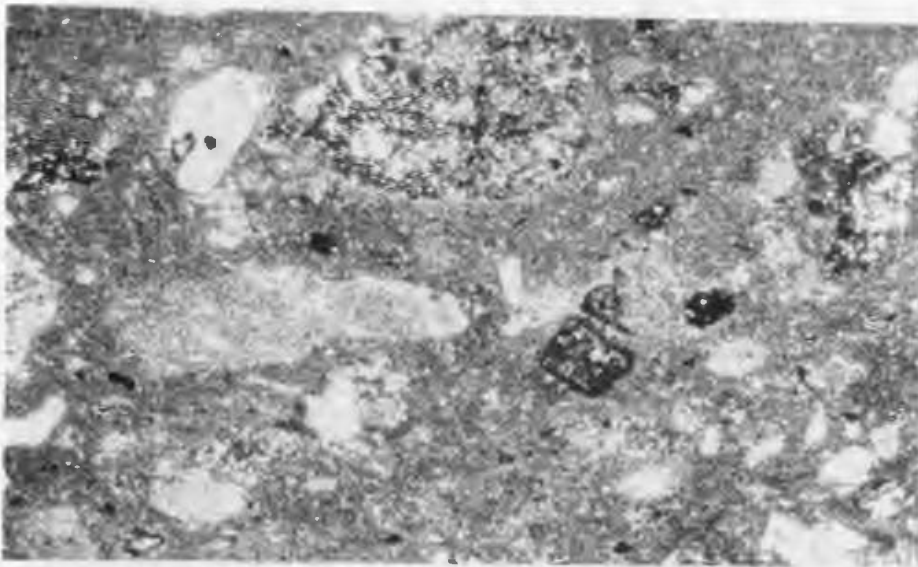
Average of 8 Measurements						
Matrix	Albite	Quartz	Rock Fragments		Pumice	Oxide
36%	16%	7%	8% Basic	28% Acid	2%	3%

(D) BASALTS:

The mafic flows are generally fine- to medium-grained aphyric rocks but may become quite coarse in patches. Sub-ophitic augite encloses laths of albite, often flow orientated. Magnetite, leucoxene and rare dusty glass have been observed. Chlorite and epidote are commonly present as alteration products. The mineralogy and petrography of the basic rocks is more aptly described as spilitic than basaltic (Plate IV-13).



A



B.

PLATE IV-14: Lithic Tuffs.

A: X-nicols X 30. Note basalt fragment.

B: Plane polarised light X 20.

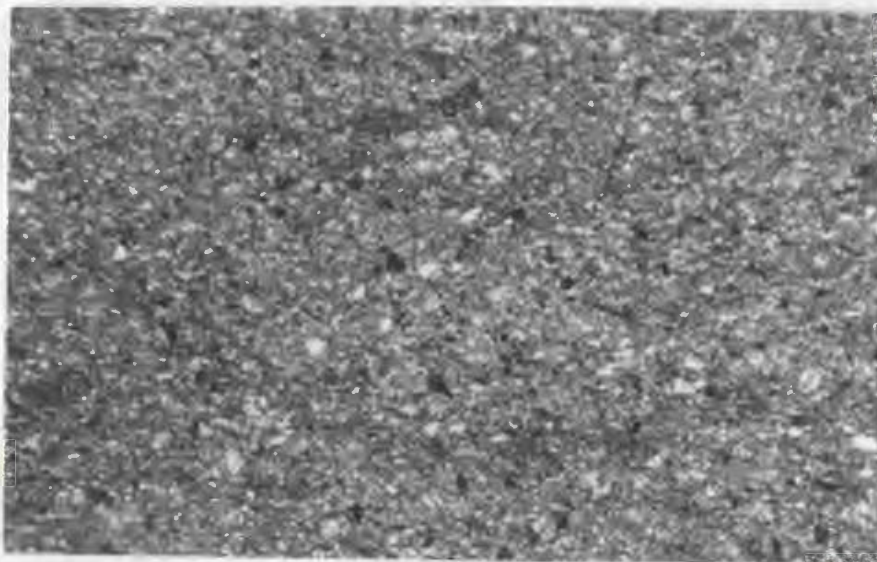
(E) TUFFS:

The tuffs range from fine-grained, often porcellanous rocks to rocks with arkosic texture and composition. Rock fragments are more common in the coarser varieties and single broken crystals in the finer varieties (Plates IV-14, IV-15).

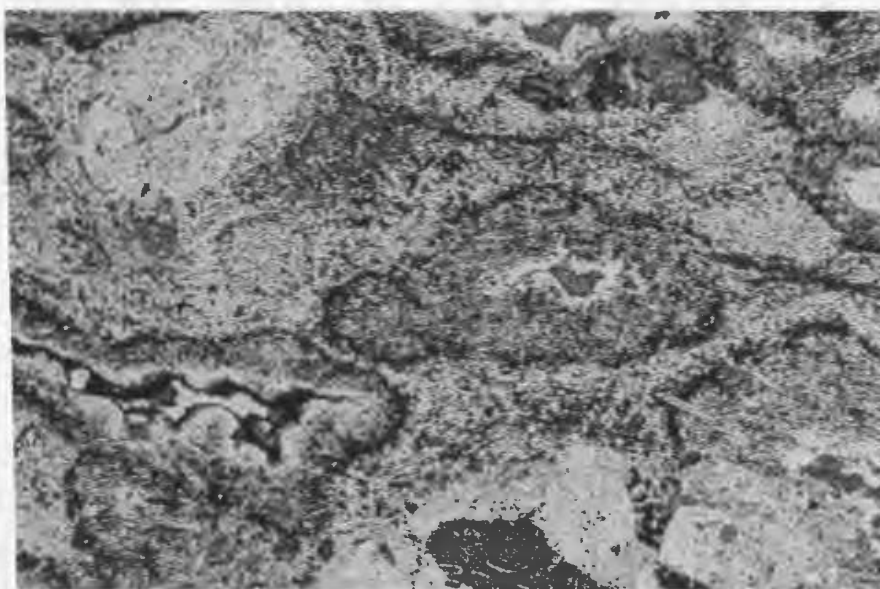
Crystals represented in the crystal tuffs resemble phenocrysts in the acid extrusives. The feldspars consist of albite crystals and turbid untwinned orthoclase, often retaining albite inclusions. The latter are most common in highly sheared tuffs collected in the Doe Hills area. Quartz is present as subangular to subrounded crystals which show both embayment and fracturing.

In the lithic tuffs, rock fragments vary from those of flow-banded rhyolites and basalts to sediments. Fragments of intermediate composition are lacking. Fragments are generally rounded, possibly as a result of reworking by water, as also indicated by fine scale cross-bedding accentuated by opaque minerals in the finer tuffs. Considerable groundmass recrystallisation is visible in the tuffs, with development of sericite and epidote (Plate IV-16). Sericite augens both rock fragments and crystals and picks out the major schistosity. Epidote imparts a green colour to the tuffs in the Doe Hills area where it is best developed. Prehnite and piemontite have been recognised.

Average modes are given in Table IV-D for two major grain-size classifications, excluding the extremely fine-grained rocks which are composed almost entirely of quartz, feldspar, epidote and sericite.



A



B

PLATE IV-15: Crystal Tuffs.

A: Fine-grained tuff, partly silicified.
X-nicols X 15.

B: Patchy alteration of fine tuff to chlorite/
epidote/quartz. Plane polarised light X 15.

TABLE IV-D: Average Modes for Tuffs.

Crystal Tuffs:			Average of 6 Measurements			
Matrix	Albite	K feld. (Sericitised)	Qtz.	Rock Frag.	Ep.	Opaques
63%	7%	4%	8%	5%	10%	3%
Lithic Tuffs:			Average of 4 Measurements			
Matrix	Albite	K feld. (Sericitised)	Qtz.	Rock Frag.	Ep.	Opaques
49%	7%	3%	6%	25%	8%	2%

K feld.: Potassium Feldspar; Qtz: Quartz; Rock Frag: Rock Fragments;
Ep: Epidote.

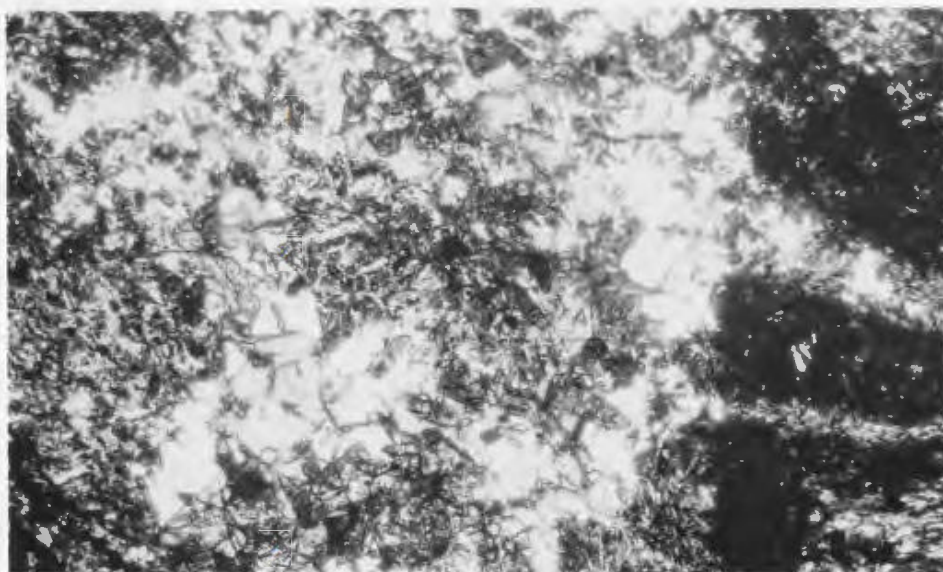


PLATE IV-16: Epidote (white) development in lithic tuff. X-nicols X 35.

CHAPTER V

PETROCHEMISTRY

Analyses of 41 specimens for major oxides and four significant trace elements are presented in Tables VA - VF. A further eleven specimens of rhyolites from the Doe Hills area have been analysed for K_2O , Na_2O , CaO , Rb and Sr. Sample locations are shown in Figure V-1. Chemical analyses and C.I.P.W. norms are presented for all specimens in Tables VA - VF.

A frequency distribution diagram (Fig. V-2) of the 41 analysed specimens which form a representative sampling of the area, shows an essentially bimodal distribution.

Major element oxides and trace elements have been plotted against SiO_2 in Figures V-3 and V-4, in an attempt to compare element abundances and possible trends, but the scarcity of intermediate rock types has reduced the significance of any petrogenetic interpretation from these Harker diagrams.

The analysed rhyolitic rocks fall into two natural divisions, here called Groups I and II, on the basis of geographic location, mineralogy (see Chapter IV) and petrochemistry. Group I, comprised of five specimens of flow breccia and three of ignimbrites from the Serrated Hill region (Fig. V-1), are the least altered of the rhyolitic rocks. Group II rocks, all of which are flow-breccias, were collected from the Doe Hills area, and show plagioclase replacement by K-feldspar.

Group I rhyolites and ignimbrites:

Chemical variations within this group are shown in the variation

TABLE V-A: Group I Rhyolites: Flows and Ignimbrites.

Specimen No.	MB910	MB69	MB100	MB58	MB117	MB11	MB56	MB68
SiO ₂ %	65.4	66.1	69.3	69.3	69.5	71.0	71.2	79.7
Al ₂ O ₃ %	14.6	16.6	15.0	13.7	14.8	13.3	13.6	8.9
ΣFe ₂ O ₃ %	4.10	1.75	1.85	2.70	1.20	2.40	1.80	1.05
CaO %	0.95	0.45	0.30	1.40	0.40	1.05	0.15	0.53
Na ₂ O %	5.05	7.50	4.33	5.12	4.20	5.09	4.58	3.15
K ₂ O %	4.59	2.35	4.33	5.00	4.05	4.30	4.30	3.05
MgO %	0.69	0.10	0.41	0.15	0.20	0.20	0.17	0.05
MnO %	0.10	0.05	0.05	0.11	0.02	0.13	0.03	0.02
TiO ₂ %	0.70	0.15	0.14	0.35	0.30	0.30	0.36	0.10
P ₂ O ₅ %	0.08	0.07	0.03	0.01	0.01	0.08	0.02	0.05
Ignition %	1.83	4.42	3.61	1.97	4.39	2.01	3.92	3.37
TOTAL	99.09	99.54	99.35	99.81	98.07	99.86	100.13	99.97
Rb ppm	160	72	185	140	150	123	170	75
Sr ppm	110	85	70	410	280	350	57	132
Ba ppm	2105	790	1130	2380	2030	1860	1520	1520
Zr ppm	321	365	215	285	255	270	215	155
Rb/Sr	1.45	0.85	2.64	0.34	0.54	0.35	2.98	0.57
<u>C. I. P. W. NORMS</u>								
q	15.8	12.8	27.2	18.7	29.9	25.5	28.5	50.4
or	28.2	14.6	26.8	30.2	25.3	26.0	26.4	18.7
ab	44.4	66.7	38.3	43.5	37.5	44.0	40.3	27.6
an	3.7	1.9	1.3	--	2.0	0.8	0.6	1.2
ag	0.5	--	--	3.1	--	2.9	--	0.9
hy	2.7	1.1	1.8	--	0.7	--	0.8	--
il	1.4	0.3	0.3	0.7	0.6	0.6	0.7	0.2
ap	0.2	0.2	0.07	0.02	0.03	0.19	0.05	0.12
ru	--	--	--	--	--	--	--	--
c	--	1.1	2.8	--	2.9	--	1.2	--
ac	--	--	--	0.6	--	--	--	--
mt	3.1	1.3	1.4	1.7	0.9	1.8	1.4	0.8
TOTALS	100.00	100.00	99.97	98.52	99.83	101.79	99.95	99.92

For the calculation of C.I.P.W. norms: Fe₂O₃ was estimated at 50% of ΣFe₂O₃
FeO was estimated at 50% of ΣFe₂O₃

ΣFe₂O₃ = Total iron measured as Fe₂O₃

TABLE V-B: Group II Rhyolites: Quartz Phenocryst-bearing Flows.

Specimen No.	MBJd	MBJc	MBJg	MBJe	MB171	MB762	MBJb	MBJa
SiO ₂ %	75.4	67.3	76.0	72.2	74.9	69.6	77.1	62.9
Al ₂ O ₃ %	12.4	16.0	9.6	11.8	11.4	14.8	10.1	17.5
Σ Fe ₂ O ₃ %	1.80	2.80	1.69	1.90	1.40	1.80	1.25	1.90
CaO %	0.20	1.71	0.30	0.15	0.32	0.25	0.15	1.65
Na ₂ O %	4.83	0.92	1.49	3.70	3.45	3.97	0.23	4.81
K ₂ O %	3.15	4.95	7.05	4.80	5.80	7.05	7.43	5.50
MgO %	0.03	1.34	--	0.03	0.05	0.08	0.09	0.22
MnO %	0.01	0.08	0.01	0.02	0.02	0.03	0.03	0.01
TiO ₂ %	--	0.25	0.03	--	0.20	--	--	--
P ₂ O ₅ %	0.04	0.06	0.03	0.03	0.02	0.04	0.04	0.03
Ignition %	1.65	2.74	3.61	3.47	2.32	1.40	3.32	4.78
TOTAL	99.51	98.15	99.81	98.10	99.88	99.00	99.71	99.30
Rb ppm	110	160	240	173	115	235	272	190
Sr ppm	45	250	35	55	70	25	45	100
Ba ppm	375	550	800	4310	2330	1000	1320	820
Zr ppm	340	335	270	295	200	300	250	265
Rb/Sr	2.44	0.64	6.86	3.15	1.64	9.4	6.04	1.9
C. I. P. W. NORMS								
q	35.2	38.7	41.5	33.3	33.4	18.9	48.4	10.2
or	19.0	30.7	43.3	30.0	35.2	42.7	45.6	34.4
ab	41.8	8.2	10.5	33.1	27.0	34.4	2.0	43.1
an	0.7	8.5	--	0.6	--	1.0	0.5	8.5
ag	--	--	1.2	--	1.3	--	--	--
hy	1.0	4.7	0.9	1.1	0.5	1.2	0.9	1.6
il	--	0.5	0.6	--	0.4	--	--	--
ap	0.10	0.15	0.07	0.07	0.05	0.10	0.10	0.07
ru	--	--	--	--	--	--	--	--
c	0.8	6.5	--	0.3	--	0.3	1.6	0.7
ac	--	--	2.3	--	2.1	--	--	--
mt	1.3	2.1	0.1	1.5	--	1.34	1.0	1.46
TOTAL	99.90	100.05	100.47	99.97	99.95	99.94	100.10	100.03

For the calculation of C.I.P.W. norms: Fe₂O₃ was estimated at 50% of Σ Fe₂O₃

FeO was estimated at 50% of Σ Fe₂O₃

Σ Fe₂O₃ = Total iron measured as Fe₂O₃

TABLE V-B (cont'd): Group II Supplementary Partial Analyses.

Specimen No.	H35	MBc	H38	MBb	MBd	H32
CaO	0.77	0.87	0.17	1.90	1.64	0.78
Na ₂ O	2.13	4.10	5.10	0.45	0.25	0.48
K ₂ O	5.26	5.35	3.70	6.60	7.25	7.61
Rb	184	76	84	197	197	202
Sr	145	61	53	409	471	122
Rb/Sr	1.27	1.25	1.58	0.48	0.42	1.66
Specimen No.	MBa	H27	H28	MBe	H29	
CaO	1.72	0.33	0.37	2.91	10.40	
Na ₂ O	0.81	0.31	0.05	0.11	0.59	
K ₂ O	7.65	7.75	9.21	10.62	2.23	
Rb	206	222	220	478	64	
Sr	369	100	74	203	1478	
Rb/Sr	0.56	2.22	2.97	2.35	0.04	

TABLE V-C: Rhyodacite. Flows.

Specimen No.	MB691	MB38	MB608	MB734
SiO ₂ %	67.3	69.2	70.8	77.5
Al ₂ O ₃ %	15.1	13.9	12.5	12.6
Σ Fe ₂ O ₃ %	3.30	3.45	3.15	2.52
CaO %	5.42	0.58	0.35	0.54
Na ₂ O %	4.50	5.41	5.00	4.55
K ₂ O %	1.85	4.15	3.29	2.45
MgO %	0.26	0.51	0.20	0.22
MnO %	0.10	0.09	0.06	0.05
TiO ₂ %	0.55	0.25	0.08	--
P ₂ O ₅ %	0.08	0.01	0.01	0.22
Ignition %	1.22	1.39	3.76	0.38
TOTAL	99.68	98.94	99.20	100.03
Rb ppm	30	175	100	100
Sr ppm	740	100	49	160
Ba ppm	0	1980	960	595
Zr ppm	143	180	895	335
Rb/Sr	0.04	1.75	2.04	0.63

C. I. P. W. NORMS

q	24.6	19.9	28.7	39.9
or	11.1	25.2	20.4	14.4
ab	38.7	47.0	44.3	38.2
an	15.8	1.4	1.8	1.2
ag	3.1	1.2	--	--
hy	--	2.2	2.1	1.9
il	1.1	0.5	0.2	--
ap	0.2	0.02	0.02	0.5
ru	--	--	--	--
c	--	--	0.1	2.0
ac	--	--	--	--
mt	2.4	2.6	2.4	1.8
TOTALS	97.0	100.02	100.02	99.9

For the calculation of C.I.P.W. norms: Fe₂O₃ was estimated at 50% of Σ Fe₂O₃

FeO was estimated at 50% of Σ Fe₂O₃

Σ Fe₂O₃ = Total iron measured as Fe₂O₃

TABLE V-D: Basalts: Flows from Doe Hills Area.

Specimen No.	MB856	MB676A	MB852	MB787	MB880
SiO ₂ %	46.8	49.3	49.6	50.0	51.5
Al ₂ O ₃ %	14.3	14.6	13.6	11.4	14.5
Σ Fe ₂ O ₃ %	12.80	12.81	13.40	9.90	11.80
CaO %	6.82	4.75	6.08	9.41	4.28
Na ₂ O %	3.50	5.43	4.30	4.13	5.35
K ₂ O %	2.80	1.41	0.53	0.35	0.30
MgO %	5.63	5.43	5.82	5.98	5.27
MnO %	0.26	0.27	0.24	0.34	0.31
TiO ₂ %	2.25	1.30	2.18	4.35	1.75
P ₂ O ₅ %	0.00	0.02	0.00	0.03	0.02
Ignition %	4.99	3.88	4.98	2.80	3.75
TOTAL	100.23	99.20	100.73	98.69	98.83
Rb ppm	65	9	30	10	25
Sr ppm	180	130	265	75	100
Ba ppm	1380	250	870	150	250
Zr ppm	108	128	120	138	148
Rb/Sr	0.36	0.07	0.11	0.13	0.05

C. I. P. W. NORMS

q	--	--	--	--	--
or	1.9	2.2	3.3	8.75	17.4
ab	47.6	36.4	38.0	37.6	20.2
an	15.4	12.0	16.9	11.9	15.8
ag	5.6	29.5	12.1	10.6	16.4
hy	13.7	8.1	10.9	--	--
fo	4.4	0.5	5.2	8.3	7.7
fa	5.6	0.6	6.9	12.1	9.8
mt	2.3	2.3	2.3	2.8	2.3
il	3.5	8.6	4.3	2.6	4.5
ap	0.05	0.07	--	0.05	--
ne	--	--	--	5.7	5.9
TOTALS	101.65	100.27	99.90	100.40	100.00

For the calculation of C.I.P.W. norms: Fe₂O₃ was taken as 2%

$$\text{FeO} = \sum \text{Fe}_2\text{O}_3 - 2\%$$

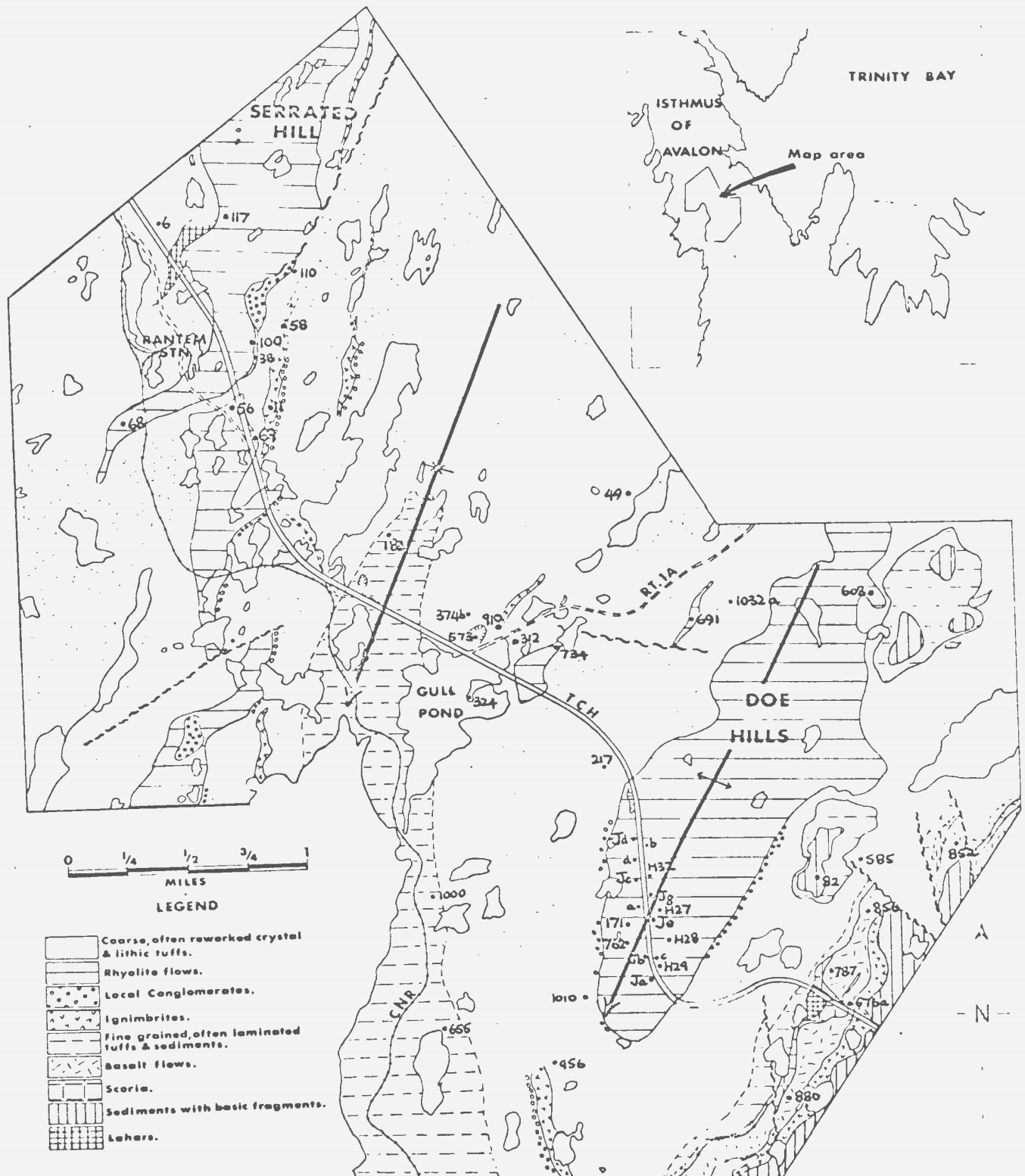
TABLE V-E: Tuffs.

Specimen No.	MB578	MB585	MB655	MB956	MB1010	MB217
SiO ₂ %	79.3	69.5	65.5	66.7	60.7	65.9
Al ₂ O ₃ %	9.8	13.9	16.6	13.9	18.2	14.0
Σ Fe ₂ O ₃ %	2.31	3.30	3.40	5.09	3.45	4.15
CaO %	1.84	1.93	4.21	1.48	0.90	3.14
Na ₂ O %	3.81	3.39	2.35	5.37	1.63	2.35
K ₂ O %	0.86	3.15	3.60	2.30	10.13	3.49
MgO %	0.57	1.25	0.90	0.45	0.96	0.89
MnO %	0.14	0.15	0.10	0.09	0.06	0.10
TiO ₂ %	0.15	0.40	0.15	0.80	0.55	0.30
P ₂ O ₅ %	0.05	0.16	0.03	0.12	0.10	0.22
Ignition%	0.78	1.73	2.00	2.81	1.77	4.17
TOTAL	99.61	98.86	98.84	99.11	98.40	98.71
Rb/Sr	0.05	0.08	0.18	0.35	3.32	0.13
Rb ppm	17	135	210	60	465	215
Sr ppm	320	1720	1175	170	140	1675
Ba ppm	340	2080	1510	650	3350	1700
Zn ppm	280	405	210	294	390	315

Specimen No.	MB1032a	MB374b	MB312	MB49	MB324	MB1000	MB6
SiO ₂ %	66.1	64.8	68.4	67.5	65.5	68.7	68.5
Al ₂ O ₃ %	14.8	14.4	13.8	16.2	15.9	13.2	12.8
Fe ₂ O ₃ %	3.50	3.00	2.15	1.66	3.15	3.80	3.60
CaO %	5.12	5.08	3.25	2.85	3.95	0.75	2.30
Na ₂ O %	3.30	3.33	1.89	2.87	3.53	5.09	3.25
K ₂ O %	2.35	2.95	3.04	4.65	3.05	4.23	3.40
MgO %	0.67	0.59	0.94	0.40	0.61	0.45	1.55
MnO %	0.10	0.11	0.09	0.14	0.07	0.08	0.18
TiO ₂ %	0.25	0.34	0.25	0.25	0.15	0.75	0.57
P ₂ O ₅ %	0.17	0.06	0.21	0.03	0.01	0.02	0.00
Ignition %	3.31	4.00	4.94	3.76	3.12	2.79	4.41
TOTAL	99.67	98.56	100.65	100.31	99.04	99.86	100.56
Rb ppm	65	145	170	245	105	108	160
Sr ppm	730	215	1035	305	410	150	500
Ba ppm	1175	1660	1755	3225	775	1570	945
Zn ppm	339	250	260	285	155	355	225
Rb/Sr	0.09	0.67	0.16	0.80	0.26	0.72	0.32

TABLE V-F: Sediments.

Specimen No.	MB82	MB110	MB183
SiO ₂ %	57.3	64.0	66.0
Al ₂ O ₃ %	17.5	14.7	13.9
Σ Fe ₂ O ₃ %	9.40	5.20	4.00
CaO %	7.72	2.79	3.03
Na ₂ O %	4.43	4.00	4.50
K ₂ O %	0.75	2.13	2.20
MgO %	1.93	0.92	0.71
MnO %	0.20	0.13	0.11
TiO ₂ %	1.10	0.57	0.50
P ₂ O ₅ %	0.01	0.02	0.02
Ignition %	0.62	4.56	4.21
TOTAL	100.96	99.02	99.18
Rb ppm	25	135	60
Sr	435	300	370
Ba	670	610	960
Zr	121	117	254
Rb/Sr	0.06	0.45	0.16



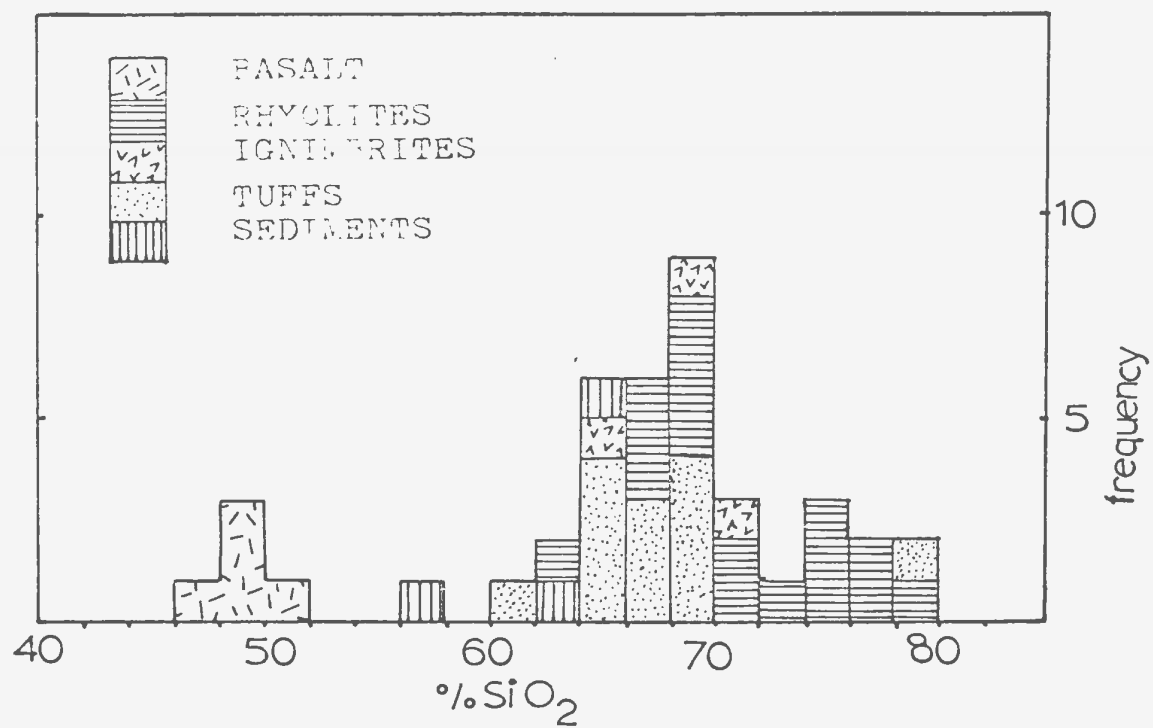


Figure V-2: Frequency distribution of the analysed rock samples from the Bull Arm Formation.

diagrams of Figures V-3, V-4, and V-5. Most oxide concentrations are fairly uniform. SiO_2 varies between 65.4% and 79.7%. Al_2O_3 varies between 13.6% and 16.6%. Specimen MB68 shows degrees of secondary silicification with recrystallisation in some quartz filled vugs and has a high $\text{SiO}_2/\text{Al}_2\text{O}_3$ ratio. It was therefore not included when drawing lines of variation. CaO is low in all specimens of Group I (average 0.371) and together with CaO/AlK ratios (average .076) possibly suggest an alkaline affinity.

All rocks of Group I have an alkaline affinity according to Wright's (1969) alkalinity index (Figure V-6). All rocks of Group I plot on the albite side of the low temperature trough on Tuttle and Bowen's (1958) quartz, albite, orthoclase diagram (Figure V-7). They are markedly more sodic than Nockold's (1954) average alkali rhyolite, the higher $\text{Na}_2\text{O} / \text{K}_2\text{O}$ ratio being reflected in albite 'phenocrysts'.

The ignimbrites, MB11, MB58, MB910, show a higher total iron content than the rhyolites. This may possibly reflect the presence of basic rock fragments which have been noted in all three ignimbrite flows.

Trace elements have also been plotted against the differentiation index used by Nockolds and Allen (1953) on Figure V-8. Although Nockolds and Allen (1953, 1954) report a negative correlation between barium content and the differentiation index in most rhyolites, the opposite appears to be true of these rocks. A positive correlation is noted between Ba and K, and the K/Ba ratio ^{declines} ~~rises~~ from 30 to 14 in the more potash rich rocks (Figure V-9). This dependency may reflect the positive correlation observed between K and Ba in early formed potash rich crystals (Mason,

Figure V-3 Major elements vs. SiO_2

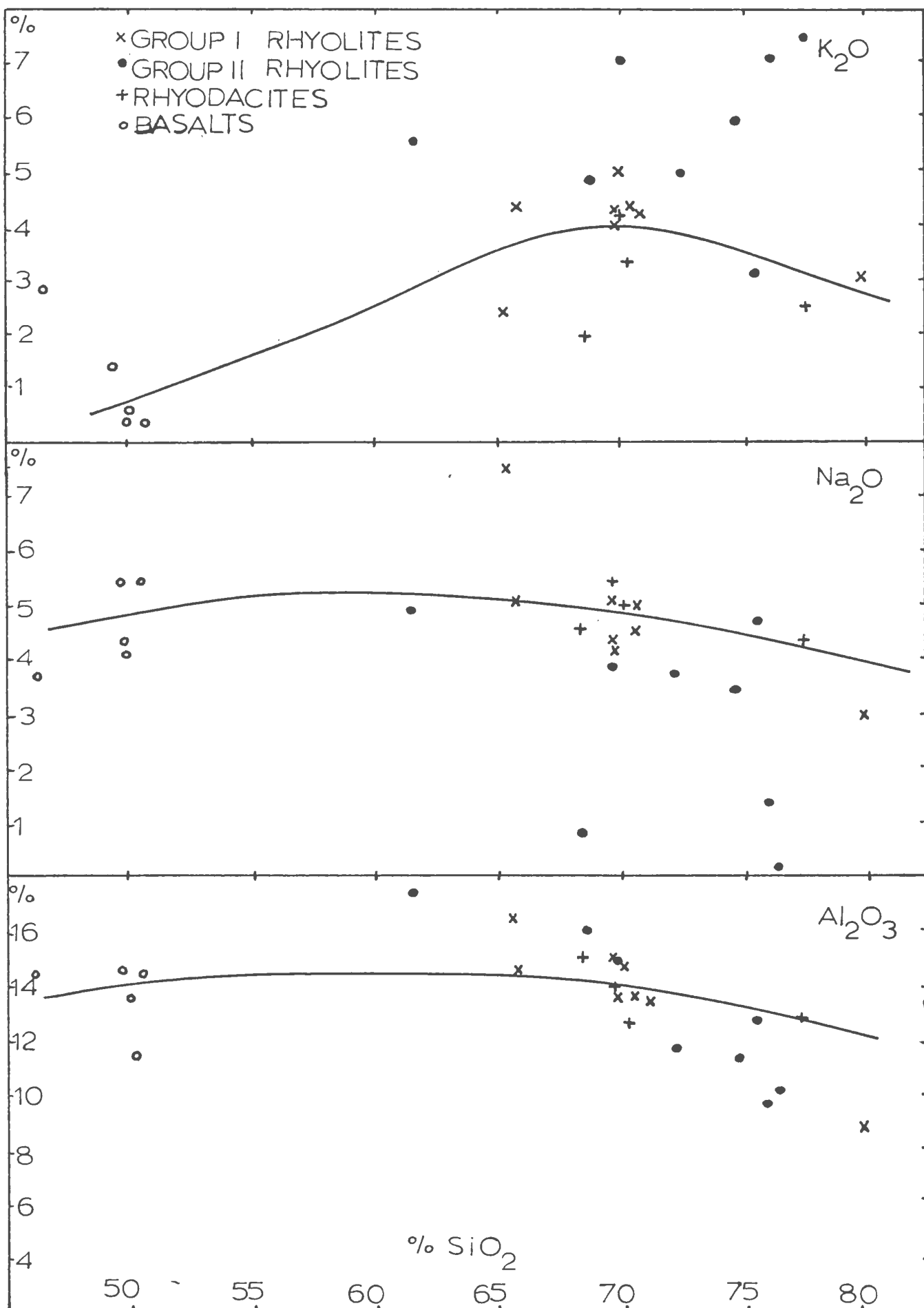


Figure V-4 Major Elements vs. SiO_2

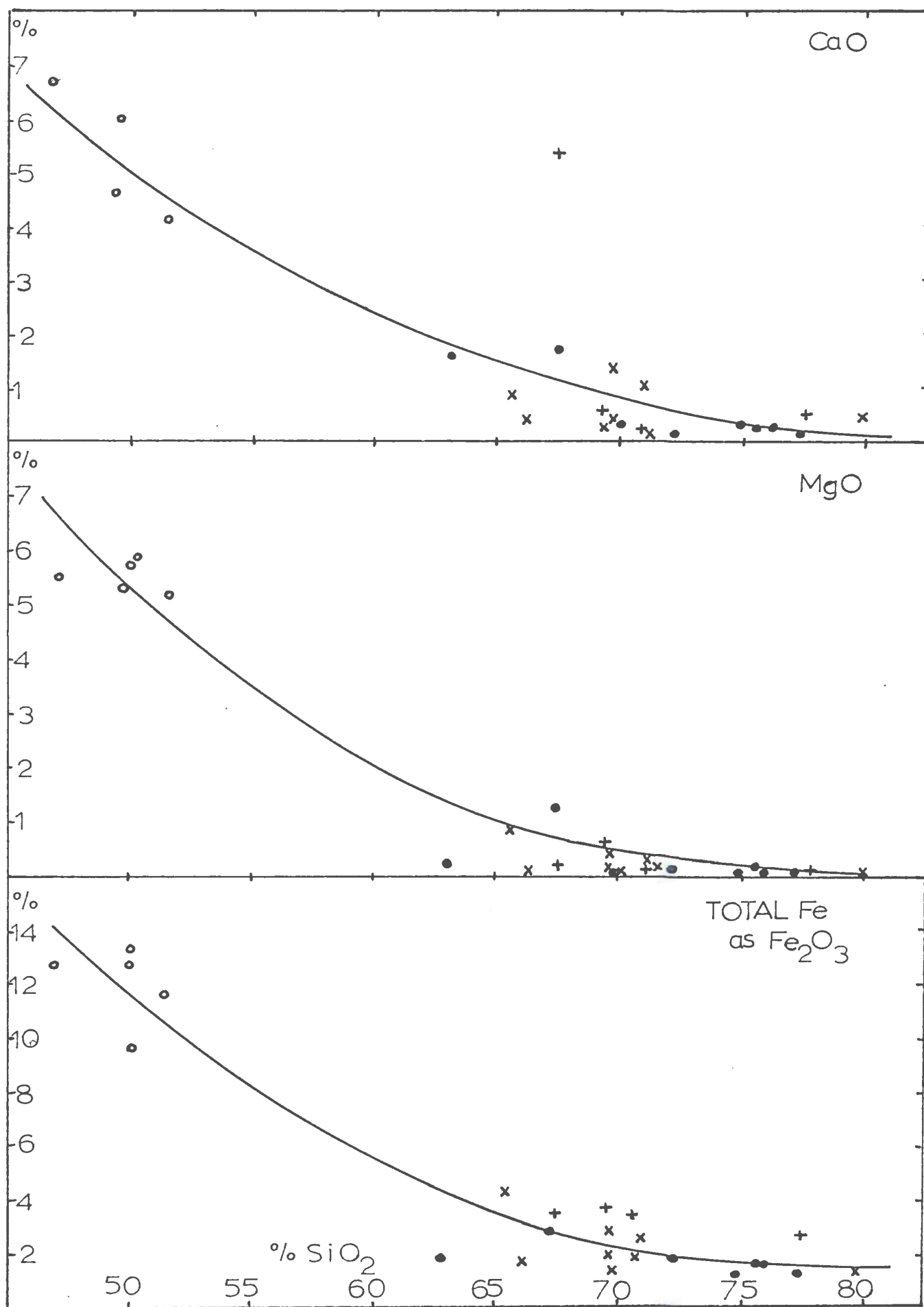
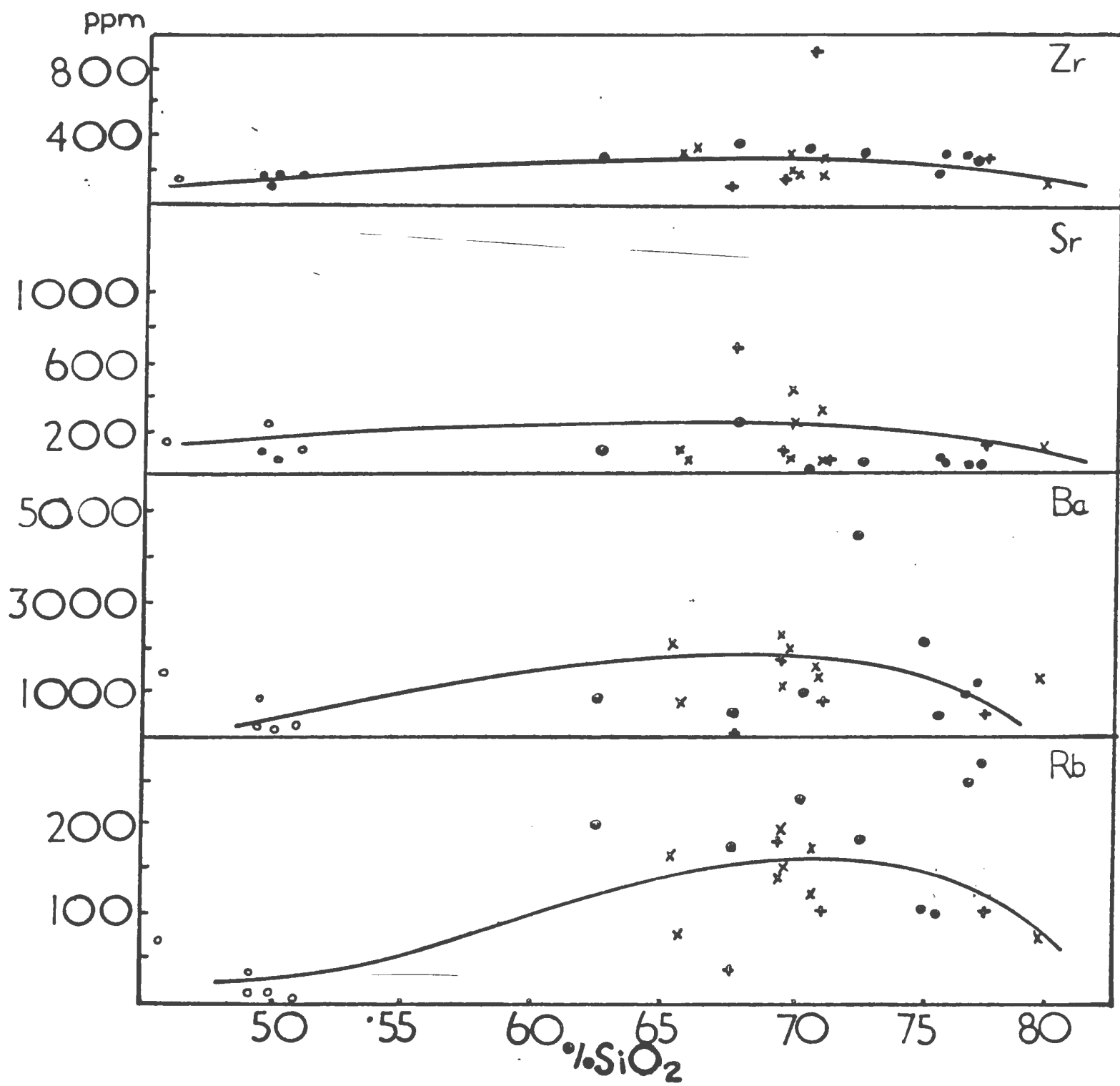


Fig. V-5: Trace Elements vs. SiO_2 . Symbols as Fig. V-3.



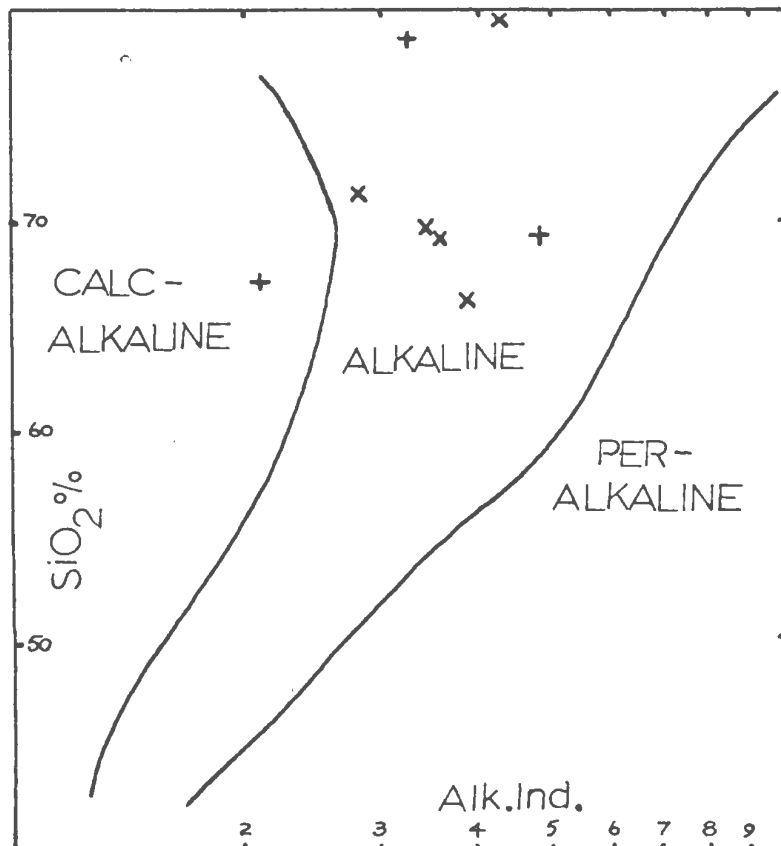


Figure V-6: Alkalinity Index (Wright '69)

vs. SiO₂.

Alk. Ind.=

$$\frac{\text{CaO} + \text{Al}_2\text{O}_3 + \text{Total Alks.}}{\text{CaO} + \text{Al}_2\text{O}_3 - \text{Total Alks.}}$$

Group I rhyolites x

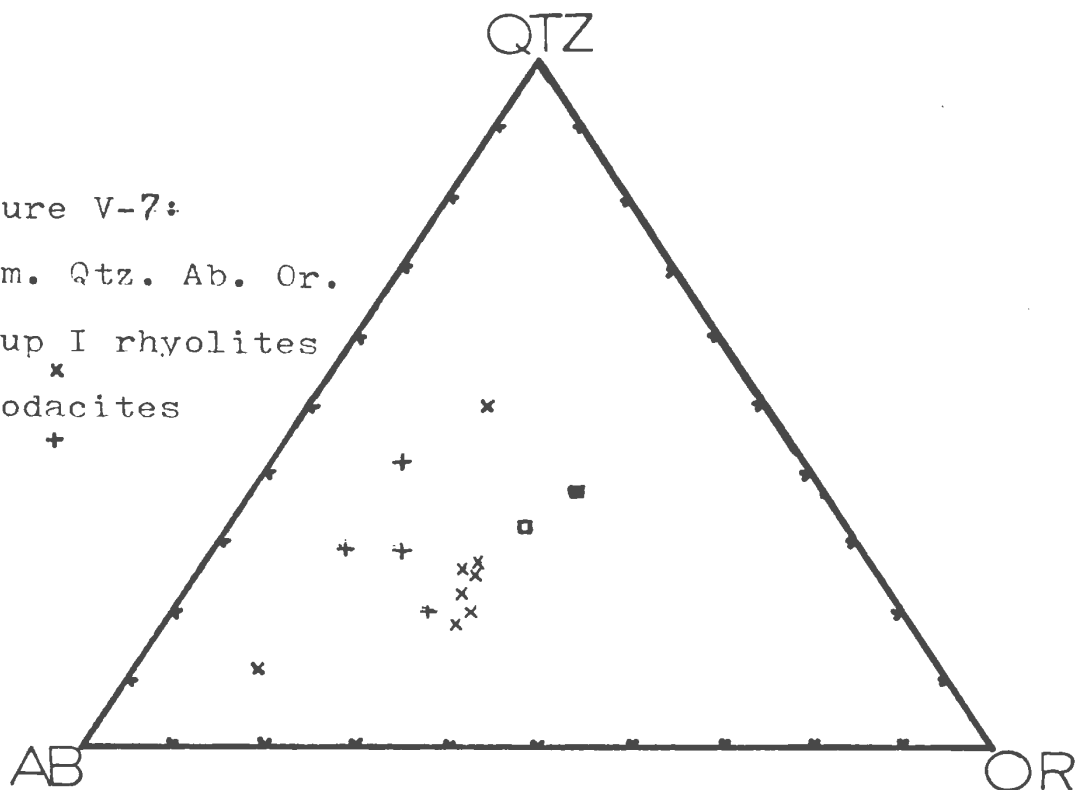
Rhyodacites +

Figure V-7:

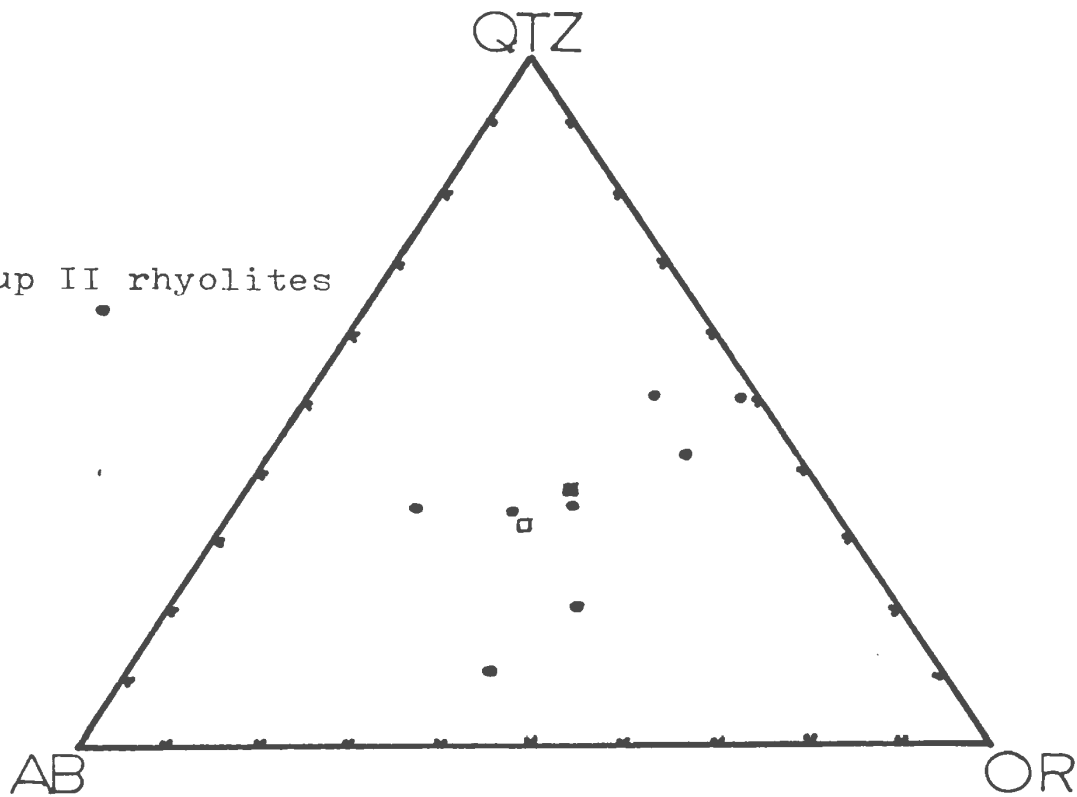
Norm. Qtz. Ab. Or.

Group I rhyolites

Rhyodacites



Group II rhyolites



Average calc-alkali rhyolite ■

Average alkali rhyolite □

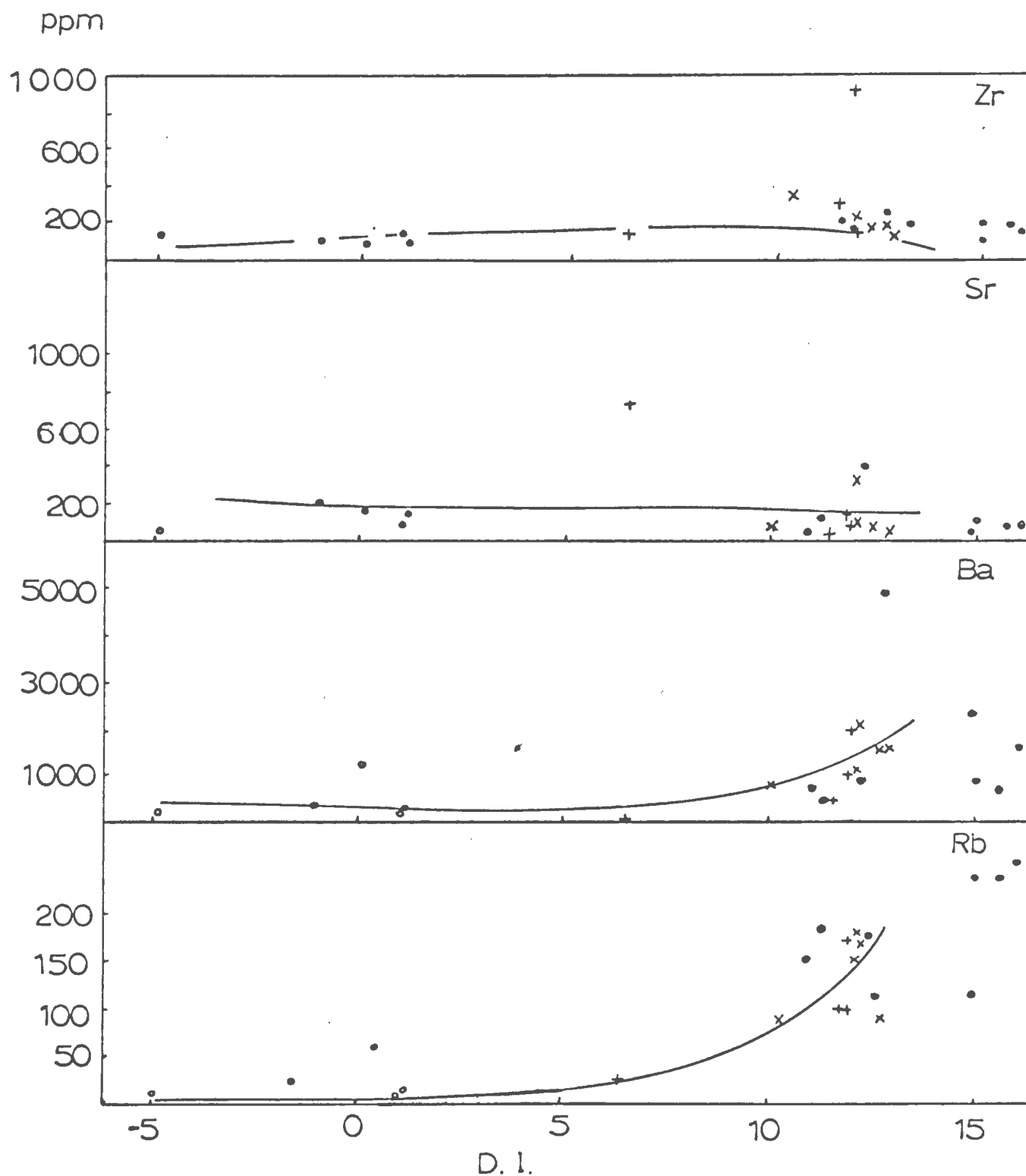


Fig.V-8: Trace element variation (ppm) with differentiation index.
 Basalts • , Rhyodacites + , Group I rhyolites, x
 Group II rhyolites • .

$$D.I. = (1/3 Si + K) - (Ca + Mg)$$

1966, p. 134). Rubidium and strontium values are variable. Rb ranges between 72 ppm and 185 ppm and averages about 130 ppm. Figure V-9 shows a poor positive correlation between K and Rb. The K/Rb ratio ranges between 400 and 150, and straddles the averages of 200 and 180 for alkaline and calc-alkaline rocks respectively, indicated by Nockolds and Allen (1953, 1954). Nockolds and Allen point out, however, that in more potassium rich calc-alkaline acid rocks, such as found at Crater Lake and in the Lesser Antilles, K/Rb ratios may be as high as 400.

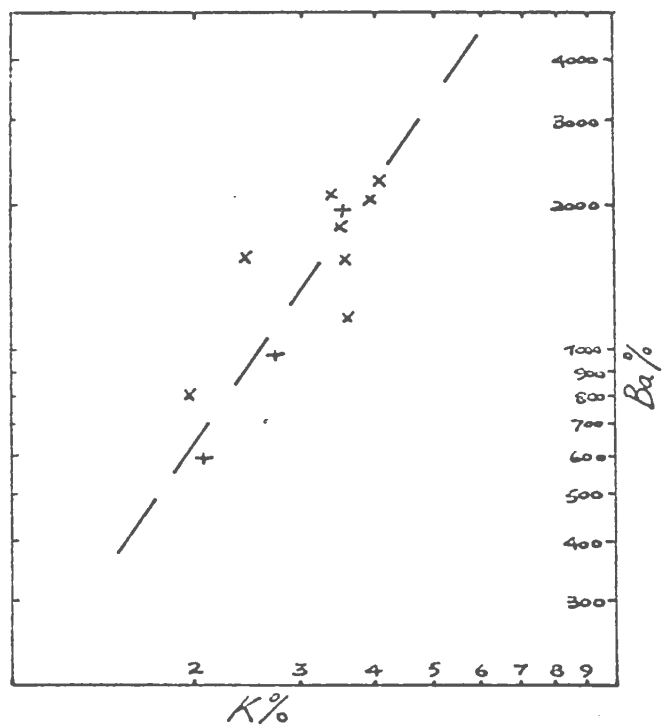
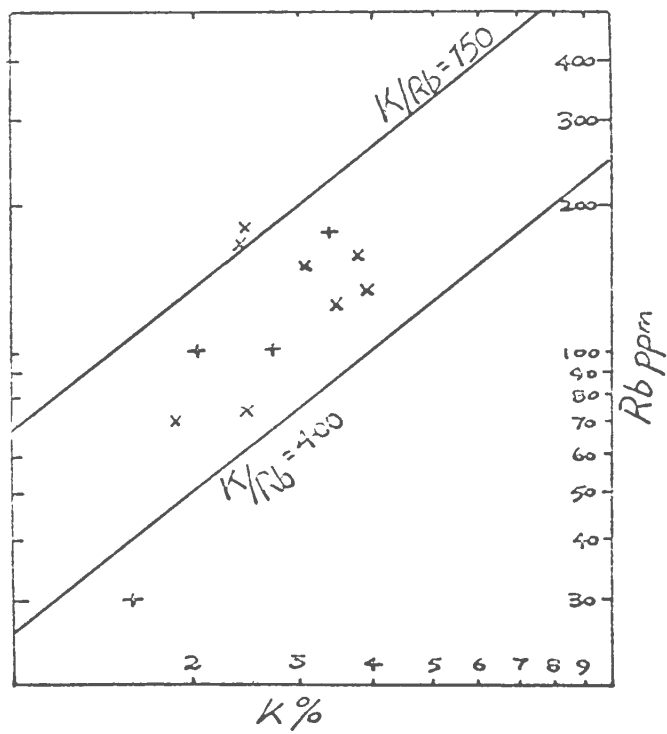
Strontium shows a positive correlation with calcium (Figure V-10), as would be expected from their similar geochemical behaviour. No apparent correlation exists between Barium and Calcium.

Concentrations of Zirconium range between 155 ppm and 365 ppm and average about 250 ppm. Nockolds and Allen report values of this order in acidic members of calc-alkaline suites, whilst significantly higher values occur in silica-rich members of alkaline suites, i.e. average ~ 200 ppm in calc-alkaline, average ~ 700 ppm in alkaline, at 70% SiO_2 .

Group II rhyolites:

Analyses of Group II rhyolites from the Doe Hills anticline are arranged in Table VB in order from the limb to the crest of the anticline.

The average SiO_2 content (71.9%) is only slightly higher than than of Group I (71.2%) although specimens MBJa and MBJb show secondary silicification with higher SiO_2 values (76.0% and 77.1% respectively), and correspondingly lower alumina (9.6% and 10.1% respectively). The Group II rhyolite plots in Figures V-3, V-4, V-5 indicate that Al_2O_3 , MgO



+ Rhyodacites
x Group I Rhyolites.

Figure V-9: A. Correlation between K and Rb
B. Correlation between K and Ba

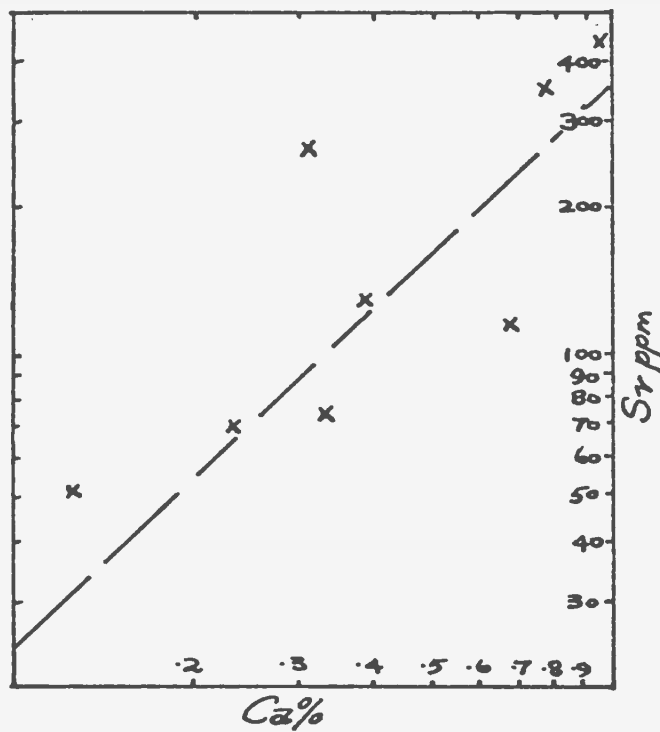


Figure V-10: Relation between
Ca and Sr in Group I rhyolites.

and total iron as Fe_2O_3 , do not differ significantly from values obtained for rhyolites of Group I except where secondary silicification affects the Al_2O_3 contents.

CaO values are low and comparable with Group I except where high CaO contents are correlatable with the sporadic development of groundmass clinozoisite and epidote (Specimens MBb, MBd, MBa, MBe, M29, MBJa and MBJe). Epidote is developed in the matrix of MBJe which has a higher value of both iron and calcium than average.

Large anomalies are, however, seen in K_2O and Na_2O . K_2O is generally higher, and Na_2O lower than in Group I rhyolites (Figure V-3). Figure V-1 shows that in general as K_2O increases so Na_2O decreases. These relations are well illustrated when Group II rhyolites are plotted on a Qtz, Ab, Or diagram (Figure V-7) where variations in the alkali contents bring about a scatter of points with noticeable changes in normative albite and orthoclase. Their wide scatter is not related either to a significantly higher content of SiO_2 or any primary crystallisation feature. The increase in K_2O does, however, correlate with the observed occurrence of secondary turbid potassium feldspar described in Chapter IV.

Rubidium varies considerably in concentration and shows a positive correlation with potassium (Figure V-12). The K/Rb ratio varies between about 400 and 200, except in MBc where it is 583, and is thus little different from that obtained in the rhyolites of Group I. Strontium is more variable than observed in Group I and is not correlatable with variations in any of the major elements. Barium varies widely from 375 ppm to 4310 ppm, twice the average value of Ba in the rhyolites of Group I.

Figure V-11: Plot of K_2O vs. Na_2O for Gp. II rhyolites showing general decrease of Na_2O with increasing K_2O .

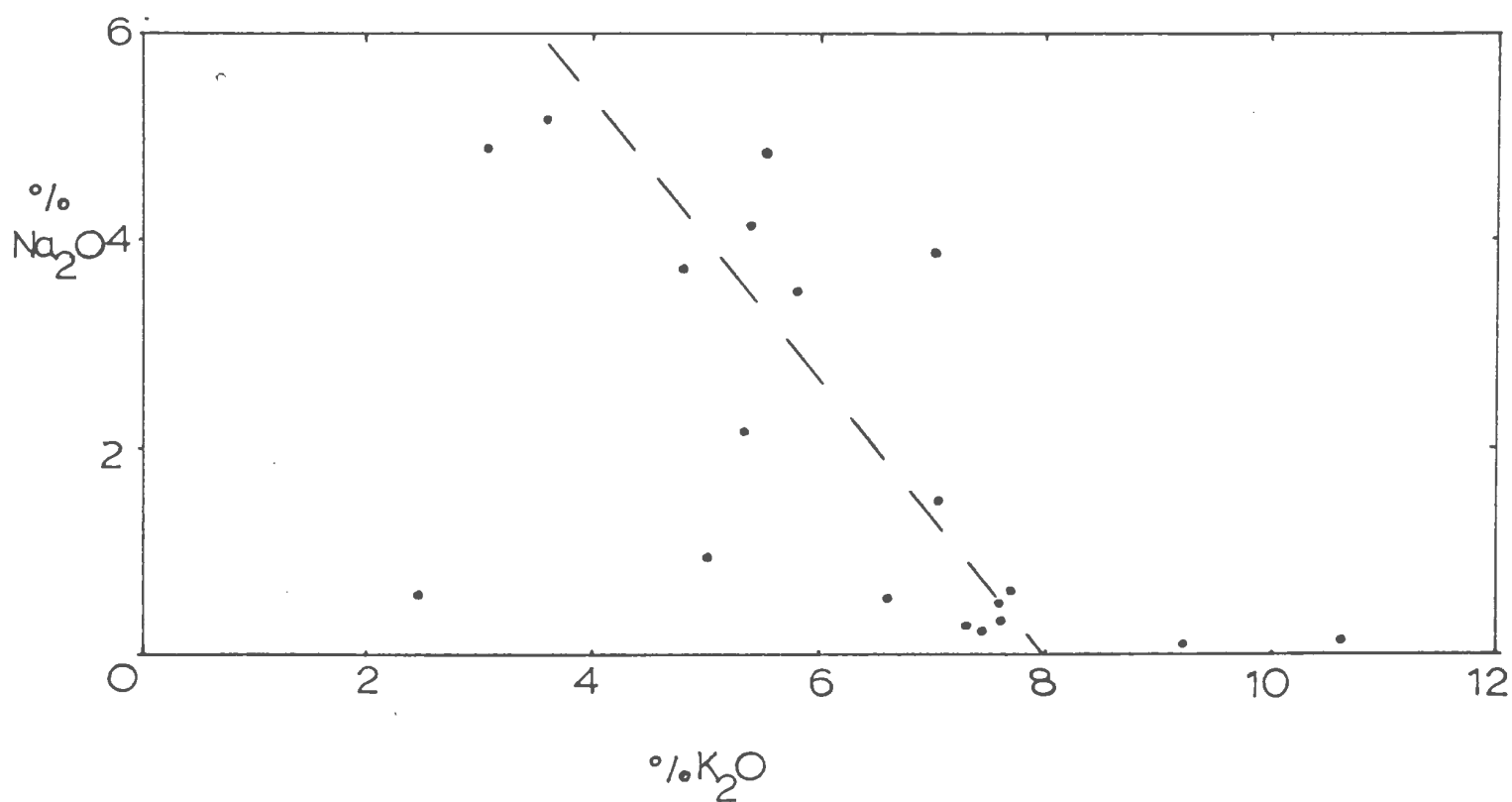


Figure V-12:

Fig. Variation of K
with Rb for Group II
rhyolites.

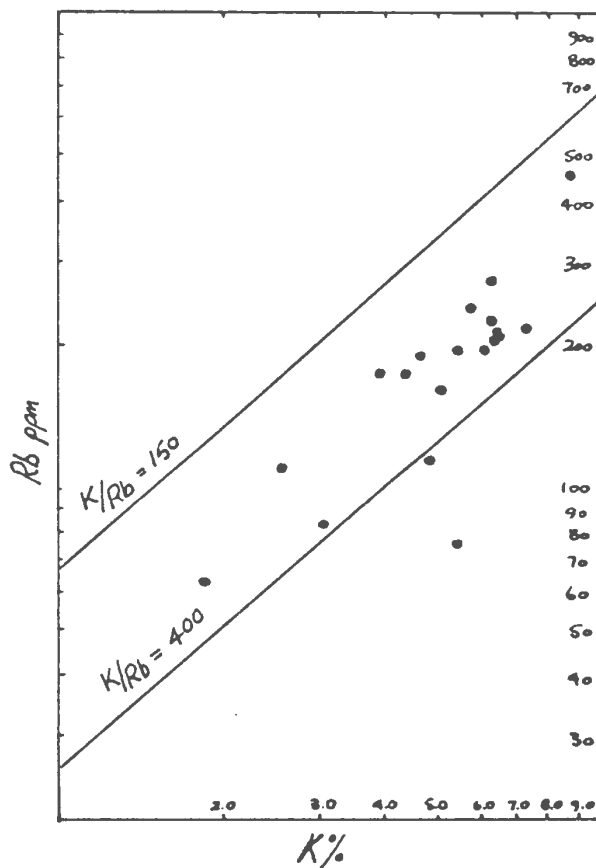
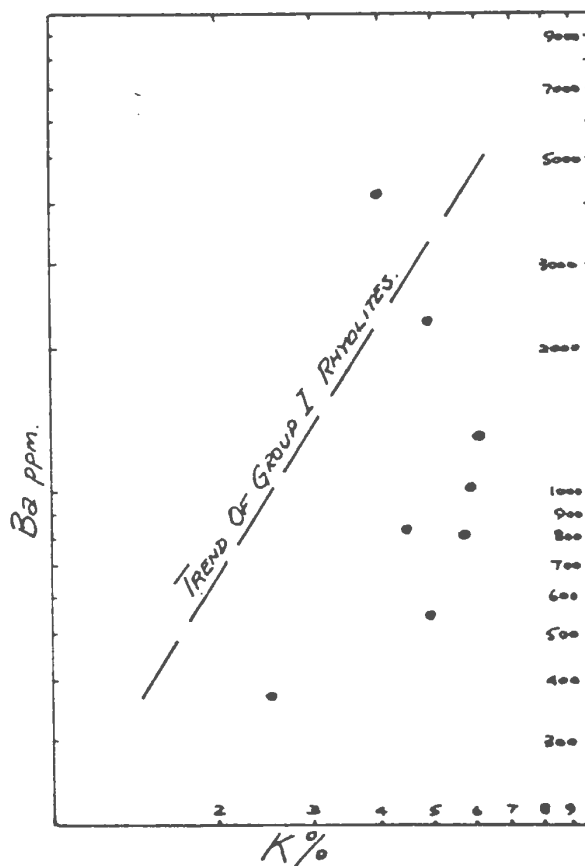


Fig. Variation of K
with Ba for Group II
rhyolites.



No significant correlation exists between Ba and K unlike in the Group I rhyolites (Figure V-11). This high figure is probably due to contamination by barite which occurs as veins and films on joint surfaces in rhyolites in the Doe Hills area.

Rhyodacites:

Analyses of specimens MB38, MB691, MB734, and MB608 are presented in Table V-C, and plotted on Figures V-2, V-3 and V-4. All contain modal mafic phenocrysts, plagioclase microlites and normative quartz $\geq 20\%$.

The high iron content ($> 2.5\%$) is a reflection of the mafic phenocrysts now pseudomorphed by chlorite. High values of Na_2O reflect the albitisation of the feldspars and most potassium must occur in the groundmass as sericite. Specimen MB691 has a high CaO content, a reflection of the development of groundmass epidote.

Trace elements are plotted against SiO_2 in Figure V-5. Zirconium shows a variation between 143 ppm and 895 ppm, the latter representing the highest value obtained in any rock from the map area, and distinctly different from any other values. Barium, Rubidium and Strontium likewise show considerable random variation. A high positive correlation is obtained between K and Ba comparable to that of the Group I rhyolites. Strontium shows a low positive correlation with calcium. A value of 740 ppm Sr in Specimen MB691 compares with a high CaO value of 5.42%.

Basalts:

Specimens MB787, MB676a, MB852, MB880 and MB856 were collected from the basic flows and scoriaceous deposits in the southeastern part of

the map area. The presence of abundant epidote veins necessitated careful sampling of the freshest material. High $\text{Na}_2\text{O}/\text{K}_2\text{O}$ ratios were generally obtained reflecting the albitisation of the feldspars, although an anomalous alkali ratio, with relatively high K_2O , was obtained for Specimen MB856. CaO values are variable.

In terms of normative criteria these basalts must be classed as transitional, with two being nepheline-normative and three hypersthene-normative. A plot of normative An, Ab, Or content of the basalts (Figure V-13) shows them to fall in the Mugearite/Hawaiite field of Barager and Irvine and Barager (1967)/(1971). A plot of $\text{Na}_2\text{O} + \text{K}_2\text{O}$ vs. SiO_2 shows all the basalts to be within the alkali field (Figure V-13) as is also shown on the alkali, alumina diagram after Kuno (Figure V-14). The basalts are, however, too poor in alumina and potash to be chemically comparable to average hawaiites and mugearites (McDonald and Katsura), Table V-G. Of the minor elements, relatively low values of Zirconium occur, in the range 100 ppm to 148 ppm. In contrast to the behaviour of Zirconium, Rubidium, Strontium and Barium show great variability and little consistency when plotted vs. SiO_2 (Figure V-5).

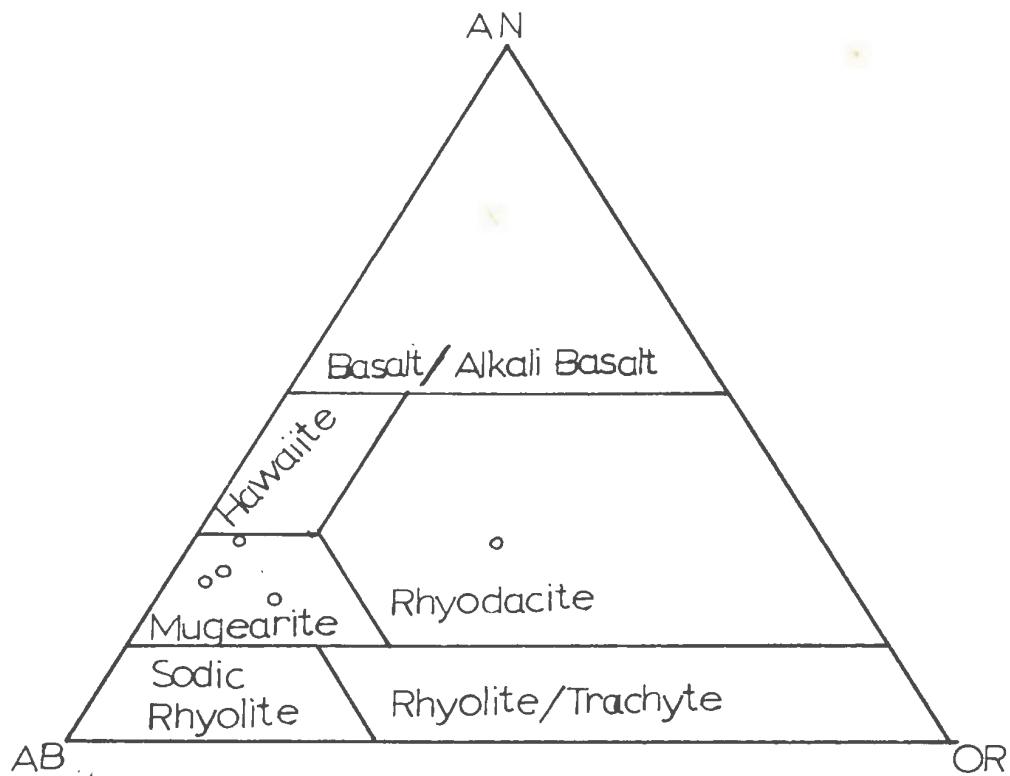


Figure V-13: Norm An Ab Or in basalts (Baragar '67)

Alks. vs. SiO_2 (McDonald and Katsura '64)

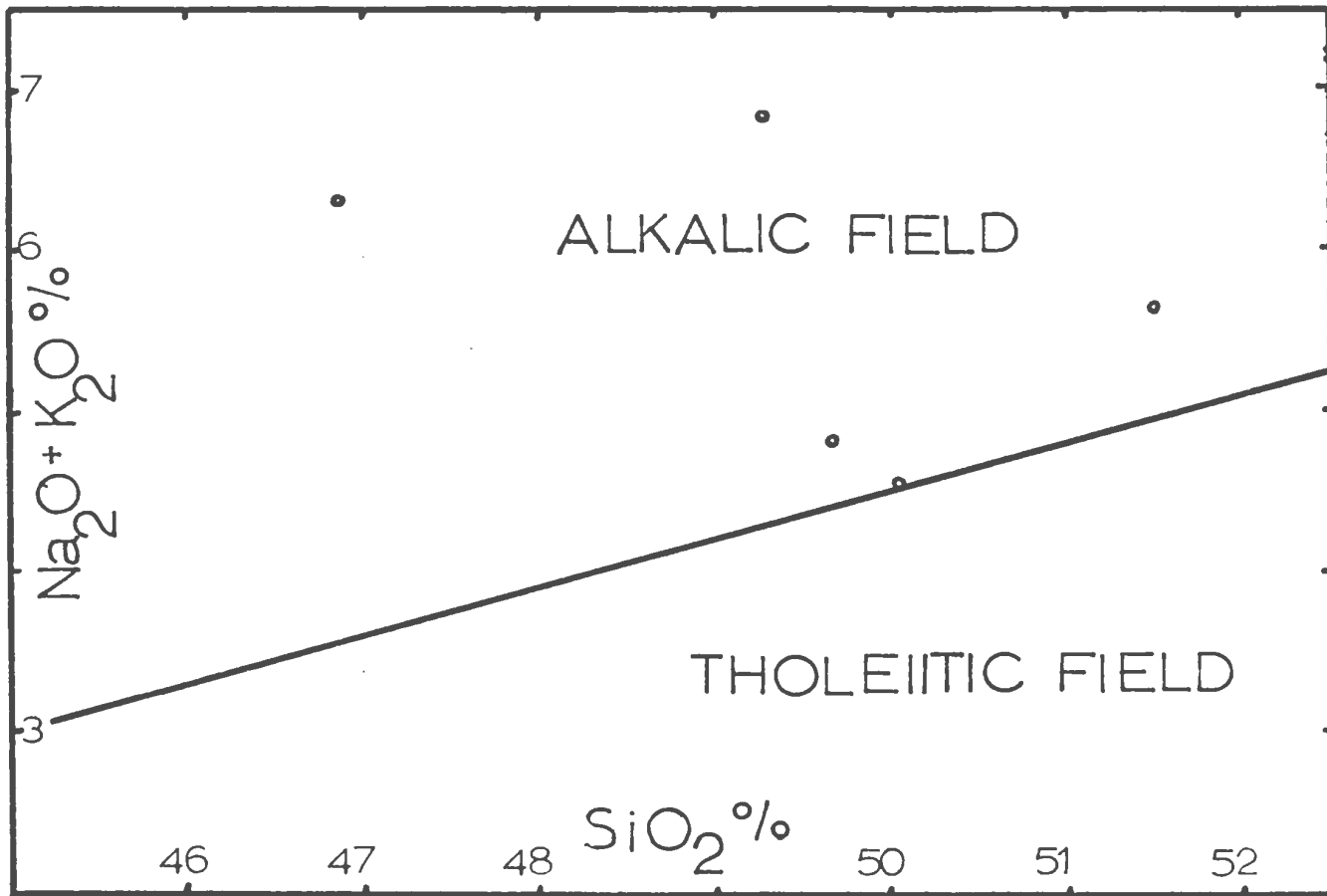


Figure V-14: Alkalies vs. Alumina (after Kuno '60)
for Bull Arm Basalts.

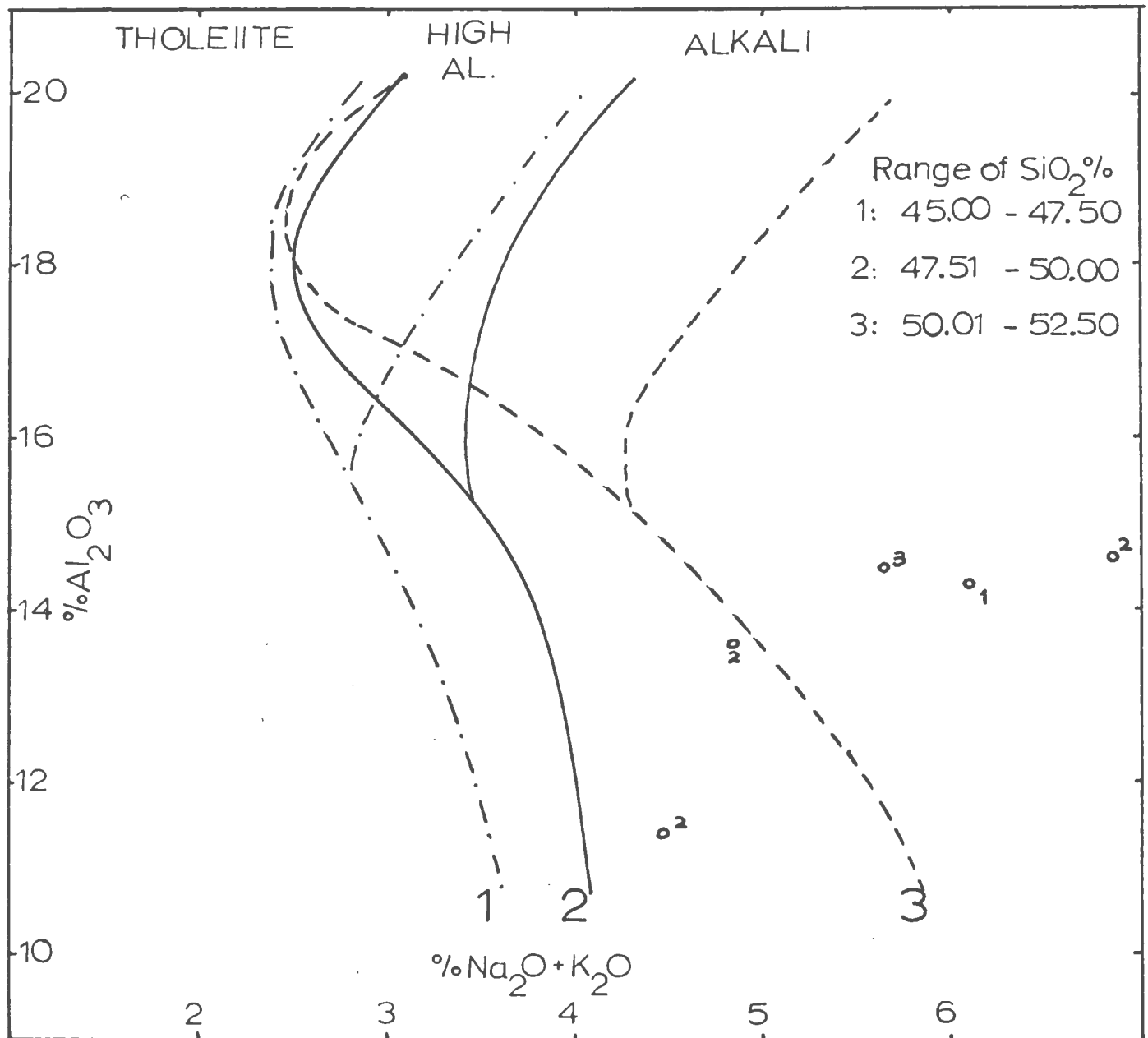


TABLE V-G: Average Hawaiite (A) and Mugearite (B).
(McDonald and Katsura, 1964).

	<u>A</u>	<u>B</u>
SiO_2	48.60	51.90
TiO_2	3.16	2.57
Al_2O_3	16.49	16.65
Fe_2O_3	4.19	4.25
FeO	7.40	6.17
MnO	0.18	0.21
MgO	4.70	3.56
CaO	7.79	6.30
Na_2O	4.43	5.22
K_2O	1.60	2.01
P_2O_5	0.69	0.93

Tuffs:

Analyses of thirteen tuffs are given in Table V-E. MB578 is porcellanous and chert-like and in thin-section can be seen to have undergone considerable secondary silicification. Its high SiO_2 content may be compared with an Al_2O_3 content of only 9.8%. Otherwise both SiO_2 and Al_2O_3 contents of the tuffs are comparable to those of Group I rhyolites.

Higher amounts of total iron and calcium than the Group I rhyolites are expressions of the higher content of epidote of the tuffs. Basaltic fragments were found in most lithic tuffs and may be the reason for high MgO values in such tuffs as MB6 and MB585. Na_2O and K_2O are comparable with rhyolites of Group I although average values are slightly lower. The $\text{Na}_2\text{O}/\text{K}_2\text{O}$ ratio generally approaches unity although there are exceptions. Specimen 1010 has an extremely high K_2O value of 10.13% and a low Na_2O value of 1.63%. This rock has a well developed cleavage along which sericite is developed. Plagioclase phenocrysts within this rock also show partial replacement by potash feldspar as in the rhyolites of Group II (see Chapter IV).

A positive correlation exists between K and Rb. Rb ranges between 465 ppm (MB1010) and 17 ppm (MB578) which have K_2O values of 10.13% and 0.86% respectively. The tuff MB1010 is notably similar to the rhyolite MBe in both its Rb and K_2O contents. Strontium is highly variable between 1720 ppm and 140 ppm but shows no correlation with major element values.

Barium shows a high positive correlation with potassium reaching a high value of 3350 ppm in 1010 and a low value of 340 ppm in MB578.

Zirconium appears not to vary much from the average of 290 ppm.

In cases other than mentioned above, and excepting CaO, the tuffs are similar in chemical composition to the Group I rhyolites. This is to be expected if both tuffs and rhyolites are of the same origin. The higher CaO content of the tuffs is a measure of the epidotisation they have undergone. The possible origin of the calcium is discussed in Chapter VI.

Sediments:

Analyses of the sediments (Table V-F) indicate that they are chemically comparable to the tuffs. Since most of the sediments are immature and poorly sorted, and generally grade from tuffs that have been reworked locally by water, this similarity was expected. Many sediments show degrees of epidotisation comparable to the tuffs. It is possible that epidotisation depends on the permeability of these rocks which are generally grit-like in grain size, whereas the flows are massive and non-vesicular. Where scoriaceous and fragmentary deposits of basalt occur, the fragments are generally found in an epidotised matrix.

CHAPTER VI

SIGNIFICANCE OF PETROCHEMISTRY AND MINERALOGY

Several questions which arise from the petrochemistry and mineralogy presented above are:

- 1) What is the origin of the albite 'phenocrysts' observed in the rhyolites?
- 2) What were the effects of metasomatism, if any?
- 3) What was the original composition of the rocks, and does it provide any indication of their petrogenesis?

(1) Origin of the Albite:

Previous Work:

Turner and Verhoogen (1960, p. 269), in discussing the problem of albite in the spilite-keratophyre suite, stated: "although the secondary nature of albite and associated low temperature minerals of some spilites has been demonstrated beyond reasonable doubt, there is a strong and persistent opinion in current literature to the effect that in other spilites the albite and even the chlorite are primary magmatic minerals." Evidence in support of albitisation in spilites reviewed by them includes relict calcic inclusions within the albite crystals, albite-filled vesicles, veinlets of albite and in some cases widespread zeolitisation.

Bathey (1955) has described both albite with normal lamellar twinning and albite with chequer-board structure in keratophyres from New Zealand. He shows that the high $\text{Na}_2\text{O}/\text{K}_2\text{O}$ ratios of sodic keratophyres

are associated with potash-rich varieties elsewhere in the sequence so that total alkalis remain constant at approximately 8% throughout the sequence, similar to that in unaltered rhyolites. Replacement of earlier plagioclase by albite is a result of redistribution of Na_2O during deep burial and deformation. Battey thus describes a process of 'autometasomatism' rather than introduction of Na_2O from external sources, and considers many keratophyres to be the metasomatic equivalents of calc-alkaline rhyolites.

Vallance (1965) concurs with the view that albites within some spilite-keratophyre suites are metasomatic, suggesting that those which he examined behaved as open systems. Although he does not deny the possible existence of primary spilitic magmas, he noted that a lack of such among recent volcanic products argues against them.

Experimental work of Yoder (1966) in the systems albite/diopside/ H_2O ; albite/chlorite/ H_2O ; anorthite/forsterite/ H_2O ; and albite/diopside/clinochlore/ H_2O , show that albite cannot be precipitated direct from a magma of basaltic composition. Evidence from the system Ab-Di- H_2O suggests that albite is a pseudomorph of a more anorthitic plagioclase that crystallised first. Even under increased $P_{\text{H}_2\text{O}}$, as suggested by Philpotts (1966), albite is not obtained on the liquidus.

Thus, the above workers conclude that spilites are not direct products of the crystallisation of even a hydrous magma, but are metasomatic products from a pre-existing basalt or gabbro assemblage. Excess Ca after albitisation occurs in epidote, zoisite or prehnite in the groundmass.

Donnelly (1966) argues that although albite replaces labradorite

phenocrysts and forms abundant microlites in spilites from the Virgin Islands, this replacement took place before consolidation of the rock. Thus, these albites are the result of a magmatic rather than a metamorphic process. Albite phenocrysts in rocks of keratophyric composition are also interpreted by Donnelly (1963) as being of primary origin for the following reasons:

(1) They show no evidence of recrystallisation and are generally clear and free of inclusions.

(2) They are often bent, apparently by viscous flow of the lava before its consolidation. They must have been albitic at this stage since replacement of an earlier feldspar in a high energy state of deformation should have produced a mosaic of smaller crystals.

(3) The albite is characterised by quasi-low temperature optics with a $2V_z$ between 90° and 100° and twin axis angles between those of low temperature and high temperature albite.

Present Work:

Phenocrysts in the Bull Arm rhyolites are similar to those described by Donnelly, many showing a lack of recrystallisation and often being bent. This bending is generally seen in specimens in which quartz-phenocrysts are also strained, and may be due to tectonic deformation rather than flow in a viscous magma. Twin planes are generally regular and distinct. Some phenocrysts are free from inclusions, although abundant amounts of epidote or zoisite are seen in others, indicating the remnants of a more calcic phase. Zoisite and epidote occur in the matrix of rhyolites but more so in the interbedded tuffs which generally have correspondingly high CaO contents.

CaO in the Group I rhyolites averages 0.65%, but in the tuffs 2.83%. The tuffs and rhyolites would be expected to have had a similar chemical composition on eruption and it is suggested that the high CaO values in the tuffs may arise as a result of diffusion on a large scale from the rhyolites during albitisation. This is somewhat similar to the zeolitisation of rocks surrounding spilites suggested by Turner and Verhoogen (1960). The bulk CaO content of the rhyolite-tuff association approximates 2.20% (see Table VI-A).

If Na_2O had been introduced into the rhyolites from external sources during a low grade greenschist metamorphism, then an appreciable change in the bulk composition of the rock would be expected. This does not occur and the average content of Na_2O in the rhyolites is no higher than the average content in average fresh rhyolite, at 4.2%. It is thus suggested that the Na_2O now in the albite phenocrysts is derived from the matrix, whilst CaO entered the matrix and diffused into surrounding rocks from the phenocrysts. Albitisation was therefore simply a result of the internal exchange of cations.

(2) Metasomatism:

The chemical composition and mineralogy of the rhyolites collected from the Doe Hills area (Group II) is that of potash-keratophyres. These rhyolites contain phenocrysts of albite that show partial to complete replacement by turbid untwinned potash-feldspar. They are also often characterised by a development of sericite and orthoclase in the matrix and correspondingly high K_2O values. Such an association of albite and

orthoclase has often been noted in keratophyric suites (Battey, 1955, p. 107; Donnelly, 1963, p. 906). No analyses of fresh rhyolitic rocks have K_2O and Na_2O values as extreme as those measured in the Doe Hills rhyolites. For example, glassy rhyolitic rocks, in apparently unaltered condition from Medicine Lake, California, and from Yellowstone, Montana, have average potash contents of 4.08% and 4.98% and soda contents of 4.02% and 3.32% respectively (Anderson, 1968). Even fresh rhyolites of more extreme composition, such as soda-rhyolites and potash-rhyolites, generally contain at least 3% of both Na_2O and K_2O . Apparently unaltered igneous rocks with alkali compositions as extreme as those reported here are wolgidite, cedricite and orendite from W. Kimberly, Australia and Leucite Hills, Wyoming (Turner and Verhoogen, 1960, p. 242). These all contain leucite and phlogopite and have low silica and are clearly not comparable to the Bull Arm rocks. Sutherland has also reported similar alkali compositions for potash trachytes from Uganda (1965) with K_2O as high as 14.96% and a corresponding Na_2O value of 0.90%, and from West Germany (1967) with K_2O up to 12.63% and a corresponding Na_2O value of 1.21%. These rock types are clearly associated with carbonatite complexes and may possibly be considered a result of fenitisation. They, again, are not comparable to the Bull Arm rocks at least in their petrogenesis.

Lipman (1965) does, however, record values of potash up to 7.97% and soda of 1.03% in devitrified rhyolites. Barker and Burmester (1970) have obtained figures as extreme as 14.48% K_2O and 0.35% Na_2O from a leached rhyolite porphyry from Llano County, Texas. Robertson (1959)

describes the occurrence of orthoclase microperthite in quartz-monzonite and alaskite in the Boulder Batholith, Montana. This apparently originated by the replacement of plagioclase. The crystallisation sequence described as leading to perthitic orthoclase was (1) the deuteric alteration of andesine to albite at the contact of invading potash-feldspar and (2) the replacement of albite by potash-feldspar which is perthitic. Robertson suggests that anorthoclase formed at an intermediate stage in the formation of orthoclase microperthite from plagioclase. Relicts of anorthoclase occur in the perthite. The temperature of formation was relatively low, below 500°C, since the sequence of mineralogical events in the deuteric stage suggest slowly decreasing temperatures throughout crystallisation.

By analogy it seems that the chemistry and mineralogy of the rhyolites of the Doe Hills could only have been derived secondarily. Since the metasomatised rocks are concentrated in an anticlinal crest with evidence of increasing degrees of replacement of plagioclase by orthoclase from the limbs to the crest, and because of the chemistry of the other rhyolites in the area, it appears that the metasomatism is structurally controlled. Thus it post-dates the crystallisation and cooling of the lavas. The possibility, therefore, that metasomatism took place during late deuteric activity is ruled out because it is localised by structural deformation of much later age.

Since an increase in K_2O is associated with the development of sericite that grows along the major schistosity in the tuffs, it seems likely that the metasomatism occurred during the deformation process. A redistribution of alkalis during burial and folding and under relatively

low temperature is envisaged by Battey (1955, p. 123), Osbourne (1925) and Terzaghis (1935, 1948). Battey points out the consistency of the total alkalis at 8%, but the rhyolites from the Bull Arm vary in total alkalis between 8% and 10% suggesting that either the original rocks crystallised from a highly alkaline magma, or that there has been some addition of alkalis from outside sources.

Truesdell (1966) showed that increased K_2O/Na_2O ratios coincide with increased contents of water in volcanic acid glasses. He concluded that potassium is adsorbed preferentially to sodium on glass, and potassium is preferentially taken up and sodium released at the same time that the glass is absorbing water and hydrogen ions. Ross and Smith (1955) noted that the water content of obsidian is only a few tenths of a percent, but perlite derived from the obsidian contains from 2 to 5 percent. They pointed out that most Tertiary glasses have undergone a secondary hydration giving rise to high water contents. Simons (1962) has described the devitrified part of a vitrophyre unit of Cretaceous ignimbrite in Arizona. The ratio K_2O/Na_2O in the glass is 1.4 whereas it is 7.7 in the devitrified rock. The losses on ignition of the rhyolites from the Bull Arm Formation, which represents H_2O^+ , H_2O^- , and CO_2 are of the order of 2-5% and most of this figure represents water. Hydrolysis is possibly a cause of the potash metasomatism. Hemley and Jones (1964) emphasize that hydration is a chemical combination of H_2O with another substance with no selective consumption of H^+ or OH^- ions, whereas hydrolysis involves a reaction with water in which either of these ions is selectively consumed. In hydrogen metasomatism, the H^+ ions apparently react with the oxygen atoms

of silicate structures to form highly polarised hydroxyl groups. Cations are concomitantly released. Thus in reactions involving hydrolytic alteration the relative stabilities of mineral assemblages in alkali-alumina-silica-water system are defined not only by pressure and temperature, but also by the pH of the aqueous phase. An increase in temperature or pressure, for example during regional metamorphism to low grades, results in reactions involving both base cation fixation and the formation of minerals such as K-mica and K-feldspar.

Geological Significance of Metasomatism:

The metasomatism also seems to have affected Rubidium/Strontium ratios (Tables VA-F). Fairbairn et al. (1966) have presented data on the abundance of Rb and Sr isotopes in the Bull Arm volcanic rocks indicating an age of 467 ± 30 m.y. and an initial $\text{Sr}^{87}/\text{Sr}^{86}$ ratio of 0.7040 ± 0.0032 . Since Lower Cambrian fossiliferous shales overlies the tuffaceous and sedimentary sequence of which the Bull Arm forms the base, this age is clearly anomalous. Fairbairn et al. (1966, p. 509) suggest that 'a small and variable diffusion of Rb into the rocks' during the later deformation may be the cause of this. Rubidium is markedly enriched in potassic rich metasomatised rhyolites, and variable strontium values are obtained, sometimes showing a positive correlation with calcium. If the volcanic rocks used in the construction of the isochron had been affected by metasomatism, even to a considerably lesser degree than the rhyolites of the Doe Hills, then a diffuse isochron, yielding an anomalous age, would have resulted.

Cormier (1969) showed that in the late Precambrian Coldbrook Group of New Brunswick, volcanic rocks with $\text{Rb}^{87}/\text{Sr}^{86}$ ratios less than unity yield an isochron age of 750 ± 80 m.y., whereas those with $\text{Rb}^{87}/\text{Sr}^{86}$ ratios greater than unity yield an isochron age of 370 ± 38 m.y. Cormier correlated the anomalously younger ages with the time of Acadian deformation, and the older age with the time of extrusion. Metasomatism in the Doe Hills area resulted in the production of rocks with widely differing Rb/Sr ratios within a small area, and this is perhaps sufficient to yield a reset isochron age for the metasomatism itself.

It is quite possible that the high value of Barium associated with the rhyolites are also a result of metasomatism. During a progressive replacement of plagioclase by orthoclase the amount of barium held in solid solution might be reduced at the lower temperatures prevailing during alteration. Barium thus released may be reprecipitated as barite on joint surfaces and in veins cutting the volcanics. Some indication of a diffusion gradient of barium towards such areas of concentration has been obtained. Specimens MBJd and MBJa were obtained from fresh massive material away from joint surfaces. They show Ba values that are well below the average (800-900 ppm) common in rhyolites. Specimen MBJa was taken closer to a joint surface and shows a higher concentration of barium. Specimens MBJb, MB171, MB762 and MBJe were taken closest to the joint surfaces. These have Ba contents generally in excess of average figures for rhyolites (specimen MBJe was probably contaminated with barite on the joint surface). The progressive increase may suggest a diffusion from the inner parts of joint surrounded blocks out towards joint planes where accumulation took place, or an inward diffusion from the joint planes.

TABLE VI-A: Major Element Analyses.

Average Group I Rhyolites.

Average Tuffs.

Average of 7

Average of 11

SiO ₂	68.8
Al ₂ O ₃	14.5
Fe ₂ O ₃	2.26
CaO	0.67
Na ₂ O	5.12
K ₂ O	4.13
MgO	0.27
MnO	0.07
TiO ₂	0.32
P ₂ O ₅	0.04
Ign.	3.16

SiO ₂	67.0
Al ₂ O ₃	14.50
Fe ₂ O ₃	3.35
CaO	3.10
Na ₂ O	3.34
K ₂ O	3.29
MgO	0.79
MnO	0.11
TiO ₂	0.38
P ₂ O ₅	0.09
Ign.	3.37

Weighted Average (Calculated Anhydrous)

SiO ₂	70.0
Al ₂ O ₃	15.0
Fe ₂ O ₃	3.01
CaO	2.20
Na ₂ O	4.19
K ₂ O	3.75
MgO	0.60
MnO	0.09
TiO ₂	0.37
P ₂ O ₅	0.07

If this diffusion was related to the period of metasomatism then the joint system would have developed during the deformation.

(3) Original Composition of Rocks and Volcanic Affinities:

The Group I rhyolites are the least altered of those analysed in the present study. Albitisation of these rocks by metasomatism requiring no intake of sodium from external sources has been suggested in Chapter VI. During this process, calcium was released from the phenocrysts and is now found in zoisite group minerals in the matrices of the rhyolites and interbedded tuffs. CaO in the Group I rhyolites averages 0.67% but in the tuffs 3.10%. Thus, since the tuffs and rhyolites would be expected to have had a similar chemical composition on eruption, their average bulk chemistry should approximate that of the original acid rock type. Such a composition is shown in Table VI-A, obtained from a weighted average of tuffs and rhyolites that show neither indication of potash-metasomatism (i.e. replacement of albite by orthoclase), nor secondary silicification, and based on relative amounts of these rock types in the sequence. This calculated analysis is as close an approximation to original composition that can be suggested. However, it should be added that mafic rock fragments in the tuffs will have minor effects on the overall amounts of total iron magnesium and maybe calcium in these rocks. Assuming that the composition in Table VI-A is correct, a high CaO/total alkali ratio suggests a calc-alkaline affinity for the acid rocks, instead of the apparent alkaline affinity.

This conclusion is supported by the Zirconium values for the total

41 specimens. Zirconium has been plotted against Nockold's and Allen's (1953) differentiation index for seven alkali provinces in Figure VI-1 and for seven calc-alkali provinces in Figure VI-2. The Bull Arm analyses are strikingly similar to those of calc-alkaline suites, with zirconium rarely reaching values above 400 ppm. Zirconium appears to remain stable throughout metasomatism.

Similar plots of Rb, Sr, and Ba show that these elements are of little use in determining the original magma type, since there are no significant differences in calc-alkaline and alkaline provinces.

This indicated calc-alkaline affinity contrasts with the conclusion reached by Papezik (1970) for the Harbour Main volcanics further east on the Avalon Peninsula. He concludes that this volcanic suite is essentially weakly alkaline in nature and draws conclusions about the tectonic setting of the Harbour Main rocks. Comparisons are Southern Nevada where block faulting of the Basin and Range type is dominant and there is associated eruption of continental alkali lavas and ignimbrites. Although mentioning alkali exchange, Papezik believes that alteration in the Harbour Main is insignificant and that the original chemistry is preserved. If not a result of metasomatism, the chemistry of the Harbour Main rocks indicates a different tectonic setting compared with the Bull Arm volcanics. However, since the Bull Arm volcanics are possibly contemporaneous with Late Harbour Main, at least in their early stages, there is an indication that the Avalon volcanic province may have been undergoing a progressive development from alkaline to calc-alkaline volcanism during Eocambrian time. Such a change through time has been recognised in the Basin and Range province

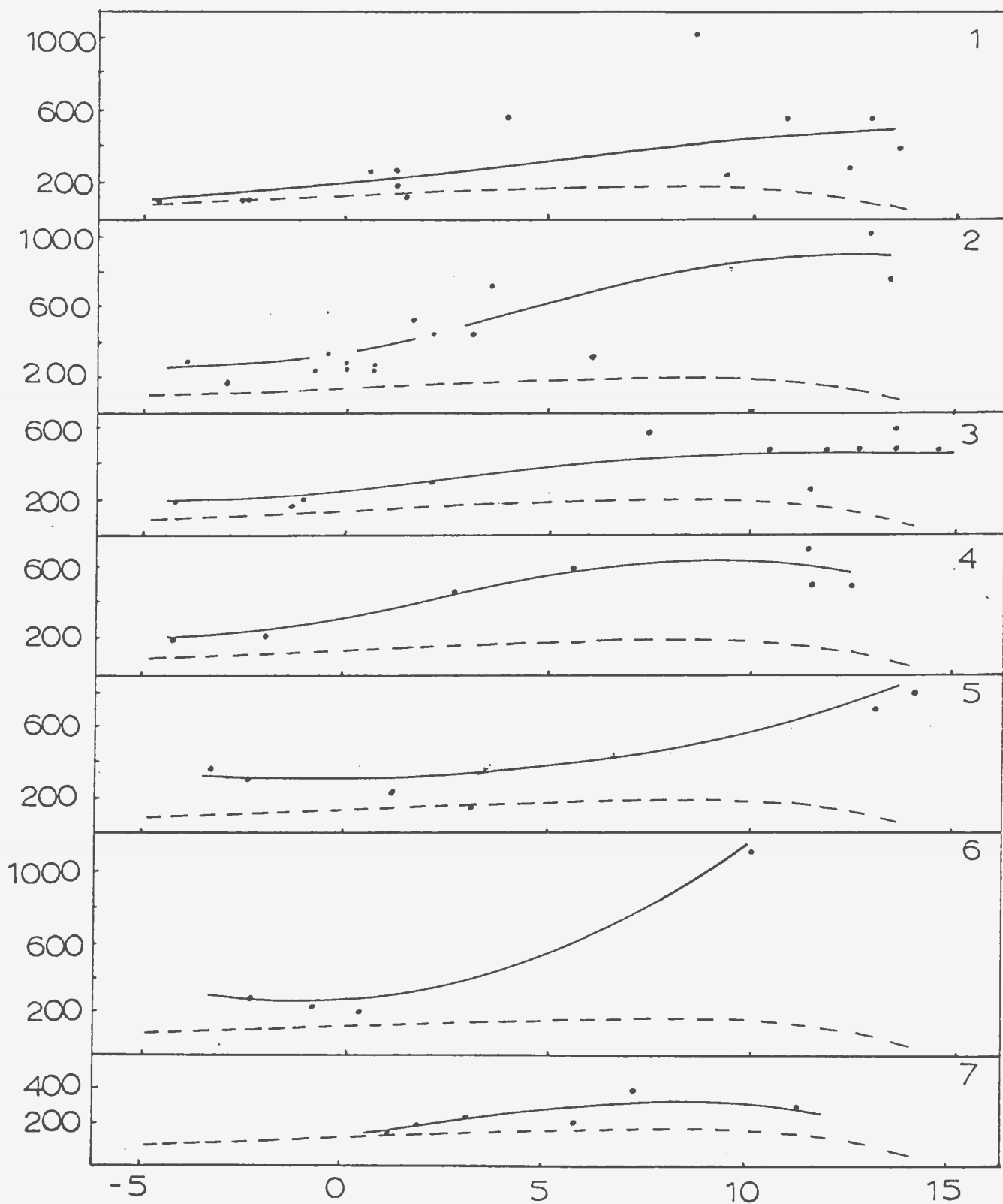


Fig VI-1: Variation in Zirconium (ppm) with differentiation index.

1 Scottish Tertiary, 2 Hawaii, 3 Polynesia I, 4 Polynesia II
5 Easter Island, 6 Braefoot, 7 Nevada Latite Series.

Bull Arm Formation superimposed as dashed line.

$$DI = (1/3 Si + K) - (Ca + Mg)$$

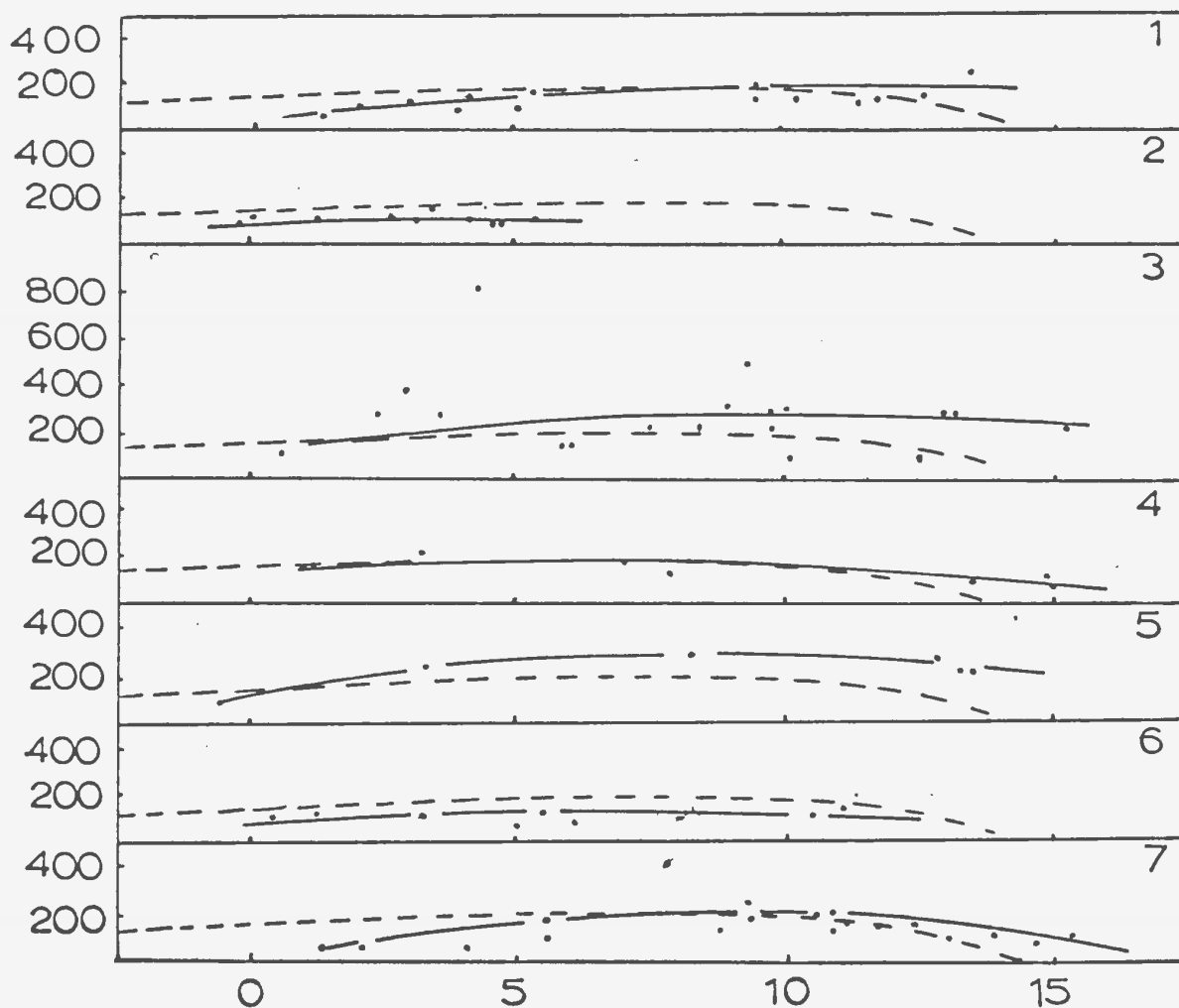


Fig VI-2 Variation in Zirconium (ppm) with Differentiation Index

1 Crater Lake, 2 Lesser Antilles, 3 Scottish Caledonian,
4 E. Central Sierra Nevada, 5 Medicine Lake Highlands,
6 Lassen Peak, 7 S. California Batholith. Zirconium

values for Bull Arm Formation superimposed as dashed line.

$$DI = (1/3 Si + K) - (Ca + Mg)$$

where alkaline volcanics overlie calc-alkaline types, and similar variations are known from Japan, where the rock types are contemporaneous but vary laterally.

However, some rocks within the Harbour Main Group are known to be metasomatised. Although only localised, examples of metasomatism from Harbour Main rocks (Hughes and Malpas, 1971) may indicate that their present chemical composition is not necessarily indicative of their composition on eruption.

The lack of intermediate rock types in the map area has been noted above (Chapter V). Perhaps little significance should be attached to the bimodal distribution of rock types in such a small area (9 square miles), especially since McCartney (1967) has recorded some intermediate rock types from elsewhere in the Bull Arm formation. These, however, are not numerous.

Some volcanic provinces which show a similar distribution of basic and acid rock types are Nuanetsi and the Hebrides. Similar rocks also occur at Thingmuli, Iceland, although here the distribution is not strictly bimodal.

A tectonic control of volcanism existed in the Nuanetsi province of Southern Rhodesia during the period of Karroo deformation. Picrites, tholeiitic basalts and rhyolites occur in association with one another. Du Toit (1929) visualized an underlying basaltic magmatic-wedge which became differentiated through both assimilation and gravitative influences to give the acid magma of the rhyolitic lavas. However, the major areas of

variation are confined to the line along which late-Karoo deformation was most intense, and it is difficult to explain differentiation occurring only in these areas and not elsewhere in the province. Cox et al. (1965) suggest that it is more likely that several primary magmas were generated in the deformed zones, whereas only one was generated in the undeformed area. Thus there appears to be a tectonic control of magma generation. Acid magma was formed by the melting of granitic crustal rocks in areas where heat flow from depth was greatest, or where tectonic relief of confining pressure was most active (Bailey, 1964; Cox et al., 1969).

The origin of the granitic rocks of the British Tertiary Province has been variously attributed to fractional crystallisation of basic magmas (Bailey et al., 1924), the metasomatism of pre-existing rock (Black, 1954) and the partial melting of country rock (Brown, 1963; Moorbath and Bell, 1965). Moorbath and Bell point out the association, in Skye, of acid and basic rocks with no gradation between the two. Strontium isotope studies suggest that the granitic rocks and marscoite suite were produced by partial melting of a shallow basin of Lewisian rocks, the heat being supplied from underlying masses of basic rocks (Thompson, 1969). In order to produce the marscoite suite, subsequent mixing of basic and acidic magma must be envisaged.

Carmichael (1964) considers that the acidic lavas of Thingmuli volcano, Iceland, are derived by a process of fractionation from a basaltic parent of olivine-tholeiite composition. The lack of sialic material in Iceland argues against any alternative.

It is not possible here to decide the origin of the acidic lavas of the Bull Arm sequence. However, the lack of intermediate types may suggest separate parental magmas. The tectonic environment suggested by Papezik (1970) with large scale block-faulting indicating local release of stress, may support this view (cf. Cox et al., 1965). The view of Hughes and Brückner (1971), see also Chapter I, of the building and erosion of a volcanic island complex, and little or no tectonic activity may argue against it. If, however, the original magmas were calc-alkaline, and the environment suggested by Hughes and Brückner is correct, then the possibility that the Avalon forms part of an island-arc complex cannot be ruled out. The likelihood that much sialic crust would be available for remelting in such a case seems doubtful, since many present day island arcs appear to form on the simatic material of ocean floors (Mitchell and Reading, 1971). The acidic magma may then have been produced by fractional crystallisation. However, the lack of intermediate rock types in an apparently calc-alkaline sequence still remains a problem.



PLATE VI-1: Development of Barite in veins and on
joint surfaces of Doe Hills rhyolites.



APPENDIX I - ANALYTICAL METHODS

The major element oxides, excluding P_2O_5 , were determined using a Perkin Elmer 303 Atomic Absorbtion Spectrometer. 0.2000 grammes of sample ground to -200 mesh was dissolved in 5 cc. of H.F. This was further diluted with 50 cc. of saturated Boric Acid and made up to 200 cc. with water. From this 'stock' solution further dilutions were made (5 in 50) for comparison with standard blends. Those standards used were both artificial and United States Geological Survey rock standards.

In the cases of CaO and MnO , 10 cc. La_2O_3 and 5 cc. HCl were added per 50 cc. solution during this further dilution to act as a releasing agent to suppress the interference of aluminium and phosphorus with these determinations.

Unknown oxides were determined both graphically and mathematically by proportionality equations.

The analyses for all trace elements were carried out by X-ray fluorescence using a Phillips PW 1220 24 channel semi-automatic spectrometer. Trace elements were determined on -200 mesh rock powders supported on mylar film, by calculating the ratios of peak to background and reading concentrations off linear calibration curves. A tungsten X-ray tube and LiF analyser crystal were used in all cases. Excitation was 40 kV and 20 mA. In the cases of Zr , Rb and Sr , the $K \alpha$ peak was recorded, in the case of Ba , the $K \beta$ peak was recorded, and background corrections made, by scintillation counter with no vacuum.

P_2O_5 was determined colorimetrically by the method described by Maxwell (1968, p. 394).

TABLE A-1: Accuracies and Precisions obtained during the Present Study are given in Table A-1:

Accuracy of Atomic Absorbtion Analysis				
Wt. %	A.	B.	A.	B.
	G-2		BCR1	
SiO ₂	69.22	69.21	54.36	54.125
TiO ₂	0.48	0.475	2.24	2.255
Al ₂ O ₃	15.33	15.420	13.56	13.665
Fe ₂ O ₃	2.69	2.675	13.40	13.355
CaO	1.98	1.965	6.94	6.915
MgO	0.77	0.755	3.46	3.485
Na ₂ O	4.06	4.095	3.26	3.290
K ₂ O	4.49	4.455	1.67	1.690
MnO	0.04	0.040	0.19	0.190

A -- Abbey's proposed values. B -- values obtained in this study.

Accuracy of X-ray Fluorescence Analysis				
ppm	A.	B.	A.	B.
	G-2		BCR1	
Rb	234	227	72.8	70
Sr	463	454	345	325
Zr	316	310	185	197
Ba	1950	2010	790	810

A -- Flanagan's proposed values. B -- Values obtained in this study.

TABLE A-1 (Continued):

Precision of Atomic Absorbtion Analysis
BCR-1

Wt. %	\bar{x}	R.	s.	n.	C%
SiO ₂	54.13	0.37	0.18	4	0.33
TiO ₂	2.26	0.10	.045	4	1.9
Al ₂ O ₃	13.67	0.25	.119	4	.09
Fe ₂ O ₃	13.36	0.49	.228	4	1.7
CaO	6.92	0.21	.118	4	1.7
MgO	3.49	0.20	.104	4	2.9
Na ₂ O	3.29	0.07	.03	4	.09
K ₂ O	1.69	0.05	.025	4	1.5
MnO	0.19	0.01	.01	4	5.3

Precision of X-ray Fluorescence Analysis
BCR-1

ppm	\bar{x}	R.	s.	n.	C%
Rb	70	15	8.66	4	12.4
Sr	325	21	9.49	4	2.9
Zr	197	20	8.31	4	4.2
Ba	810	71	31.2	4	3.9

\bar{x} = Mean determinations; R = Range (max.-min.); s = Standard dev. from mean; n = no. of determinations; c = coefficient of variation.

BIBLIOGRAPHY

- ANDERSON, C.A. 1968. Metamorphosed Precambrian Silicic Volcanic Rocks in Central Arizona. *Studies in Volcanology; Mem. Geol. Soc. Amer.* 112, Ed. Coats, R.R., Hay, R.L. and Anderson, C.A., 678 pp.
- ANDERSON, J.E. Jr., 1969. Development of snowflake texture in a welded tuff, Davis Mountains, Texas. *Geol. Soc. Amer. Bull.*, v. 80, pp. 2075-2080.
- _____, 1970a. Snowflake texture not diagnostic of Devitrified Ash-flow tuffs: Reply. *Geol. Soc. Amer. Bull.*, v. 81, pp. 2529-2530.
- _____, 1970b. Recognition and Time Distribution of Texturally Altered Welded Tuff. *Geol. Soc. Amer. Bull.*, v. 81, pp. 287-291.
- ANDERSON, M.M. And MISRA, S.B. 1968. Fossils found in the Precambrian Conception Group of South-Eastern Newfoundland. *Nature*, v. 220, No. 5168, pp. 680-681.
- BAILEY, D.K. 1964. Crustal warping, a possible tectonic control of alkaline magmatism. *J. Geo. Res.*, v. 69, No. 6, pp. 1103-1111.
- BAILEY, E.B., GOUGH, C.T., WRIGHT, W.B., RICHEY, J.E. and WILSON, G.V. 1925. The Tertiary and Post Tertiary Geology of Mull, Loch Aline, and Oban. *Mem. Geol. Surv. Scot. (Sheet 44 etc. Geol.)*.
- BARAGER, W.R. 1967. Unpublished report of Vulcanology Sub-committee of Geodesy and Geophysics. *Nat. Res. Council Canada*.
- BARKER, D.S. and BURMESTER, R.F. 1970. Leaching of Quartz from Precambrian Hypabyssal Rhyolite Porphyry, Llano Co., Texas. *Contr. Miner. and Petrol.* 28, pp. 1-8.

- BATTEY, M. H. 1955. Alkali Metasomatism and the Petrology of some Keratophyres. *Geol. Mag.*, v. 92, No. 2, pp. 104-126.
- BLACK, G. P. 1954. The acid rocks of western Rhum. *Geol. Mag.*, v. 91, pp. 257-272.
- BROWN, G. M. 1963. Melting relations of Tertiary Granitic Rocks in Skye and Rhum. *Min. Mag.*, v. 33, pp. 533-562.
- BRÜCKNER, W. D. 1969. Geology of Eastern Part of Avalon Peninsula, Newfoundland - A Summary. *Amer. Assoc. Pet. Geol. Mem.* 12, pp. 130-138.
- BRÜCKNER, W. D. and ANDERSON, M. M. 1971. Late Precambrian Glacial Deposits in Southeastern Newfoundland - A Preliminary Note. *Geol. Assoc. Canada Proc.*, v. 24, no. 1, pp. 95-102.
- BUDDINGTON, A. F. 1916. Pyrophyllitisation, Puritization and Silicification of rock around Conception Bay, Newfoundland. *J. Geol.*, v. 24, pp. 130-152.
- _____, 1919. Precambrian rocks of Southeast Newfoundland. *J. Geol.*, v. 27, pp. 449-479.
- CARMICHAEL, I. S. E. 1963. The Crystallisation of Feldspar in Volcanic Acid Liquids. *Quart. Jour. Geol. Soc. (Lond.)*, v. 119, pp. 95-131.
- _____, 1964. The Petrology of Thingmuli, a Tertiary Volcano in E. Iceland. *J. Pet.*, v. 5, pt. 3, pp. 435-460.
- CORMIER, R. F. 1969. Radiometric dating of the Coldbrook Group of southern New Brunswick, Canada. *Can. J. Earth Sci.*, v. 6, pp. 393-398.
- COX, K. G., JOHNSON, R. L., MONHUA, L. J., STILLMAN, C. J., VAIL, J. R. and WOOD, D. N. 1965. The Geology of the Nuanetzi Igneous Province. *Phil. Trans. Roy. Soc.*, v. 257, pp. 71-218.
- CURTIS, G. N. 1954. Mode of Origin of Pyroclastic Debris in the Meluten Formation of the Sierra Nevada. *Univ. Calif. Publ. Bull. Dept. Geol. Sci.*, v. 29, pp. 453-502.

- DALE, N. C. 1915. The Cambrian Manganese Deposits of Conception and Trinity Bays, Newfoundland. Proc. Am. Philos. Soc., v. 54, pp. 371-456.
- DONNELLY, T. W. 1963. Genesis of Albite in Early Orogenic Volcanic Rocks. Amer. Jour. Sci., v. 261, pp. 957-972.
- _____, 1966. Geology of St. Thomas and St. John, U. S. Virgin Islands. in Caribbean Geological Investigations. (H. H. Hess, ed.); Mem. Geol. Soc. Amer. 98, pp. 85-176.
- Du TOIT, A. L. 1929. The Volcanic Belt of Lerbombo, a Region of Tension. Trans. Roy. Soc. S. Afr., v. 18, pp. 189-217.
- FAIRBAIRN, H. W., BOTTINO, M. L., PINSON, W. H., and HURLEY, P. M. 1966. Whole rock age and initial Sr^{87}/Sr^{86} of Volcanics underlying Lower Cambrian in the Atlantic Provinces of Canada. Can. J. Earth Sci., v. 3, pp. 509-521.
- GREEN, J. C. 1970. 'Snowflake' Texture not Diagnostic of Devitrified Ash Flow Tuffs. Geol. Soc. Amer. Bull., v. 81, pp. 2527-2528.
- HAYES, A. O. 1948. Geology of the Area between Bonavista and Trinity Bays, Eastern Newfoundland. Geol. Surv. Nfld. Bull. 32, pt. I.
- HEMLEY, J. T. and JONES, W. R. 1964. Chemical aspects of Hydrothermal Alteration with emphasis on Hydrogen Metasomatism. Econ. Geol., v. 59, pp. 538-569.
- HENDERSON, E. P. 1960. Surficial Deposits, St. John's, Newfoundland. Geol. Surv. Can. Map 35-1959.
- HJELMQUIST, S. 1955. On the Occurrence of Ignimbrite in the Precambrian. Sveriges. Geol. Undersökning. Ars. 49, ser. C., No. 542, pp. 1-12.
- HOWELL, B. F. 1925. The Faunas of the Cambrian Paradoxides Beds at Manuels, Newfoundland. Bull. Am. Palaeo., v. 11, no. 43, pp. 1-140.

- HUGHES, C.J. 1970. The Late Precambrian Avalonian Orogeny in Avalon, Southeast Newfoundland. *Amer. Jour. Sci.*, v. 269, pp. 183-190.
- HUGHES, C.J. and BRÜCKNER, W.D. 1971. Late Precambrian Rocks of Eastern Avalon Peninsula, Newfoundland - A Volcanic Island Complex. *Can. J. Earth Sci.*, v. 8, no. 8, pp. 899-915.
- HUGHES, C.J. and MALPAS, J.G. 1971. Metasomatism in the Late Precambrian Bull Arm Formation in Southeastern Newfoundland: Recognition and Implications. *Geol. Assoc. Canada Proc.*, v. 24, no. 1, pp. 85-93.
- HUTCHINSON, R.D. 1953. Geology of the Harbour Grace map-area, Newfoundland. *Geol. Surv. Canada Mem.* 275.
- _____, 1962. Cambrian stratigraphy and trilobite faunas of S.E. Newfoundland. *Geol. Surv. Can. Bull.* 88.
- IRVINE, T.N. and BARAGER, W.R. 1971. A Guide to the Chemical Classification of the Common Volcanic Rocks. *Can. J. Earth Sci.*, v. 8, No. 5, pp. 523-548.
- JAKES, P. and SMITH, I.E. 1970. High Potassium Calc-alkaline Rocks from Cape Nelson, Eastern Papua. *Contr. Mineral. and Petrol.*, v. 28, pp. 259-271.
- JENNESS, S.E. 1960. Late Pleistocene Glaciation of Eastern Newfoundland. *Geol. Soc. Amer. Bull.*, v. 71, pp. 161-179.
- _____, 1963. Terra Nova and Bonavista Map Areas, Newfoundland. *Geol. Surv. Canada Mem.* 327.
- JUKES, J.B. 1843. General Report of the Geological Survey of Newfoundland during the years 1839-1840. V. I & II, 160 pp; John Murray, London, England.
- KAY, G.M. 1953. North American Geosynclines. *Geol. Soc. Amer. Mem.* 48, 143 pp.
- KEATS, H.F. 1970. Geology and Mineralogy of the Pyrophyllite Deposits South of Manuels, Avalon Peninsula, Newfoundland. Unpublished M.Sc. Thesis, Memorial Univ. of Nfld.

- KUNO, H. 1960. High Alumina Basalt. J. Pet., v. 1, pp. 121-145.
- LIPMAN, P. W. 1965. Chemical Comparison of Glassy and Crystalline Volcanic Rocks. U.S.G.S. Bull. 1201-D.
- _____, 1966. Water Pressures during Differentiation and Crystallisation of some Ash-Flows from Southern Nevada. Amer. Jour. Sci., v. 264, pp. 810-826.
- MAHER, J. B. 1971. Stratigraphy and Petrology of the Pouch Cove, Cape St. Francis Area, Newfoundland. Unpublished M.Sc. Thesis, Memorial Univ. of Nfld.
- MARSHALL, P. 1935. Acid Rocks of the Taupo-Rotorua Volcanic District. Roy. Soc. New Zealand Trans., v. 64, pp. 323-366.
- MASON, B. 1966. Principles of Geochemistry. 3rd. Ed., 329pp. John Wiley, N.Y.
- MAXWELL, J. A. 1968. Rock and Mineral Analysis. 584 pp. John Wiley, N.Y.
- MCCARTNEY, W. D. 1956a. Argentia, Newfoundland. Geol. Surv. Canada Prelim. Map. Paper 55-11.
- _____, 1956b. Dildo, Newfoundland. Geol. Surv. Canada Prelim. Map. 13-1956.
- _____, 1958. Sunnyside, Newfoundland. Geol. Surv. Canada Paper 58-8.
- _____, 1967. Whitbourne Map-Area, Newfoundland. Geol. Surv. Canada Mem. 341.
- _____, 1969. Geology of the Avalon Peninsula, Southeast Newfoundland. Amer. Assoc. Pet. Geol. Mem. 12, pp. 115-129.
- MCCARTNEY, W. D., POOLE, W.H., WANLESS, R.K., WILLIAMS, H. and LOVERIDGE, W.D. 1966. Rb/Sr age and geological setting of the Holyrood Granite, Southeast Newfoundland. Can. J. Earth Sci., v. 3, pp. 947-957.

- MCDONALD, G. A. and KATSURA, T. 1964. Chemical composition of Hawaiian Lavas. *J. Pet.*, v. 5, pp. 82-133.
- MITCHELL, A. H. and READING, H. G. 1971. Evolution of Island Arcs. *J. Geol.*, v. 79, pp. 253-284.
- MOORBATH, S. and BELL, J. D. 1965. Strontium Isotope Abundance Studies and Rb/Sr Age Determinations on Tertiary Igneous Rocks from the Isle of Skye, NW Scotland. *J. Pet.*, v. 6, pt. 1, pp. 37-66.
- MURRAY, A. and HOWLEY, J. P. 1881. Map of the Peninsula of Avalon. *Geol. Surv. Nfld.*
- NEALE, E. R. W., BELAND, J., POTTER, R. R., and POOLE, W. H. 1961. A Preliminary Map of the Canadian Appalachian Region based on Age of Folding. *Can. Inst. Min. Met. Trans.*, v. 64, pp. 405-412.
- NOCKOLDS, S. R. 1954. Average Chemical Composition of Some Igneous Rocks. *Geol. Soc. Amer. Bull.*, v. 65, pp. 1007-1032.
- NOCKOLDS, S. R. and ALLEN, R. 1953. The Geochemistry of Some Igneous Rock, Series I. *Geochem. Cosmochem. Acta*, v. 4, pp. 105-142.
- _____, and _____, 1954. The Geochemistry of Some Igneous Rock, Series II. *Geochem. Cosmochem. Acta*, v. 5, pp. 245-285.
- ORVILLE, P. M. 1963. Alkali-ion Exchange between Vapour and Feldspar Phases. *Amer. Jour. Sci.*, v. 261, pp. 201-237.
- OSBOURNE, G. D. 1925. Geology and Petrography of the Clarencetown-Paterson District, pt. IV. *Petrography Proc. Linn. Soc. of N.S.W.*, pp. 112-138.
- PAPEZIK, V. S. 1969. Late Precambrian Ignimbrites of the Avalon Peninsula, Newfoundland. *Can. J. Earth Sci.*, v. 6, pp. 1405-1414.
- _____, 1970. Petrochemistry of Volcanic Rocks of the Harbour Main Group, Avalon Peninsula, Newfoundland. *Can. J. Earth Sci.*, v. 7, pp. 1485-1498.

TERZAGHI, R. D. 1935. The Origin of Potash Rich Rocks. Amer. Jour. Sci., v. 229, pp. 369-380; v. 230, pp. 141-142.

_____, 1948. Potash rich Rocks of Esterel, France. Amer. Miner., v. 33, pp. 18-30.

THIEME, J. G. 1970. The Geology of the Mansa Area: explanation of Degree Sheet 1128, parts of N.W. Quarter and N.E. Quarter. Rep. Geol. Surv. Zambia.

THOMPSON, R. N. 1967. The 'Rhyolite' of Fionn Choire, Isle of Skye. Geol. Soc. London Proc., no. 1642, pp. 212-214.

_____, 1969. Tertiary Granites and Associated Rocks of the Marsco Area, Isle of Skye. Q. J. Geol. Soc. London, v. 124, pp. 349-385.

TRUEDELL, A. H. 1966. Ion-Exchange Constants of Natural Glasses by the Electrode Method. Amer. Miner., v. 51, pp. 110-122.

TURNER, F. J. and VERHOOGEN, J. 1960. Igneous and Metamorphic Petrology. McGraw-Hill, N.Y., 694 pp.

TUTTLE, O.F. 1952. Optical Studies on Alkali Feldspars. Amer. Jour. Sci. Bowen vol., pt. 2, pp. 553-567.

TUTTLE, O.F. and BOWEN, N. L. 1958. The Origin of Granite in the Light of Experimental Studies in the System $\text{NaAlSi}_3\text{O}_8$ - KAlSi_3O_8 - SiO_2 - M_2O . Geol. Soc. Amer. Mem. 74, 153pp.

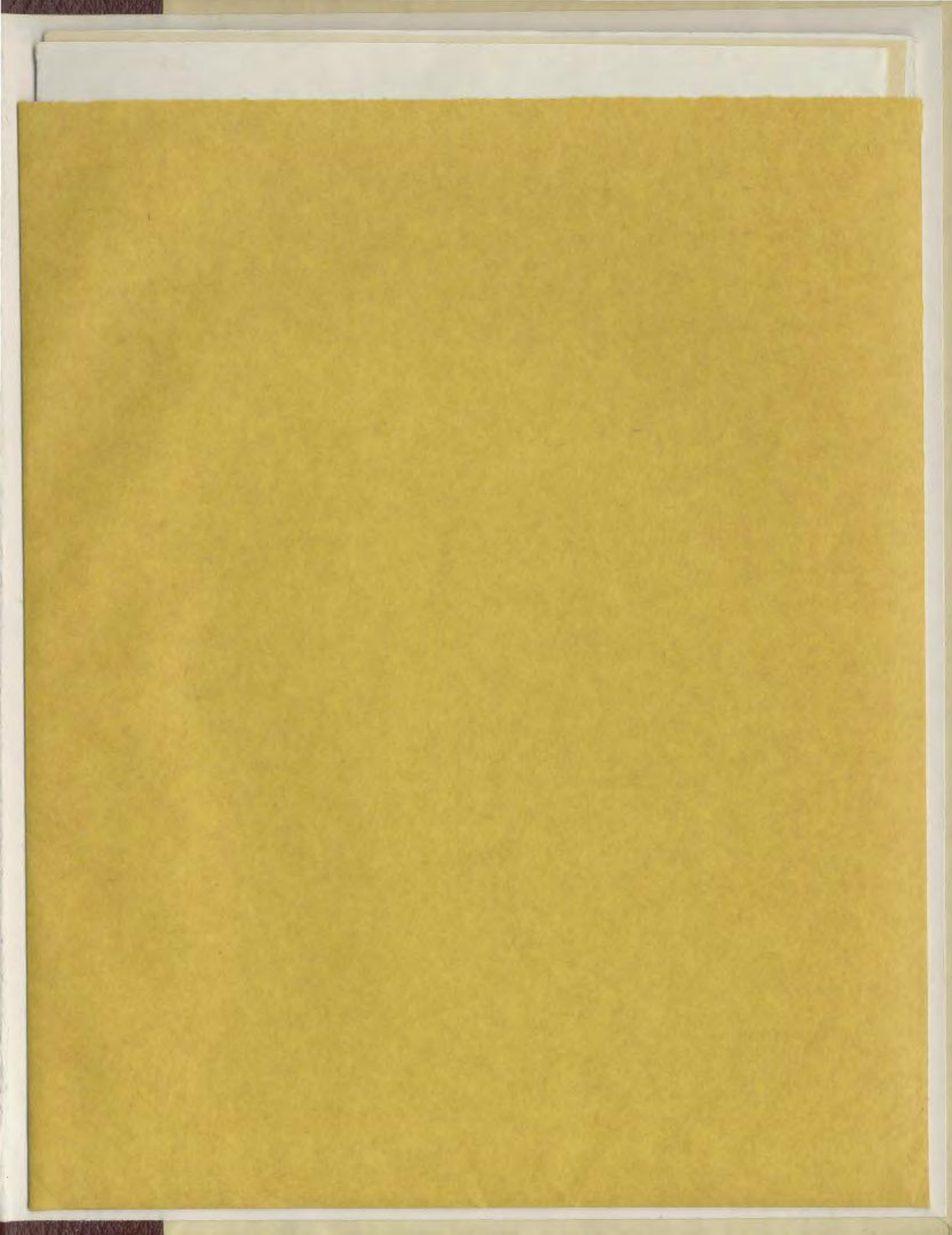
VALLANCE, T. G. 1965. On the Chemistry of Pillow Lavas and the Origin of Spilites. Min. Mag., v. 34 (Tilley Volume), pp. 471-481.

WILLIAMS, H. 1964. The Appalachian in N.E. Newfoundland - A Two-Sided Symmetrical System. Amer. Jour. Sci., v. 262, pp. 1137-1158.

_____, 1967. Silurian Rocks of Newfoundland. Geol. Surv. Can. Sp. Paper 4 (H. Lilly Mem.), pp. 93-137.

WRIGHT, J. B. 1969. A Simple Alkalinity Ratio and its Application to Questions of Non-Orogenic Granite Gneiss. Geol. Mag., v. 106, no. 4, pp. 370-384.

YODER, H. S., Jr. 1966. 'Spilites and Serpentinities'. Annual Report of the Director, Geophysical Lab. Carnegie Inst. Washington, pp. 269-279.



- PHILPOTTS, A. R. 1966. Origin of the Anorthosite-Mangerite Rocks in Southern Quebec. *J. Pet.*, v. 7, pp. 1-64.
- POOLE, W. H. 1967. Tectonic Evolution of Appalachian Region of Canada. *Geol. Surv. Can. Spec. Pap. 4 (H. Lilly Mem.)*, pp. 9-51.
- ROBERTSON, F. 1959. Perthite Formed by Reorganisation of Albite from Plagioclase during Potash-Feldspar Metasomatism. *Amer. Miner.*, v. 44, pp. 603-619.
- RODGERS, J. 1967. Chronology of Tectonic Movements in the Appalachian Region of eastern North America. *Am. Jour. Sci.*, v. 265, pp. 408-427.
- _____, 1968. The Eastern Edge of the North American Continent during the Cambrian and Early Ordovician; in *Studies of Appalachian Geology*. ed. Zen, E., White, W.S., Hadley, J.B., Thompson, J.B.; John Wiley, N.Y., pp. 141-149.
- ROSE, E. R. 1948. Geology of the Area between Bonavista, Trinity and Placentia Bays, Eastern Newfoundland. *Geol. Surv. Nfld. Bull. 32*, pt. 2, pp. 39-49.
- _____, 1952. Torbay Map-Area, Newfoundland. *Geol. Surv. Canada Mem. 265*.
- ROSS, C. S. and SMITH, R. L. 1955. Water and Other Volatiles in Volcanic Glasses. *Amer. Miner.*, v. 40, pp. 1071-1089.
- SIMONS, F. S. 1962. Devitrification Dikes and Giant Spherulites from Klondyke, Arizona. *Amer. Miner.*, v. 47, pp. 871-885.
- SUTHERLAND, D. S. 1965. Potash-trachytes and ultra-potassic rocks associated with the carbonatite complex of the Teror Hills, Uganda. *Min. Mag.*, v. 35, pp. 363-378.
- _____, 1967. A note on the occurrence of potassium-rich trachytes in the Kaiserstuhl carbonatite complex, West Germany. *Min. Mag.*, v. 36, pp. 334-341.